Universidade de Aveiro Departamento de Biologia
Ano 2016

**Mónica
da Silva Sá**

Estudo do mecanismo molecular envolvido na retenção de esporozoítos de *Plasmodium* nos sinusoides hepáticos

Dissecting the molecular basis for the arrest of *Plasmodium* sporozoites in the liver sinusoids

DECLARAÇÃO

Declaro que este relatório é integralmente da minha autoria, estando devidamente referenciadas as fontes e obras consultadas, bem como identificadas de modo claro as citações dessas obras. Não contém, por isso, qualquer tipo de plágio quer de textos publicados, qualquer que seja o meio dessa publicação, incluindo meios eletrónicos, quer de trabalhos académicos.

Universidade de Aveiro Departamento de Biologia
Ano 2016

Mónica da Silva Sá

Estudo do mecanismo molecular envolvido na retenção de esporozoítos de *Plasmodium* nos sinusoides hepáticos

Dissecting the molecular basis for the arrest of *Plasmodium* sporozoites in the liver sinusoids

Dissertação apresentada à Universidade de Aveiro para cumprimento dos requisitos necessários à obtenção do grau de Mestre em Microbiologia, realizada sob a orientação científica da Doutora Joana Alexandra Pinto da Costa Tavares, Investigadora Auxiliar, Instituto de Biologia Molecular e Celular/ Instituto de Investigação e Inovação em Saúde da Universidade do Porto, da Professora Doutora Anabela Cordeiro-da-Silva, Professora Associada com Agregação, Faculdade de Farmácia da Universidade do Porto e da Professora Doutora Maria de Fátima Matos Almeida Henriques de Macedo, Professora Auxiliar Convidada do Departamento de Ciências Médicas da Universidade de Aveiro.

A investigação conducente à obtenção destes resultados foi financiada pela Fundação para a Ciência e Tecnologia (FCT)/ Ministério da Educação e Ciência (MEC) cofinanciada pelo FEDER através dos projetos: EXPL/JTavares-IF/00881/2012/CP0158; EXPL/IMI-MIC/1331/2013 e Unidade de Investigação No. 4293. Este trabalho recebeu também financiamento do projeto Norte-01-0145-FEDER-000012, suportado pelo NORTE 2020, através do PORTUGAL 2020, FEDER.

Aos meus Pais e às minhas Avós.

o júri

presidente

Doutora Isabel da Silva Henriques
equiparada e investigadora auxiliar, Universidade de Aveiro.

Doutora Inês Marina Soares Loureiro
investigadora de pós doutoramento, Instituto de Biologia Molecular e Celular/ Instituto de Investigação e Inovação em Saúde da Universidade do Porto.

Doutora Joana Alexandra Pinto da Costa Tavares
investigadora auxiliar, Instituto de Biologia Molecular e Celular/ Instituto de Investigação e Inovação em Saúde da Universidade do Porto.

agradecimentos

Em primeiro lugar, gostaria de agradecer à Doutora Joana Tavares pela confiança que depositou em mim desde o primeiro dia, por todo o seu incansável apoio e por me ter guiado e aconselhado durante a minha primeira aventura pelo mundo da Ciência. Todo este trabalho se deve a si. Muito Obrigado.

À Professora Anabela por me ter acolhido tão bem no seu grupo, e por me ter dado a fantástica oportunidade de participar em projetos fora do âmbito da minha dissertação, fornecendo-me todos os meios para que eu pudesse aprofundar os meus conhecimentos teóricos e práticos no que concerne a purificação de proteínas e ensaios enzimáticos.

À Professora Fátima Macedo, por se ter demonstrado sempre disponível durante este percurso.

Ao David. Acho não tenho palavras suficientes para te agradecer, mas aqui vai a minha tentativa: muito obrigado por NUNCA me teres recusado ajuda, por toda a (infinita!) paciência que tiveste comigo e por todas as conversas que tivemos (mesmo por vezes fora de horas). Este trabalho também é teu.

Aos restantes membros do grupo por me terem feito sentir em casa. Passar um ano convosco foi deveras uma experiência única :)

À Carla, Sara e ao Gustavo, por nunca me terem deixado de apoiar e por me fazerem sempre ver o lado B da vida.

Aos meus pais e avós, por serem o meu maior suporte. Este trabalho é para vocês.

E por fim, a ti Miguel, por todo o carinho e apoio que me deste durante este percurso, por nunca me teres falhado, e acima de tudo, por nunca teres deixado de acreditar em mim.

palavras-chave

Malaria, *Plasmodium*, esporozoíto, fase pré-eritrocitária, imagem em tempo real, TRAP, MAEBL

resumo

A malária é uma doença grave causada por parasitas do género *Plasmodium* e transmitida a mamíferos através da picada de um mosquito fêmea infetado do género *Anopheles*. A fase pré-eritrocitária do ciclo de vida dos parasitas é assintomática, englobando o percurso dos esporozoítos desde a pele até ao fígado, a sua multiplicação dentro de hepatócitos e libertação de merozoitos, as formas responsáveis pela infeção de eritrócitos. Uma etapa crucial para a infeção do fígado pelos esporozoítos envolve a retenção dos mesmos nos sinusoides. A proteína "thrombospondin-related adhesion protein" (TRAP) é a uma molécula candidata para a mediação deste evento, uma vez que esporozoítos "knockout" da TRAP não ficam retidos no fígado. Contudo, esta proteína possui uma estrutura complexa composta por domínios adesivos na sua porção extracelular, para além de estar ligada ao motor de actina-miosina do esporozoíto através do domínio citoplasmático em C terminal. Assim, de modo a explorar o papel da TRAP como mediador da retenção de esporozoítos no fígado, construímos parasitas bioluminescentes capazes de expressar a TRAP sem a cauda citoplasmática, uma vez que a deleção deste domínio torna os parasitas imóveis mas não altera a apresentação da proteína à superfície do esporozoíto. Como estes parasitas não conseguem invadir as glândulas salivares dos mosquitos e portanto maturarem completamente, criamos "knockouts" da *maebl* como controlo, uma vez que com base na literatura estes permanecem na hemolinfa de mosquitos mas infetam normalmente o fígado. Surpreendentemente, descobrimos que esporozoítos "knockout" da *maebl* têm um defeito na retenção hepática e consequentemente na capacidade de infetarem o fígado. Adicionalmente estudos *in vitro* demonstraram que os esporozoítos knockout da maebl têm um defeito na capacidade de atravessarem e invadirem hepatócitos. Com base nestes resultados, sugerimos que os esporozoítos de *Plasmodium* possam utilizar um mecanismo conservado que lhes permita reconhecer moléculas expressas à superfície das glândulas salivares do mosquito e das células hepáticas do hospedeiro mamífero.

keywords

Malaria, *Plasmodium*, sporozoite, pre-erythrocytic phase, live imaging, TRAP, MAEBL

abstract

Malaria is a devastating disease caused by *Plasmodium* parasites and transmitted to mammals through the bite of an infected anopheline female mosquito. The asymptomatic pre-erythrocytic phase of the parasite life cycle comprises the journey of sporozoites from the skin to the liver, their asexual multiplication in hepatocytes and the release of merozoites, the red blood cells infective forms. A crucial event for successful liver infection comprises the arrest of sporozoites in the sinusoids. The thrombospondin-related adhesion protein (TRAP) is a promising candidate to mediate this event, since trap knockout sporozoites cannot home to the liver. However, TRAP contains several adhesion domains in its extracellular portion and is also connected to the sporozoite actin-myosin motor through its C- terminal cytoplasmic domain. Thus, to further explore the role of TRAP in mediating the homing of sporozoites to the liver, we have successfully engineered bioluminescent parasites to express TRAP without the cytoplasmic tail. Indeed, the deletion of this domain renders sporozoites immotile but do not alter the surface presentation of the protein. As these sporozoites cannot invade the mosquito salivary glands and attain complete maturation, we have generated *maebl* knockouts as a control, a mutant line that based on previous findings remains in the mosquito hemolymph but do infect the liver as wild type parasites. Unexpectedly, we found that *maebl* knockout sporozoites have an impaired capacity to target and infect the liver of mice. Indeed, *in vitro* experiments demonstrate defective hepatocytes traversal and invasion by the *maebl* knockout sporozoites. These findings suggest that *Plasmodium* sporozoites may use a conserved mechanism for the recognition of molecules expressed by the mosquito salivary glands and the liver in the mammalian host.

Abreviation list

ACT	artemisinin-based combination therapy
AMA-1	apical membrane antigen 1
APC	antigen-presenting cells
ATP	adenosine triphosphate
BbTRAP	*Babesia bovis* TRAP homologue
C-cys	cysteine-rich region
CDPK	calcium dependent protein kinase
CDS	coding sequences
CelTOS	cell traversal protein for ookinetes and sporozoites
CSP	circumsporozoite protein
CT	cell traversal
CTD	cytoplasmic tail domain
CTRAP	CS-and-TRAP-related protein
DBL	Duffy-binding like
DC	dendritic cells
EBA	erythrocyte binding antigen
EBL	erythrocyte binding- like
EBL-1	erythrocyte-binding ligand-1
EC	endothelial cells
EEF	exoerythrocytic form
FACS	fluorescence-activated cell sorting
G6PD	glucose-6-phosphate dehydrogenase

GAGs	glycosaminoglycans
gDNA	genomic DNA
GEST	gamete egress and sporozoite traversal
GFP	green fluorescent protein
GPI	glycosylphosphatidylinositol
HBV	hepatitis B virus
HEMO	hemolymph
HSPGs	heparan sulphate proteoglycans
i.p.	intraperitoneal
i.v.	intravenous
IFA	wide-field immunofluorescence
IMC	inner membrane complex
IPTi	intermittent preventive treatment in infants
IPTp	intermittent preventive treatment in pregnancy
IRS	indoor residual spraying
KC	Kupffer cells
KO	knockout
LLIN	long-lasting insecticidal net
LN	lymph node
MAEBL	apical membrane antigen/erythrocyte binding-like
MHC	major histocompatibility complex
MG	midgut
MIC	microneme protein

MIDAS	metal ion-dependent adhesion site
MPL	monophosphoryl lipid A
MTOCs	microtubule-organizing centres
MTRAP	merozoite TRAP homologue
Myo A	myosin A
ORF	open reading frame
PCR	polymerase chain reaction
PE	pre-erythrocytic
PI	propidium iodide
PL	phospholipase
PV	parasitophorous vacuole
RBC	red blood cell
ROI	region of interest
ROM	rhomboid protease
s.c.	subcutaneous
SC	stellate cells
SG	salivary glands
SMC	seasonal malaria chemoprevention
SPECT	sporozoite microneme proteins essential for cell traversal
SR-BI	scavenger receptor BI
TEM	transmission electron microscopy
TJ	tight junction
TLP	TRAP-like protein

TRAP	thrombospondin-related anonymous protein
TRAPC1	thrombospondin-related adhesive protein of *Cryptosporidium* 1
TREP	TRAP-related protein
TRSP	thrombospondin-related sporozoite protein
TSR	thrombospondin type I
TV	transient vacuole
UTR	untranslated region
wt	wild type
VWA	von Willebrand factor A
WHO	World Health Organization

Index of figures

Table of contents

Chapter I

Introduction

Section I – Malaria, vectors and parasites

1. Key facts about malaria

Despite the scientific community awareness of malaria being more than a century old, this devastating parasitic disease still affects millions of people every year. At this moment, malaria is endemic in 95 countries placing 3.2 billion people at risk (World Health Organization, 2015a). The latest global evaluation reported in 2015, 214 million cases of paludism leading to 438 thousand deaths (World Health Organization, 2015a) (Fig.1). The malaria burden is higher in Africa since 90% of the global deaths occurred in that continent. The most vulnerable group of people are children under five year old, pregnant women, and non-immunized migrants (Desai *et al.,* 2007; Jensenius *et al.*, 2013; World Health Organization, 2015a). Young children are particularly susceptible to develop severe forms of malaria, entering as the fourth highest cause of infant mortality in WHO Africa Region (World Health Organization, 2015a).

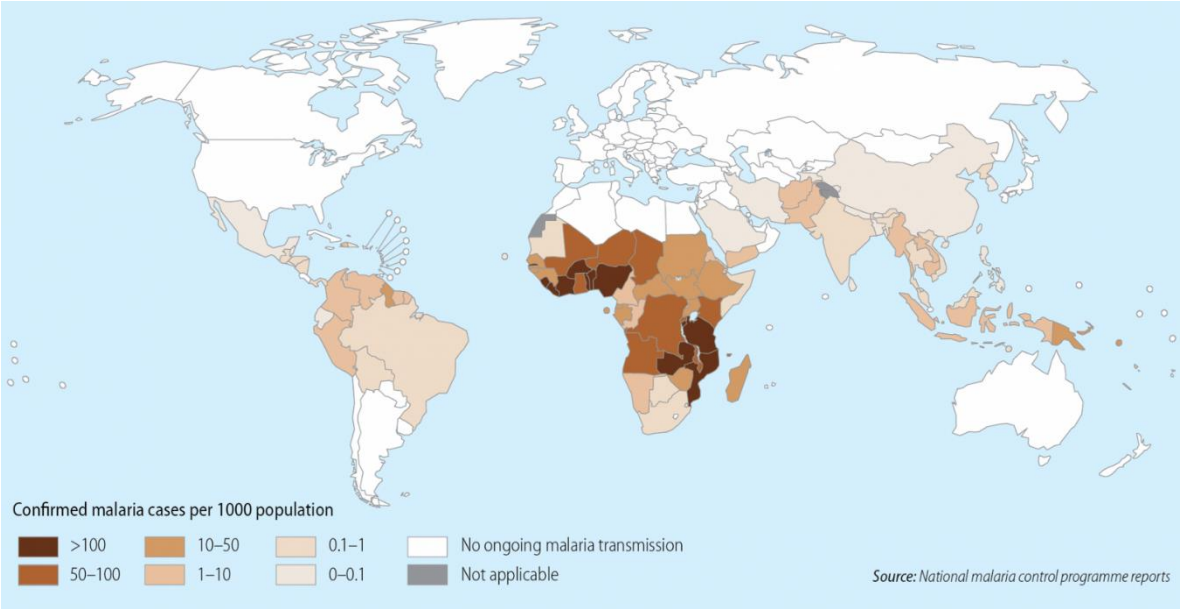

Figure 1- Countries with ongoing malaria transmission. Adapted from World Health Organization, 2014.

2. Vectors

The transmission of parasites responsible for malaria is restricted to female mosquitoes from the genus *Anopheles*. Not all anopheline mosquitoes can act as human malaria vectors. From all the 450 species of the genus *Anopheles*, only 60 are capable of transmitting the parasite to humans, although at different levels of concern to public health (Sylvie *et al.,* 2008). Despite living in sympatry, the endemicity of a region is maintained by a single *Anopheles* specie, called dominant vector (Sinka *et al.,* 2012).

Besides being outnumbered, dominant species have higher vectorial capacity, which is governed by intrinsic (genetic factors) and extrinsic factors. With the recent sequencing of the genome of

several anopheline mosquitoes, including some major malaria vectors such as *Anopheles gambiae,* it was possible to understand some of the genetic determinants of mosquito competence (Holt *et al.,* 2002). In particular, many biological traits of mosquitoes, concerning their morphology, physiology and behaviour, influence their vectorial capacity. Some examples of those traits are reproduction, host identification and preference, blood-feeding behaviours, resistance to insecticides and immunity (Neafsey *et al.,* 2015). Concerning the non-genetic influences on the vectorial capacity of mosquitoes, it is possible to highlight the climatic factors, diet, gut microbiota, infection history, maternal effects and immune priming (Lefèvre *et al.,* 2013). Among them, climatic factors (and especially temperature) are particularly important because not only have an impact in vector competence by influencing the mosquito development and parasite viability, but also dictate the geographical distribution of dominant vectors and consequently, parasites biodiversity (Kiszewskl *et al.*, 2004; Autino *et al.,* 2012).

3. Parasites

a. *Plasmodium* phylogeny

Plasmodium are obligate intracellular parasites that belong to the phylum Apicomplexa, a large phylogenetic group of unicellular protozoans. Besides *Plasmodium,* this phylum includes other genera of parasites with marked impact on public health affecting cattle or humans, such as *Babesia* (Brayton *et al.,* 2007), *Toxoplasma* (Montoya & Liesenfeld 2004), *Theileria* (Gardner *et al.,* 2005; Pain *et al.,* 2005) and *Cryptosporidium* (Abrahamsen *et al.,* 2004) (Fig.2).

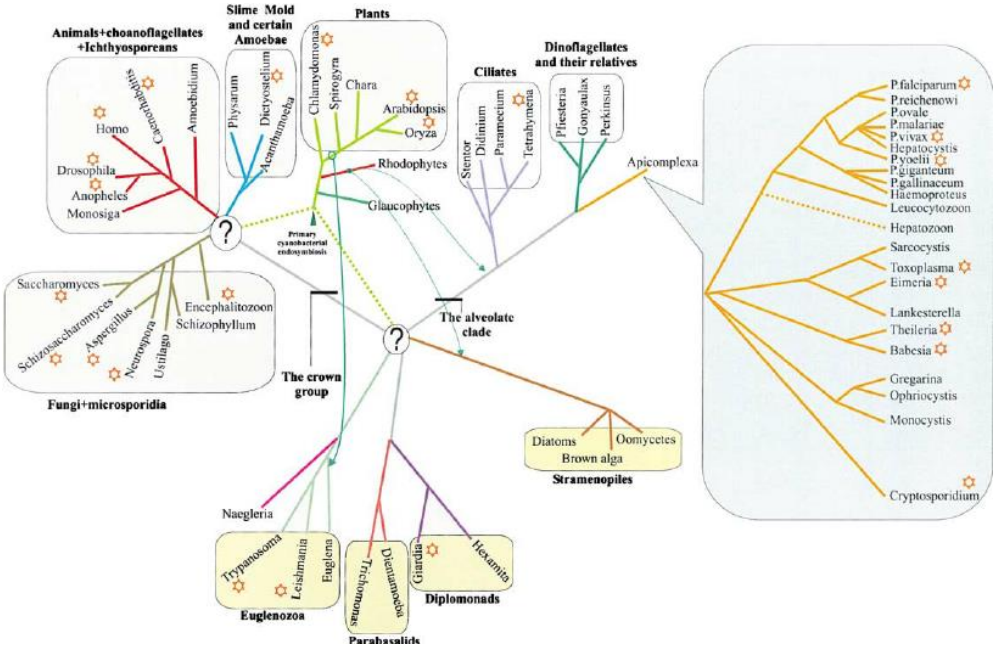

Figure 2- Phylogenetic context of the genus *Plasmodium.* Adapted from Aravind et al., 2003.

There are more than 200 species of *Plasmodium*, capable to infect mammals, reptiles and birds (Ramasamy, 2014). Among them, only five can cause human malaria, namely *Plasmodium vivax*,

Plasmodium ovale, *Plasmodium malariae*, *Plasmodium knowlesi* and *Plasmodium falciparum*, being the latest the deadliest one (Oddoux *et al.,* 2011; World Health Organization, 2015a). The rodent malaria species *Plasmodium berghei* and *Plasmodium yoelii,* are also important since they are used as model of choice in *in vivo* experimental malaria research (Ménard *et al.,* 2013).

b. *Plasmodium* spp. life cycle

Despite requiring different hosts, the life cycle of mammalian *Plasmodium* species is very similar (Fig.3). Indeed, it can be divided into three main phases: the pre-erythrocytic (PE) phase, where there is an asymptomatic asexual multiplication of the parasite in the liver of the vertebrate host; the erythrocytic phase during which parasite asexual multiplication inside red blood cells leads to the symptoms and complications of malaria; and the mosquito phase characterized by sexual and asexual multiplications of the parasites turning the invertebrate host into a potential transmission vector. In brief, while having a blood meal, an infected female mosquito injects sporozoites in the skin of the mammalian host, which travel to the liver and invade hepatocytes. Inside them, parasites transform into spherical exoerythrocytic forms (EEFs), which subsequently undergo several rounds of nuclear division to generate thousands of red blood cells (RBCs) infective forms, called merozoites. Once mature, merozoites are released into the bloodstream inside merosomes. This pre-erythrocytic phase lasts about 2 and 7-10 days in rodents and humans, respectively (Kaiser *et al.,* 2003; Ménard *et al.,* 2013; Ferguson *et al.,* 2014). However, some parasite species can form hypnozoites, a latent form that remains dormant in the liver for weeks to years, until they reactivate and generate blood infective forms, termed relapse (Chamchod & Beier 2013). Inside erythrocytes, merozoites multiply again, developing through ring, throphozoite and schizont stages (Cowman & Crabb 2006). Each merozoite can generate up to 30 new infective merozoites, which are released into the bloodstream. This cyclic process is responsible for clinical manifestations of the disease and lasts nearly 24 and 48-72 hours in rodents and humans, respectively (Cowman & Crabb, 2006; Ménard *et al.,* 2013). However, a small proportion of parasites transforms into sexual stages termed gametocytes, which are ingested by a mosquito during a blood meal. In the mosquito midgut lumen, the female and male gametocytes egress from red blood cells into non-motile macro and highly motile flagella-like microgametes, respectively (Matuschewski, 2006). The sexual reproduction occurs giving rise to a motile zygote, called ookinete that invades the epithelial layer of the mosquito midgut to reach the basal lamina and where it starts to transform into an oocyst. The oocyst undergoes several mitotic divisions, forming sporoblasts containing thousands of sporozoites. After 10 to 14 days of maturation, sporozoites egress from the sporoblast and enter in the mosquito circulatory system, the hemolymph (Siden-Kiamos & Louis 2004; Matuschewski, 2006). In the last step of their journey in the vector, sporozoites invade the salivary glands, completing their maturation and being ready for transmission into a new mammalian host (Ménard *et al.,* 2013; Ferguson *et al.,* 2014).

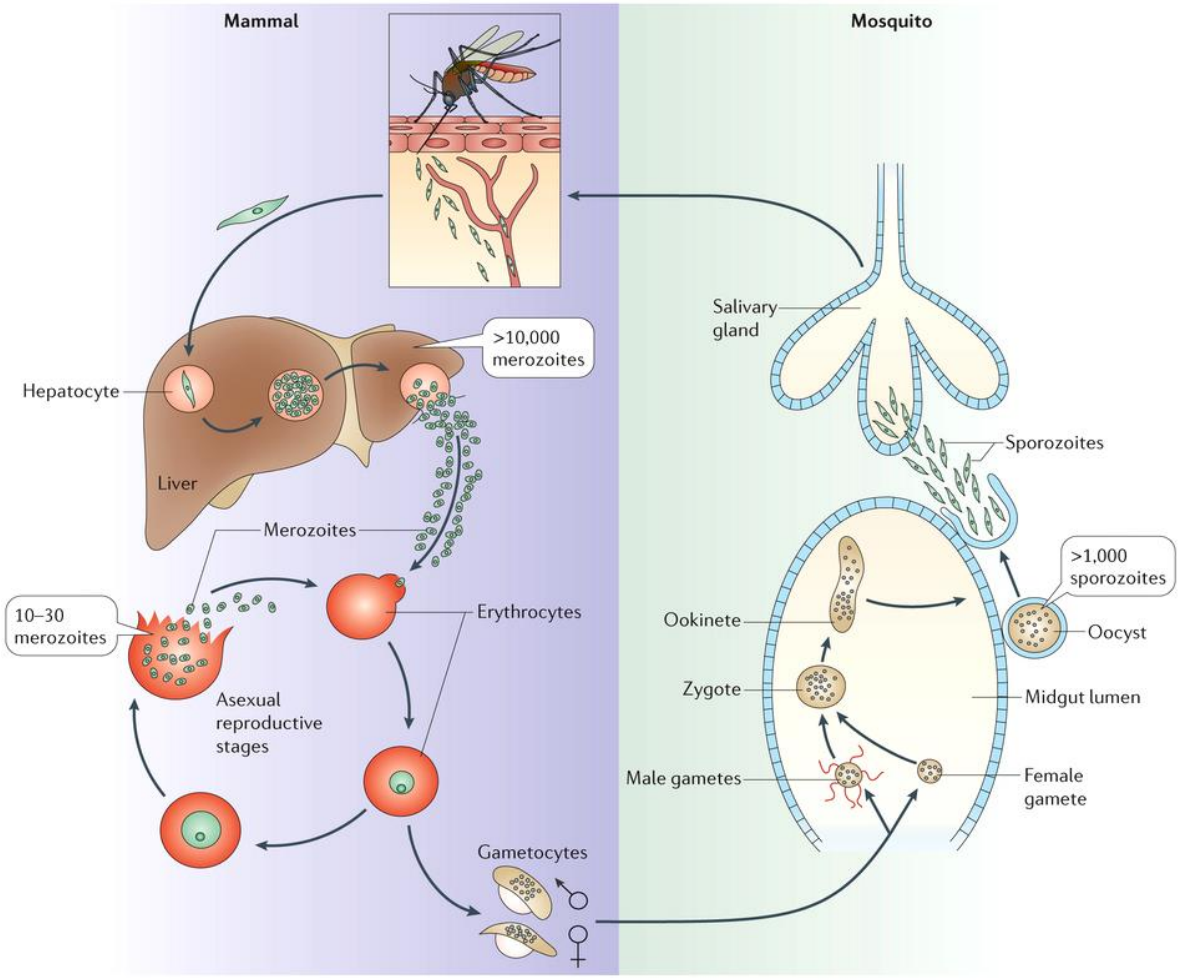

Figure 3- The life cycle of mammalian *Plasmodium* species. *Plasmodium* sporozoites are inoculated in the skin of the mammalian host through the bite of an infected anopheline female mosquito. Once in the skin, sporozoites enter the bloodstream and rapidly target the liver invading hepatocytes. Inside these cells, they undergo schizogony and generate thousands of merozoites, which are released into the bloodstream inside merosomes. Merozoites initiate repetitive cycles of asexual replication inside red blood cells. These cycles are responsible for malaria symptoms and complications. Meanwhile, some parasites transform into gametocytes, which are ingested by a mosquito during a blood meal. Inside the mosquito, parasites initially suffer sexual replication and then undergo sporogony, which results in the release of thousands of sporozoites into the mosquito hemocoel. Finally, sporozoites target the mosquito salivary glands and invade those structures. Infectious sporozoites can be transmitted to a new host during a mosquito blood meal, completing the cycle. Adapted from Ménard *et al.,* 2013.

4. Disease control

By applying strategies such as vector control, chemoprevention and case management, it was possible between 2000 and 2015 to decrease the global malaria incidence and mortality rates among children under five years of age by 37% and 65%, respectively. The most astonishing accomplishments were related to the decrease of malaria burden in Africa, since it was possible to reduce the incidence of the disease by 42% and the mortality rates in young children by 71% over the past fifteen years (World Health Organization, 2015a).

a. Vector control

Vector control has been particularly useful to reduce the malaria morbidity and mortality (World Health Organization, 2015a). The two core measures of this strategy were long-lasting insecticidal nets (LLINs) and indoor residual spraying (IRS). Whereas IRS relies only in the susceptibility of vector to insecticides, LLINs have the advantage of providing a physical barrier between mosquitoes and humans (World Health Organization 2016a). These measures can be supplemented with larval source control to reduce malaria vectors population, by modifying the natural habitat of mosquitoes, treating the mosquitoes breeding areas with larvicidal compounds and applying biological control measures (World Health Organization, 2015a).

b. Chemotherapy

Another effective strategy used in malaria control is the chemoprotection of pregnant woman and young children. The three main treatment strategies widely used in the field are: intermittent preventive treatment in pregnancy (IPTp), seasonal malaria chemoprevention (SMC) and intermittent preventive treatment in infants (IPTi). All these measures cannot be effective without a proper case management in the field, which involves the rapid detection, diagnose and treatment of ill people. Malaria diagnosis can be divided in two main categories: suspected malaria and parasitological diagnosis. The diagnosis by suspected malaria is based on the observation and recognition of symptoms characteristics of malaria, such as fever. Since malaria symptoms are non-specific, this method is highly unreliable and usually leads to overtreatment. Thus, it is always necessary to confirm the suspected malaria using other methods that rely on the direct or indirect detection of malaria parasites, such for example by microscopic analysis of Giemsa or Fields's blood smears or using rapid diagnostic tests (Moody & Chiodini, 2000; World Health Organization, 2015b). The treatment of malaria depends on the clinic picture of the patient, which can be classified in severe or uncomplicated malaria (World Health Organization, 2015b). To treat uncomplicated malaria, the World Health Organization (WHO) recommends the use of artemisinin-based combination therapy (ACT), i.e. a combination of an artemisinin derivate with another long-lasting drug with a distinct mode of action. Additionally, patients infected with *P. vivax* are treated with primaquine in order to prevent relapses (World Health Organization, 2015b). In contrast, the treatment for severe *P. falciparum* malaria is composed by an initial parenteral (or rectal) administration of an antimalarial drug, such as artesunate, following oral administration of an ACT (World Health Organization, 2015b).

c. Vaccines

Even after decades of study, there is still no approved human vaccine for malaria. The most advanced vaccine at the moment it the RTS,S/AS01 that is now under phase IV pharmacovigilance studies and under regulatory review for paediatric use (World Health Organization, 2016b). The RTS, S is a subunit vaccine that is composed of 16 tandem repeats of the immunodominant epitope of the *P. falciparum* circumsporozoite protein (CSP) together with the protein's C-terminus fused to the pre-S2 region of the hepatitis B virus (HBV) surface antigen. The hybrid protein self-assembles into virus-like

particles similar to native HBV surface antigen, with exposure of the CSP epitopes. The current formulation includes adjuvant AS01 that is a mixture of 3-deacylated monophosphoryl lipid A (MPL) and the saponin QS21 in a liposome formulation. This vaccine is able to protect infants against uncomplicated malaria by 27% to 39% and decrease the incidence of severe malaria by 31.5% (The RTS,S Clinical Trials Partnership, 2014). Vaccine efficacy is strictly correlated with the anti-CSP antibodies titres and their decay over time is correlated with the loss of RTS,S-induced immune responses (White *et al.,* 2015). Despite conferring moderate protection against severe and clinical malaria the vaccine fails short of the goals established for preventing disease and eradicating the parasite.

d. Current challenges

Despite the greatest advances towards malaria control and eradication, the scientific community is now facing some important challenges. One of the most concerning issue is the crescent reported cases of *P. vivax* malaria worldwide (World Health Organization, 2015a). *P. vivax* malaria may be particularly challenging in terms of vector control, diagnostic and treatment. *P. vivax* parasites can undergo sporogony at lower temperatures than *P. falciparum*, meaning that parasites can survive in vectors at higher latitudes. Additionally, 95% of *P. vivax* infections occurs outside Africa, in regions were primary vectors have a higher zoophilic feeding-behaviour, i.e. their prefer to feed on other animals rather than humans, meaning that the control of *P. vivax* parasites transmission is harder to achieve using LLINs and IRS (KiszewskI *et al.,* 2004; World Health Organization, 2015a). Moreover, as patients infected with *P. vivax* develop lower levels of parasitaemia compared to those infected with *P. falciparum*, the detection of *P. vivax* infections can be easily missed using the conventional methods for malaria diagnosis (Gething *et al.,* 2012; World Health Organization, 2015a). Besides that, there is no effective method to detect hypnozoites, which can cause debilitating effects to patients during chronic relapses, such as severe anaemia (Anstey *et al.,* 2012). These latent hepatic forms can only be treated with long-term primaquine, which is linked to high levels of morbidity and mortality in patients with severe forms of glucose-6-phosphate dehydrogenase (G6PD) deficiency (Baird, 2015; World Health Organization, 2015b).

e. Resistances

Antimalarial drug resistance on *Plasmodium* parasites has been a concerning issue for decades, since *P. falciparum* gained resistance to chloroquine. This drug was discovered in the 1940s and integrated in global malaria control and eradication programs a decade later. However, the efforts to eradicate malaria were severely hampered by the emerging of chloroquine-resistant parasites (Payne, 1987). Consequently, patients with *P. falciparum* malaria started to be treated with sulfadoxine-pyrimethamine, which resulted to the rapidly acquisition of resistance to this drug by parasites (Clyde & Shute 1957; Nair *et al.,* 2003; Roper *et al.,* 2003). Thus, this harsh scenario resultant from the use of antimalarial drugs as monotherapies led to the current use of ATC as the first-line treatment for *P. falciparum* malaria (Antony & Parija, 2016). However, despite the actual high effectiveness of the treatment, *P. falciparum* resistance to artemisinin was already reported in 5 countries of the Greater

Mekong Subregion (Cambodia, Lao People's Democratic Republic, Myanmar, Thailand and Vietnam) (Ashley *et al.,* 2014; World Health Organization, 2015a).

As parasites gained resistance to antimalarial drugs, mosquitoes are also developing resistances to insecticides used in vector control. Indeed, there is an increase spread of resistance to pyrethroids, the most used class of insecticides in malaria vector control, being used in all LLINs (Hemingway, 2014). Despite the overuse of pyrethroids, which contributed to disseminate resistances in all major malaria vectors, including the *P. falciparum* vectors such *A. gambiae* and *Anopheles funestus,* LLINs remain effective for now (Ranson *et al.,* 2011; Riveron *et al.,* 2013; World Health Organization, 2015a).

Section II - Biology of *Plasmodium* sporozoites

As obligate intracellular parasites, apicomplexan must invade host cells at one or more steps in their life cycle. To do this, parasites transform into specialized extracellular stages, usually called "zoites" (Ménard, 2001). In the mammalian host, the *Plasmodium* zoites suffer drastic morphologic transformations during their life cycle, varying between the banana-shaped sporozoites and the round-shaped merozoites (Bannister *et al.,* 2000). These alterations are extremely relevant in the journey of parasites inside the host, providing to zoites the capacity to invade and colonize different tissues (Morrissette & Sibley, 2002).

Among the several types of *Plasmodium* zoites, sporozoites have a unique capacity to become invasive twice in their lifetime (Sultan, 1999). Similarly to other apicomplexan parasites, *Plasmodium* sporozoites are elongated and polarized cells, 5 to 15 µm long and 2 to 5 µm wide (Levine, 1973) (Fig.4). Sporozoites are limited by the pellicle that continuously interacts with a set of cytoskeleton elements, such as actin, myosin and intermediate-like proteins. Specifically, the pellicle is composed by the plasma membrane along with an underlying platform of one or more flattened vesicles (alveolar membranes), interrupted at both anterior and posterior pole of the parasite. The alveolar membranes along with the cytoskeleton comprise the inner membrane complex (IMC) of the sporozoite (Morrissette & Sibley, 2002). Another important structure is the apical complex, a set of specialized organelles located at their apical pole, which includes the rhoptries, the micronemes and the apical polar ring. The rhoptries and the micronemes are two crucial secretory organelles essential for motility, cell traversal, adhesion and invasion of the host cells (Morrissette & Sibley, 2002; Ishino *et al.,* 2004). Moreover, the apical polar ring is one of the three microtubule-organizing centres (MTOCs) of sporozoites, being the other two the spindle pole plaques and centrioles bodies (Sinden 1978; Chobotar & Scholtyseck, 1982). This highly organized structure determine the number and orientation of subpellicular microtubules, which in turn provide the rigidity, cell shape and apical polarity to sporozoites (Russell & Burns, 1984; Nichols & Chiappino, 1987; Stokkermans *et al.,* 1996; Morrissette & Sibley, 2002). Sporozoites also have dense granules, likely involved in the invasion of host cells and an apicoplast, an essential non-photosynthetic plastid which participate in the synthesis of fatty acids, isoprenoids and heme (Mercier *et al.,* 2005; Mizushima & Sahani, 2014).

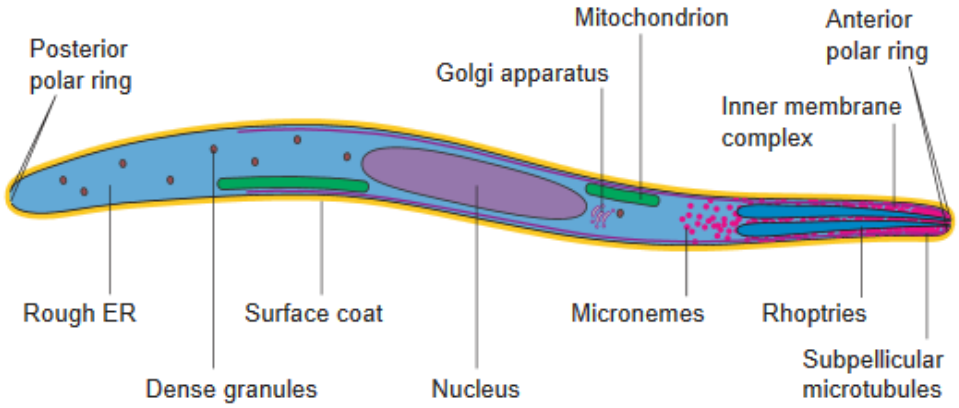

Figure 4- The *Plasmodium* sporozoite. As other apicomplexan parasites, the hallmarks of sporozoites include the apical complex, the inner membrane complex (IMC), dense granules and the apicoplast (not represented). The apical complex includes the polar ring and two secretory organelles, the micronemes and rhoptries. Whereas the rhoptries are teardrop-shaped organelles, whose ducts opens to the apical end of the parasite, micronemes are small and round structures dispersed in the cytoplasm of sporozoites (Jayabalasingham *et al.,* 2010). Another important feature is their IMC composed by the alveolar membranes and the parasite cytoskeleton. Dense granules are small microspheres of approximately 200 nm that act as secretory organelles during host cell invasion (Mercier *et al.*, 2005). Adapted from Frevert, 2004**.**

1. Gliding motility

Although they do not have cilia or flagella, sporozoites are highly motile. They have a substrate-dependent type of locomotion, called gliding motility, characterized by the absence of morphological distortion and locomotory organelles (Heintzelman, 2015). Instead, their motility is powered by an actin-myosin motor anchored to the IMC and regulated by calcium-dependent mechanisms (Ménard, 2001; Carey *et al.,* 2014; Harding & Meissner, 2014).

Three conditions are necessary for a successful locomotion, namely, i) the formation of transient contact points between the substrate and the adhesive molecules present at the parasite surface; ii) a molecular bridge linking the adhesins to the motor apparatus and iii) the anchorage of the motor internally, in order to generate mechanical force that push the parasite forward on the substrate (Heintzelman, 2015). Münter and colleagues in 2009 described the sporozoite gliding motility as “an alternating sequence of periods of run and firm adhesion”. In fact, it was demonstrated that sporozoite gliding relies on repetitive cycles of adhesion and posterior deadhesion to the substrate, generating sufficient tension to the parasite slip onwards (Münter *et al.,* 2009). *Plasmodium* sporozoites can move at a maximum speed of 4 µm per second and their gliding pattern can vary between a circular and a corkscrew-like motion in a 2D and 3D matrix, respectively (Amino *et al.,* 2008; Kudryashev *et al.,* 2012; Heintzelman, 2015).

After many years of research, it was possible to understand (at least in part) how the glideosome works and which its molecular components are. Indeed, whereas the mechanistic components of the motor are conserved among Apicomplexa parasites, the adhesive molecules are specie and stage-specific, allowing the parasite interaction with different host cells and tissues (Morahan *et al.,* 2009).

At the moment three proteins linking the host receptors to the motor apparatus were described, namely the thrombospondin-related adhesion protein (TRAP) (Sultan *et al.,* 1997; Kappe *et al.,* 1999), TRAP-like protein (TLP) (Heiss *et al.,* 2008) and TRAP-related protein (TREP) (Combe *et al.,* 2009). Actin and myosin A (MyoA) molecules are the core components of the glideosome, since myosins can convert the chemical energy of adenosine triphosphate (ATP) into mechanical energy and pull the actin filaments, propelling the parasite forwards (Boucher & Bosch, 2015; Heintzelman, 2015).

Interestingly, a potential role of CSP in sporozoites gliding motility was proposed in late 1980s, after seeing that antibodies against this protein rendered parasites non-motile (Stewart *et al.,* 1986). Despite not being associated with the glideosome, CSP is one of the most abundant proteins expressed on the sporozoite surface (Swearingen *et al.,* 2016). In fact, it was later proposed that CSP may provide the substrate-binding sites required for gliding motility because once released from the apical end of the sporozoite, it forms adhesion patches with the substrate and is translocated along the surface of the sporozoite towards the posterior pole before being shed on the substrate (Stewart & Vanderberg, 1988, 1991; Sultan *et al.,* 1997).

2. Host cell traversal

Besides gliding on a solid surface, sporozoites can also disrupt the host cells plasma membrane, glide through their cytosol and exit from it (Mota *et al.,* 2001). This migratory behaviour was observed in several cell types, such macrophages, epithelial cells, fibroblasts, and hepatocytes, indicating that cell-type specificity apparently does not seem to exist (Vanderberg *et al.,* 1990; Mota *et al.,* 2001; Amino *et al.,* 2008; Hamaoka & Ghosh, 2014). Regarding the fate of traversed cells, some can reseal their membrane integrity while others don't (Mota *et al.,* 2001; Tavares *et al.,* 2013; Formaglio *et al.,* 2014; Hamaoka & Ghosh, 2014). Many years of research using reverse genetics led to the identification of parasite molecules important for sporozoite cell traversal (CT), such as the sporozoite microneme proteins essential for cell traversal (SPECT) and SPECT2 (Ishino *et al.,* 2004, 2005a), a surface phospholipase (PL) (Bhanot *et al.,* 2005), TLP (Moreira *et al.,* 2008), the gamete egress and sporozoite traversal (GEST) (Talman *et al.,* 2011) and cell-traversal protein for ookinetes and sporozoites (CelTOS) (Kariu *et al.,* 2006). Interestingly, it seems to exist a dichotomy among the proteins necessary for gliding motility and cell traversal. Whereas proteins associated with sporozoite gliding motility have adhesion properties, those associated with cell traversal possess membrane-lytic activity capable to disrupt the host cell membrane (Lacroix & Ménard, 2008). This behaviour seems to be important for the progression of sporozoites in different host tissues and to avoid parasite clearance by phagocytic cells (Amino *et al.,* 2008; Tavares *et al.,* 2013). However, it remains to be elucidated whether sporozoites CT contribute to host cell tolerance or immunity to parasite antigens and to the stimulation of anti-inflammatory mediators from traversed cells (Tavares *et al.,* 2013). The role of CT in the pre-erythrocytic stage will be addressed in more detail on section III. Moreover, it was recently reported that sporozoites can migrate through host cells within a non-replicative vacuole, named transient vacuole (TV). Indeed, sporozoites enter the cells inside of a TV and exit from it using pH sensing and SPECT2-dependent mechanism (Risco-Castillo *et al.,* 2015).

3. Host cell invasion

During host cell invasion, sporozoites enter in host cells inside a parasitophorous vacuole (PV). Initially, a tight connection is formed between the sporozoite and the host cell, called tight junction (TJ) (Besteiro *et al.,* 2011). This interaction starts at the apical pole of the sporozoite and subsequently moves to the posterior pole, surrounding the whole parasite as it enters the cell (Besteiro *et al.,* 2011). The establishment of the TJ benefits the sporozoite in several ways; besides assisting the parasite entrance into the PV, the TJ is also involved in the vacuole biogenesis, i.e. participate in the selection of the biochemical components of the vacuole membrane (Besteiro *et al.,* 2011). Interestingly, sporozoites remodel the PV membrane in order to exclude components of the host plasma membrane, and thus avoiding degradation by the host lysosomal system (Zheng *et al.,* 2014; Risco-Castillo *et al.,* 2015). After their entrance, sporozoites establish themselves in the host cell cytoplasm and multiply inside the PV (Ménard *et al.,* 2013).

Section III - The *Plasmodium* pre-erythrocytic phase

1. The skin phase

While taking a blood meal, the mosquito puncture directly a blood vessel or ingest blood from hematomas, which are small blood pools created during the blood feeding probing phase, i.e. when the mosquito probes the host skin for blood with it mouthpart stylets while injecting saliva (Clements, 1992; Jin *et al.,* 2007). Importantly, it is during this phase that sporozoites are transmitted to the mammalian host (Sidjanski & Vanderberg, 1997; Matsuoka *et al.,* 2002; Vanderberg & Frevert, 2004; Medica & Sinnis, 2005; Amino *et al.,* 2006; Yamauchi *et al.,* 2007). However, rather than being injected directly in the blood vessels, sporozoites are inoculated in the avascular area of the skin (in dermis and epidermis), subcutaneous tissue and even in muscle (Vanderberg & Frevert, 2004; Jin *et al.,* 2007). The size of the parasite inoculum delivered to the mammalian host is very small, usually not exceeding some dozens of sporozoites (Amino *et al.,* 2006). This phenomenon can be explained by several determinants. For example, despite the large number of sporozoites capable to colonize the mosquito salivary glands, just a small portion are free and yet a lower fraction are motile. Only this fraction, termed releasable pool, can colonize the mosquito salivary ducts and thus be transmitted to the new host. Additionally, it was also demonstrated that sporozoites are re-ingested when the mosquito starts to ingest host blood (Frischknecht *et al.,* 2004; Kebaier & Vanderberg, 2006).

After being injected at a rate of 1 to 2.5 parasites per second, the majority of sporozoites exhibit forward gliding motility at rate of 1 to 2 µm per second, following a tortuous path (Amino *et al.,* 2006; Jin *et al.,* 2007). Then, these highly motile sporozoites face a tripartite fate (Fig.5). Based on time-lapse microscopic analysis of *P. berghei* sporozoites, it was verified that in 1 hour, approximately 50% of them leave the bite site by invading actively blood (≈ 70%) or lymphatic vessels (≈ 30%), while the other part remain in the bite site (Amino *et al.,* 2006). In the “lymphatic pathway”, sporozoites are drained to the proximal lymph node (LN) where the vast majority are captured by dendritic cells (DC).

Despite some can transform into EEFs inside podoplanin-expressing cells those are unable to complete their development (Amino *et al.,* 2006; Ménard *et al.,* 2013). Regarding the sporozoites that remain in the bite site some can also develop into EEFs inside a PV in dermal and epidermal cells, as well as in association with hair follicles. In contrast to lymphatic EEFs, these can induce detachable merosome-like extensions in host cells full of infective merozoites. Surprisingly, it was observed that EEFs associated with hair follicles can be detected during several weeks. This maintenance of parasites viability is probably due to the presence of an immunosuppressed environment characterized by the absence of major histocompatibility complex (MHC) class I molecules in these immunoprivileged sites (Gueirard *et al.,* 2010).

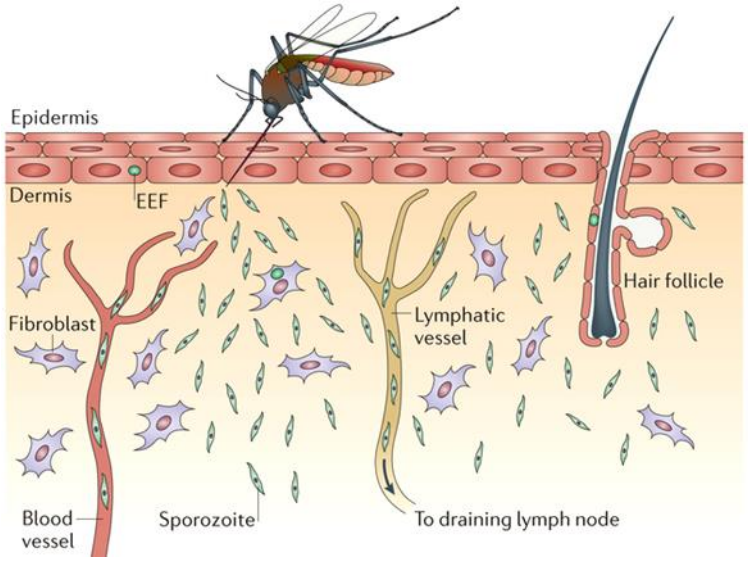

Figure 5- The tripartite fate of *Plasmodium* sporozoites in the skin of the mammalian host. After being inoculated, sporozoites may cross the endothelial barrier of blood or lymphatic vessels or remain in the skin, near the bite site. Only the sporozoites that invade blood vessels reach the liver. Adapted from Ménard *et al.,* 2013.

The role of CT in the skin phase started to be depicted some years ago, when the fate of *P. berghei spect* and *spect2* knockout (KO) sporozoites, which have a severe defect in cell traversal but not in gliding motility, was imaged in the skin of mice (Ishino *et al.,* 2004, 2005a; Amino *et al.,* 2008). After the observation that subcutaneous injected mutant sporozoites were less infectious to mice compared to mutant sporozoites injected intravenously, it was suggested that CT would have a role in the sporozoite passage through the host skin. In fact, the majority of mutant sporozoites was found to be immotile after being inoculated in the skin, contrasting with the highly motile wild-type (wt) parasites. Using advanced microscopic techniques, it was discovered that CT-defective sporozoites were rapidly immobilized in the host skin by leukocytes and that were highly associated with dermal fibroblasts. In contrast, it was not found any defect in their ability to actively cross either blood or lymphatic vessels. Thus, it seems that the major role of sporozoite CT is to avoid parasite clearance by phagocytic cells and allow the free movement of sporozoites in the dermis, avoiding non-specific

invasion events (e.g. invasion of fibroblasts), until sporozoite entry in the host circulatory system (Amino *et al.,* 2008).

The consequences of *Plasmodium* skin phase in the host immune system cannot be ignored. In rodent malaria models, the skin draining LN receives about 70% of the parasite antigens inoculated by the mosquito, i.e. antigens of dead lymphatic and skin sporozoites, and importantly, antigens of abortive EEFs. This antigenic drainage occurs in an important immunogenic context, in contrast to what occurs in the liver, where a strong immunotolerant environment prevails (Gueirard *et al.,* 2010; Protzer *et al.,* 2012). Indeed, $CD8^+$ T-cells activated inside LN are major players in the fight against liver stage malaria, since they act against infected hepatocytes that present parasite antigens through their MHC complex (Chakravarty *et al.,* 2007). Furthermore, it also known that the mosquito saliva is capable to trigger the mouse immune system *per se* since it causes mast cell degranulation, which induces the recruitment of antigen-presenting cells (APC) to the bite site. In addition, this recruitment is followed by the relocation of APC to the host lymph nodes, contributing to the host T and B lymphocyte priming (Demeure *et al.,* 2005). This phase may also be clinically important, since hair follicles may constitute a small niche for *Plasmodium* erythrocytic infective forms that can eventually lead to malaria recurrences in mammals (Gueirard *et al.*, 2010). The natural contribution of skin derived merozoites in the establishment of a blood-stage infection is hard to access as eliminating hepatic EEFs contribution is experimentally challenging (Gueirard *et al.,* 2010). However, by using mutant *P. berghei* sporozoites unable to exit the inoculation site, it was demonstrated that skin EEFs can, in fact, induce blood-stage infection (Coppi *et al.,* 2011).

2. The liver phase

The liver is a complex organ composed by several types of cells, such as hepatocytes, endothelial cells (EC), macrophages and hepatic stellate cells (SC). The hepatocytes are spatially arranged in cords separated by the liver sinusoids, which in turn are lined by a unique epithelium, composed by fenestrated EC. In addition, the sinusoids are surrounded by resident macrophages, called Kupffer cells (KC), which are mainly anchored to the endothelial walls and form cytoplasmic extensions capable to penetrate the gaps between adjacent EC. Between the liver sinusoids and hepatocytes, exists a perisinusoidal compartment, called space of Disse, composed by plasma and connective tissue (Motta, 1984; Senoo, 2004; Ishibashi *et al.,* 2009; Krishna, 2013).

Once inside the host bloodstream, sporozoites only take a few minutes to reach the liver, suggesting that a very specific recognition event takes place between parasite molecules and liver cells (Frevert *et al.,* 2005). Although studied for decades, the molecular basis of this phenomenon is still debatable since it is mostly based on indirect and/or *in vitro* experiments. It has been proposed that CSP mediates the targeting of sporozoites to the liver. This protein has a conserved structure that comprises the signal peptide, a central repetitive domain and a C-terminal hydrophobic sequence (McCutchan *et al.,* 1996). The CSP from different *Plasmodium* species share conserved domains flanking the repetitive region, such as the Region I, composed by the pentapeptide KLKQP at the N

terminus and the cell adhesive motif termed thrombospondin repeat type I (TSR) at C terminus (Adams & Tucker, 2000).

Several studies demonstrated that CSP can bind to heparan sulphate proteoglycans (HSPGs) present on the surface of hepatocytes (Cerami *et al.,* 1992; Frevert *et al.,* 1993; Sinnis *et al.,* 1994). However, the protein domains responsible for this interaction are a debated issue: whereas some studies demonstrated that the TSR domain was mediating this interaction (Cerami *et al.,* 1992; Frevert *et al.,* 1993; Sinnis *et al.,* 1994), others found that a charged motif in the N-terminal region of CSP, upstream from the Region I, was involved (Aley *et al.,* 1986; Suarez *et al.,* 2001; Rathore *et al.,* 2002). Despite being expressed by the majority of mammalian cells, the glycosaminoglycan chains (GAGs) of HSPGs structure are amenable to chemical alterations that lead to a substantial level of structural heterogeneity among them. Sporozoites exploit this phenomenon and preferentially interact with highly sulphated GAGs, expressed mostly by SC, hepatocytes and KC (Lyon *et al.,* 1994; Ying *et al.,* 1997; Pradel *et al.,* 2004).

The precise underlying mechanism of CSP-HSPGs interaction started to be disclosed when it was observed that sporozoites stop migration and invade host cells upon contact with highly sulphated HSPGs. Specifically, the change in the sporozoite behaviour was concomitant with the proteolytic cleavage of CSP (within the Region I) by a papain family cysteine protease expressed by the parasite upon calcium dependent protein kinase (CDPK) 6 signalling (Coppi *el al.,* 2005, 2007). More recently, the same group demonstrated that CSP has two distinct conformational states in sporozoites (Coppi *et al.,* 2011). Indeed, they found that the C-terminus of the protein was exposed in oocysts sporozoites and masked in hemolymph or salivary glands sporozoites by the N-terminus. Moreover, the presence of highly sulphated HSPGs triggered the cleavage of CSP, exposing the TSR adhesive domain at C-terminal. In the light of these results, the model that explains sporozoites progression to the liver and consequently invasion of hepatocytes was proposed (Fig.6): i) during the journey of sporozoites from the mammalian host skin to the liver, the N-terminus of CSP is masking the adhesion domain TSR, conferring a migratory behaviour to sporozoites and preventing non-specific adhesion events; ii) upon contact with the highly sulphated HSPGs, CSP is cleaved within the Region I, exposing the cell-adhesive TSR domain; iii) without the N-terminal region of CSP, sporozoites are able to invade hepatocytes (Coppi *et al.,* 2011).

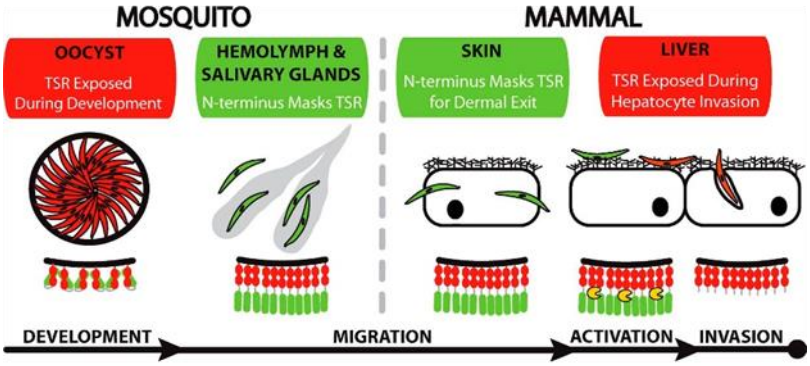

Figure 6- The two conformational states of CSP during the sporozoite journey from the mosquito oocyst to the liver. During sporozoite development inside the oocyst, the C-terminus (red) of CSP is exposed. Once released to the hemolymph, the C-terminus is masked by the N-terminus (green) allowing sporozoites to acquire a migratory behaviour until reaching the liver. Upon contact with liver HSPGs, CSP is cleaved by a protease (yellow) in the Region I near the tandem repeats (grey), exposing the C-terminal region of the protein. With the adhesive TSR domain exposed, sporozoites are activated to invade hepatocytes. Adapted from Coppi *et al.,* 2011.

After their arrest in the liver, sporozoites need to cross the endothelial barrier in order to reach the hepatocytes. The way that sporozoites manage to overcome this barrier has been a long debated issue. Initially, it was thought that these crossing events occurred solely *via* KC traversal, a hypothesis known as "the gateway model" (Frevert *et al.,* 2006). Since the first evidence that KC might act as portals for sporozoite passage was found in 1983 using transmission electron microscopy (TEM), numerous studies using cell biological, biochemical and microscopy data have been published supporting this hypothesis (Meis *et al.,* 1983, 1985; Vreden *et al.,* 1993; Pradel & Frevert, 2001; Pradel *et al.,* 2002; Ishino *et al.,* 2004, 2005a, 2005b; Frevert *et al.,* 2005; Baer *et al.,* 2007a). Recently, a new explanation for this phenomenon arose from an intravital imaging study performed by Tavares and colleagues in 2013. In this study, the dynamics of sporozoites in the liver sinusoids was imaged using fluorescent *P. berghei* parasites and transgenic mice capable of expressing green fluorescent protein (GFP) in EC. In addition, the KC of mice were immunolabeled and membrane impermeable dies used to visualize wounded cells. Unexpectedly, it was verified that the sporozoite crossing events can be classified by CT-dependent or CT-independent mechanisms. In fact, sporozoites mainly use the CT-machinery (≈77%) to reach the hepatocytes but contrary to the expectations, the majority of the events occurred via EC (≈53%) rather than KC. Concerning the CT-independent crossing events (≈23%), it was hypothesized that the sporozoites cross the sinusoidal walls by the paracellular pathway, i.e. passing between two EC or between an EC and KC, or by the transcellular pathway, i.e. passing through EC, by means of host cellular channels or fenestrations (Tavares *et al.,* 2013). The most important conclusion drawn from this study is that CT is not essential for sporozoites to reach the liver parenchyma. However, and similar to what was reported in the skin, this behaviour seems to play a role in avoiding the parasite clearance by phagocytic cells (Amino *et al.,* 2008). Indeed, the majority of CT-deficient sporozoites were trapped and killed by KC (Tavares *et al,.* 2013). Besides the dual role of CT in this phase, it may also affect the adaptive immunity of the host, since traversed cells are able to present antigens (Ebrahimkhani *et al.,* 2011), allowing the host to mount an immune response to sporozoites. However, this scenario may be hampered due to the fact that the majority of traversed KC cannot reseal their plasma membrane, ending up dying (Tavares *et al.,* 2013).

Once outside the bloodstream, sporozoite traverse several hepatocytes before invading and establishing in a final one (Mota *et al.,* 2001, 2002; Frevert *et al.,* 2005) (Fig.7). Researchers have long debated the role of hepatocyte traversal by sporozoites. Initially, it was suggested that this behaviour benefits the sporozoites, triggering their invasion mechanisms and rendering the surrounding hepatocytes susceptible to invasion (Mota *et al.,* 2002; Carrolo *et al.,* 2003; Leirião *et al.,* 2005). However, the normal infectivity of CT deficient sporozoites in KC-depleted animals unequivocally demonstrates that hepatocyte traversal is not mandatory to invasion (Ishino *et al.*, 2004).

Besides CSP, several other proteins have also been reported to mediate sporozoite infection of hepatocytes. According to reverse genetic studies, P36 and P36p seems to have a key role in this process (Ishino *et al.,* 2005b). Whereas *in vitro* studies shown that *p36* and *p36p* KO sporozoites have a defect in hepatocyte invasion and EEF development, their migratory behaviour through hepatocytes was enhanced compared to wt parasites, suggesting that these proteins are involved in commitment of sporozoite host cells invasion. Moreover, these proteins may also be involved in the hepatic development of parasites, since EEFs formed by mutant sporozoites could not develop beyond nuclear division (Ishino *et al.*, 2005b; van Dijk *et al.,* 2005). Furthermore, a recent study reported that the absence of the protein P113 in salivary glands sporozoites delays pre-patency (the time between sporozoite inoculation and detection of blood stage parasites) when parasites are transmitted to the mammalian host through the bite of infected mosquitoes. The expression of this protein is upregulated in infectious sporozoites and it seems to be related with the transformation of intracellular sporozoites into early liver stages, since it was revealed that *p113* KO parasites can adhere and infect normally hepatocytes, although producing a lower number of liver stage merozoites (Offeddu *et al.,* 2014). Finally, the thrombospondin-related sporozoite protein (TRSP), a TSR-containing protein mainly expressed in sporozoites, was also implicated in invasion of hepatocytes (Kaiser *et al.,* 2004; Labaied *et al.,* 2007). In the absence of this protein, sporozoites could not properly invade hepatocytes *in vitro* and were less infectious to mice compared to wt parasites (Labaied *et al.,* 2007). Another sporozoites protein required for host cell invasion is TRAP, which will be addressed in detail on section IV.

Besides the liver proteoglycans, a few host molecules were identified as receptors for the sporozoite adhesion and/or invasion of hepatocytes (Pradel *et al.,* 2004). It is known that the tetraspanin CD81 expressed on the hepatocytes surface is required for *P. yoelii* and *P. falciparum* infectivity (Silvie *et al.,* 2003). Indeed, *P. yoelii* failed to infect CD81 deficient hepatocytes *in vivo* and *in vitro*, contrary to *P. berghei* sporozoites, suggesting that CD81-dependent infection of hepatocytes may rely on a species-specific mechanism (Silvie *et al.,* 2003). Later, it was verified that CD81 act as a co-receptor along with the scavenger receptor BI (SR-BI), which also affects the intracellular development of sporozoites (Rodrigues *et al.*, 2008; Yalaoui *et al.,* 2008). More recently, it was verified that the EphA2 receptor expressed by hepatocytes interacts with the sporozoite protein P36, being necessary for the establishment of a functional PV by sporozoites during liver infection (Kaushansky *et al.,* 2015).

After invasion, parasite multiplies through schizogony in order to form thousands of merozoites, which eventually bud off into the sinusoidal lumen inside merosomes (Fig.7). After being released, these vesicle-like structures accumulate in the lungs, being capable of avoiding disintegration during their journey. As the merosomes membrane is from host origin, parasites can evade the host immune system, escaping from phagocytic attack by KC after being released from hepatocytes. Indeed, merosomes disintegrate only in the lung microvasculature, releasing 100 to 200 merozoites to the bloodstream and initiate the erythrocytic phase of the parasite's life cycle (Baer *et al.,* 2007b).

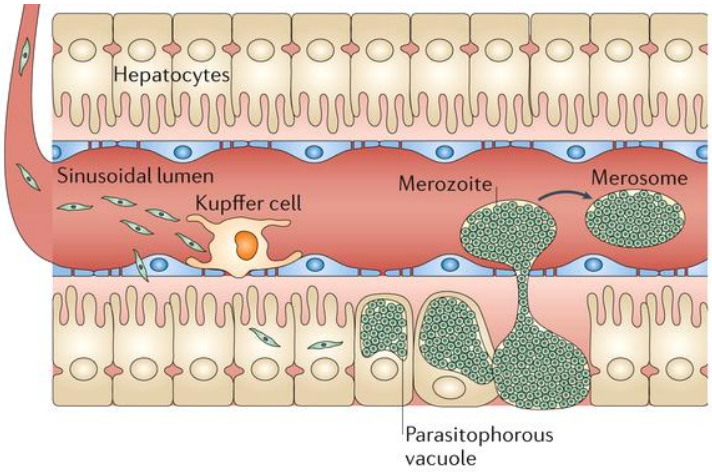

Figure 7- The sporozoite passage through the host liver. Once crossing the endothelial barrier of dermal capillaries, sporozoites enter into the bloodstream and rapidly arrest in the liver sinusoids. Sporozoites are able to cross the endothelial barrier using CT-dependent or independent mechanisms, reaching the liver parenchyma, in which they traverse several cells before invading a final one inside a PV. After schizogony, thousands of merozoites are formed and released in the host bloodstream inside merosomes. Adapted from Ménard *et al.,* 2013.

Section IV – Aims

At the moment, malaria is still a major public health problem worldwide. The poor efficacy of the most advanced malaria vaccine, along with the increasing reports of *P. vivax* malaria cases and antimalarial drug and insecticide resistances, renders the identification of new *Plasmodium* antigens for the development of vaccines a priority. The asymptomatic but metabolically active pre-erythrocytic phase of *Plasmodium* life cycle appears as an appealing vaccine target (Duffy *et al.,* 2012). This phase represents a bottleneck in the *Plasmodium* life cycle, characterized by the extremely low numbers of parasites in the mammalian host (Pimenta *et al.,* 2015). Furthermore, *P. falciparum* and *P. vivax* take almost a week to complete their development inside the liver, providing time to the host immune system to act (Mauduit *et al.,* 2009). Moreover, this phase is immunologically relevant, since sporozoites during their journey in the mammalian host traverse and invade cells expressing MHC class I molecules (Amino *et al.,* 2008; Duffy *et al.,* 2012; Tavares *et al.,* 2013).

The research proposal for this thesis was based on the work developed by the group in collaboration with Rogerio Amino team at Pasteur Institute in Paris aiming at identifying sporozoites molecules involved in crucial steps of the parasite journey in the mammalian and that could, eventually, be targeted by vaccine approaches. The specific homing of sporozoites to the liver is one of the crucial events that precedes liver infection and that the lab is interested into explore. As above mentioned, in the current model sporozoites target the liver due to the interaction of the major sporozoites surface protein, CSP, with proteoglycans expressed by liver cells (Pradel *et al.,* 2004; Coppi *et al.,* 2011).

Unpublished data from the lab shows that KC depletion in mice by i.v. injection of clodronate liposomes do not affect the sporozoites capacity to target or infect the liver (data not shown). The team developed an assay using whole mice live imaging and *P. berghei* bioluminescent sporozoites to quantify the percentage of bioluminescent signal in the liver immediately (7 minutes) after i.v. injection of parasites. Based on this assay around 70% of the total bioluminescent signal is detected in the liver when sporozoites from salivary glands are injected (Fig.8). The specificity of this arrest is given by the approximately 20% bioluminescent signal in the liver when merozoites prepared from blood schizonts are injected (data not shown). Surprisingly, sporozoites capacity to home to the liver increases with the progression of its journey in the mosquito. Indeed, homing to the liver increases from 24.5 ± 2.2% to 45.5 ± 0.4% to 67.4 ± 7.1% for sporozoites collected 19 days after mosquito infection respectively from midgut (MG), hemolymph (HEMO) and salivary glands (SG) (Fig.8A). Similarly, for sporozoites collected at day 23, homing to the liver increased from 26.7 ± 2.7% to 52.4 ± 3.9% to 74.0 ± 13.6% for sporozoites from MG, HEMO and SG (Fig.8A). These observations were unexpected since midgut sporozoites have the CSP adhesive domain exposed (Coppi *et al.,* 2011). A well-known difference between the MG and SG sporozoites is the gliding motility. To investigate the role of the gliding motility in the arrest of sporozoites in the sinusoids, parasites pre-incubated with cytochalasin D were allowed to glide on a glass slide and imaged on a fluorescent microscope. The projection of the several images clearly shows that sporozoites treated with cytochalasin D remain immotile at least during 15 minutes upon drug treatment (Fig.8B). Cytochalasin D treated sporozoites and DMSO treated sporozoites were injected intravenously in mice and their capacity to arrest in the liver quantified. No significant differences were found on the capacity of cytochalasin D treated sporozoites compared to control, to arrest in the liver (Fig.8B). However, a significant reduction in liver infection at 24 hours was detected in the mice infected with cytochalasin D treated sporozoites, evidencing a role for the motility on hepatocytes infection (Fig.8B). In order to better understand the parasite molecules mediating this phenomenon, potential candidates were selected based on a proteomic profiling of *P. falciparum* sporozoites collected either from the mosquito midgut or salivary glands (Lasonder *et al.,* 2008) by applying two consecutive filters: i) up-regulation in infectious sporozoites; ii) presence of a signal peptide, a transmembrane domain or a glycosylphosphatidylinositol (GPI) anchor in its structure. The TRAP molecule was among the selected candidates and importantly, TRAP knockout sporozoites were shown to be defective in the homing to the liver (Fig.8C).

The work developed in this thesis aimed to disclose the molecular mechanisms underlying the role of TRAP in mediating the arrest of sporozoites to the liver. Previous gene-targeting studies have shown that this protein is crucial for sporozoite motility and infectivity (Sultan *et al.,* 1997). This protein has two adhesive domains, a TSR domain and a von Willebrand factor A domain (VWA-domain), capable to bind proteoglycans expressed in liver cells, and an acidic cytoplasmic tail anchored to the sporozoite glideosome by the aldolase (Pradel *et al.,* 2002; Buscaglia *et al.,* 2003; Morahan *et al.,* 2009). Despite the data obtained using cytochalasin D-treated sporozoites suggests that the gliding motility is not involved in the homing, it was necessary to validate them using a

genetic approach, since the inhibitory effect of cytochalasin D is reversible (Schliwa, 1982). For that, we have engineered parasites to express TRAP without the cytoplasmic tail, since the deletion of this domain renders sporozoites incapable of gliding but do not alters the surface presentation of the protein (Kappe *et al.,* 1999). Similar to the phenotype of *trap* KO sporozoites, sporozoites expressing a truncated TRAP do not invade the mosquito salivary glands, therefore do not attain complete maturation remaining in the hemolymph (Kappe *et al.,* 1999). For that reason, *maebl* KO sporozoite were engineered as a control, since apical membrane antigen/erythrocyte binding-like (MAEBL) protein is required for sporozoite infection of mosquito salivary glands but dispensable for liver infection (Kariu *et al.,* 2002).

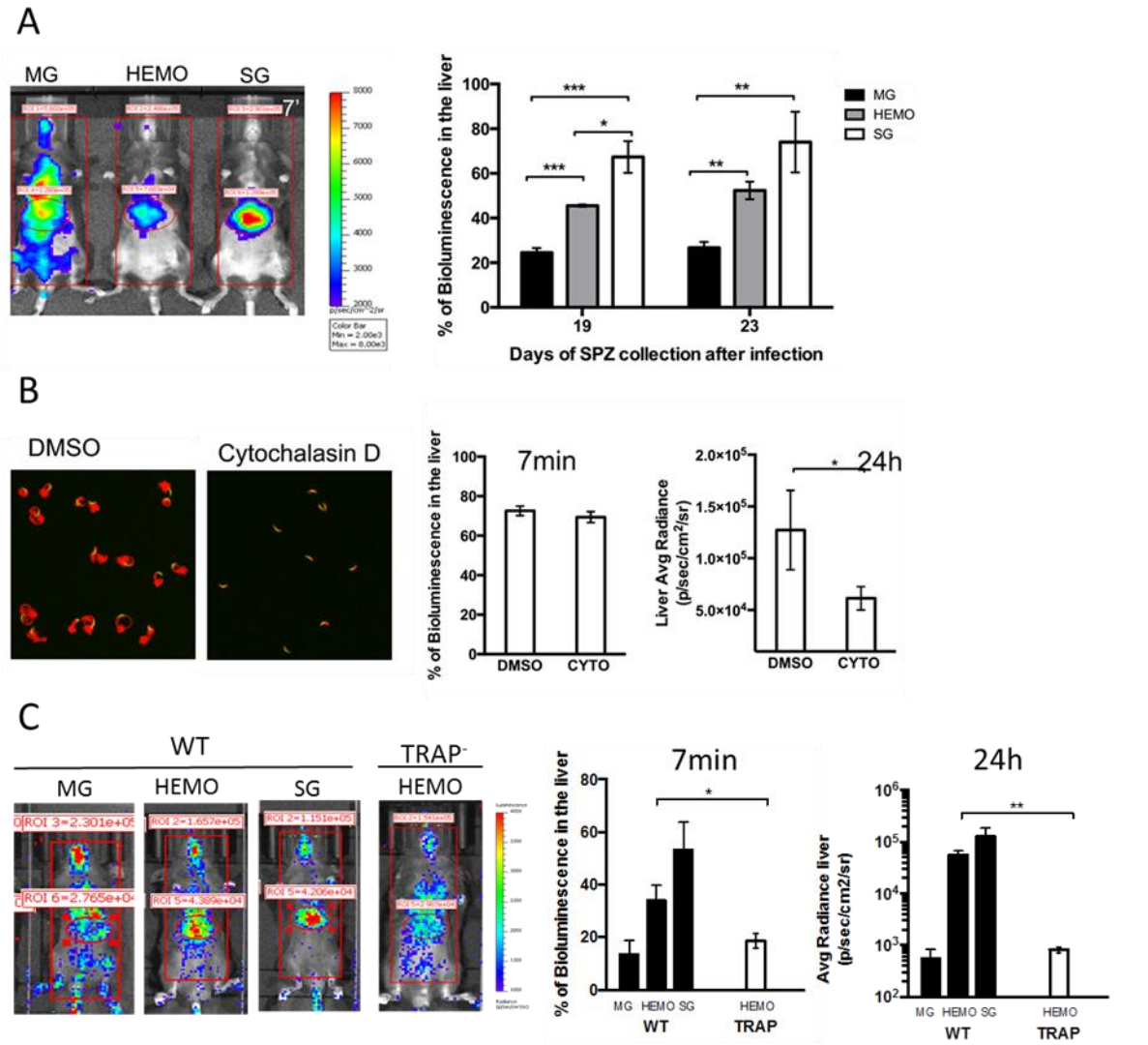

Figure 8- Homing of *Plasmodium* sporozoites to the liver. A. *P. berghei* GFP$^+$:LUC$^+$ sporozoites collected from the mosquito midgut (MG), hemolymph (HEMO) and salivary glands (SG) at day 19 and 23 after the infectious blood meal (left) were intravenously injected in C57BL/6 mice previously treated with clodronate and recorded 7 min after infection. The percentage of bioluminescent signal in the liver versus total body was calculated and is shown (mean ± SD; n = 3). **B.** Sporozoites were incubated with 10 µM cytochalasin D (CYTO) for 10 min on ice and their gliding motility was imaged for 5 min and projected in red. DMSO or cytochalasin D treated sporozoites were intravenously injected in C57BL/6 mice previously treated with clodronate liposomes (3 days before infection) and recorded 7 min after infection following injection of luciferin. The percentage (mean ± SD; n = 3) of bioluminescent signal in the liver versus total body signal is represented. The quantification of the bioluminescent signal in the liver was also done at 24 h after infection and the average radiance (p/sec/cm^2/sr) (mean ± SD; n=3) is shown. **C.** GFP$^+$:LUC$^+$ wt sporozoites collected from mosquitos midgut (MG), hemolymph (HEMO) or salivary glands (SG) and GFP$^+$:LUC$^+$ TRAP knockout sporozoites were intravenously injected in C57BL/6 mice previously treated with clodronate liposomes (3 days before infection) and recorded 7 min after infection following the injection of luciferin. The percentage (mean ± SD; n=3) of bioluminescent signal in the liver versus total body signal is represented. The quantification of the bioluminescent signal in the liver was also done at 24 h after infection and the average radiance (p/sec/cm^2/sr) (mean ± SD; n=3) is shown. Statistical analysis, an unpaired two-tailed Student's t-test was used, *, p<0.05; **, p < 0.01; ***, p<0.001. Tavares *et al.,* unpublished.

1. A review of the role of TRAP and MAEBL on the sporozoites journey from the mosquito to the mammalian host

a. Thrombospondin-related adhesion protein

TRAP belongs to a family of proteins characterized by the presence of at least two adhesive modules in the extracellular portion of the protein, i.e. the TSR domain and the VWA-domain (Fig.9) (Kappe *et al.,* 2004). The emergence of this family within the Apicomplexa phylum occurred earlier, since it is possible to find TRAP-like proteins across other Apicomplexan genera, such as *Toxoplasma gondii* microneme protein 2 (TgMIC2) in *Toxoplasma* (Wan *et al.,* 1997), the *Eimeria tenella* microneme protein 1 (EtMIC1) in *Eimeria* (Tomley *et al.,* 2001), *Neospora caninum* microneme protein 2 (NcMIC2) in *Neospora* (Lovett *et al.,* 2000), *Babesia bovis* TRAP homologue (BbTRAP) in *Babesia* (Gaffar *et al.,* 2004) and thrombospondin-related adhesive protein of *Cryptosporidium* 1 (TRAPC1) in *Cryptosporidium* (Spano *et al.,* 1998). In *Plasmodium,* several members of TRAP family of proteins are expressed, such as the TRAP in sporozoites, the CS-and-TRAP-related protein (CTRAP) in ookinetes and the merozoite TRAP homologue (MTRAP) in blood-stages (Trottein *et al.,* 1995; Baum *et al.,* 2006).

The 200-amino-acid long VWA-domain is present in a superfamily of proteins that include soluble proteins, extracellular matrix proteins and also integral membrane proteins (Fig.9) (Morahan *et al.,* 2009). The crystal structure of this domain revealed that this protein unit acquires a classic α/β Rossman fold consisting in seven amphipathic α–helices surrounded by a β-sheet (Emsley *et al.,* 1998; Li *et al.,* 1998). This domain also encompasses a metal ion-dependent adhesion site (MIDAS), an important motif for divalent cation binding, receptor recognition and cell adhesion, composed by 5 non-contiguous amino acids (Asp-X-Ser-X-Ser), which shelters a Mg^{2+} ion at the centre of its binding site (Springer, 2006; Morahan *et al.,* 2009). In addition, structural studies of TRAP revealed that the WVA-domain encompasses two ligand-binding sites, namely the MIDAS motif and a basic heparin-binding site (Akhouri *et al.,* 2004; Pihlajamaa *et al.,* 2013). Similar to CSP, TRAP also has the TSR adhesive domain (Fig.9). This domain is found on transmembrane and extracellular matrix proteins with important roles on matrix organization, cell guidance and direct interaction between cells (Morahan *et al.,* 2009). Commonly, the TSR domain is composed by approximately 60 amino acids and shelters a central motif encompassing Trp-Ser-X-Trp followed by Cys-Ser-X-Thr-Cys-Gly (Morahan *et al.,* 2009). The ligand-binding site is located at the N terminal portion of the domain and similar to the CSP, TRAP TSR domain has affinity to heparan sulphate proteoglycans expressed on the surface of hepatocytes (Robson *et al.,* 1995; Müller *et al.,* 1993; Tossavainen *et al*., 2006). Using a surface plasmon resonance technology to analyse the interaction between TRAP and heparin, Akhouri and colleagues in 2004, demonstrated the affinity to heparin to TRAP increases when the TSR and VWA-domain act together, which may explain the conformational changes that occur in the protein upon binding to the receptor and suggests that both adhesion domains may participate in the sporozoite adherence and invasion of host cells (Akhouri *et al.*, 2004; Morahan *et al.,* 2009). Indeed, this hypothesis was in agreement with a previous study that used genetically modified parasites

harbouring loss-of-function mutations in the TSR and VWA-domain of TRAP: whereas mutants harbouring mutation in one domain were less infective to cultured cells, mosquito salivary glands and rodent liver, mutants bearing mutation in both domains were non-infective (Matuschewski *et al.,* 2002a).

Contrarily to the adhesion domains, the structure of TRAP cytoplasmic tail (Fig.9) is not similar among the members of this family of proteins, being the only resemblance among them the presence of a conserved tryptophan residue at the C-terminal region, the YXXϕ motif (where ϕ is any hydrophobic residue) and the abundance of acidic amino acids (Robson *et al.,* 1988; Morahan *et al.,* 2009). The cytoplasmic tail is required for TRAP sorting, since the tyrosine-based motif is responsible for a proper targeting of the protein to micronemes and sporozoite surface (Bhanot *et al.,* 2003).

Figure 9- Domain architecture of the thrombospondin-related adhesion protein (TRAP). The extracellular portion of TRAP is composed of a signal peptide (SP), two adhesion domains, namely a von Willebrand factor A domain (VWA-domain) and a thrombospondin type-I domain (TSR), and portion of tandem amino acid repeats (Tandem repeats). The protein has also a transmembrane domain (TD), along with an acidic cytoplasmic tail (CTD) (Adapted from Kappe *et al.,* 2004).

TRAP was originally detected in *Plasmodium* blood stages but was found to be predominantly expressed by infectious sporozoites (Robson *et al.,* 1988, 1995; Rogers *et al.*, 1992). This protein is rapidly secreted to the sporozoites surface upon contact with host cells (Gantt *et al.*, 2000). Immunofluorescence analysis showed that the protein usually appears as a faint patchy pattern at the surface of sporozoites, although sometimes forms a "cap" over a pole of the parasites or one or two rings surrounding their surface (Kappe *et al.,* 1999; Gantt *et al.,* 2000).

The role of TRAP in gliding motility started to be depicted when Sultan and colleagues in 1997 reported that *trap* KO sporozoites were not capable of gliding, invading mosquito salivary glands or infecting the rodent liver. Later on, it was shown that sporozoites engineered to express TRAP without the 14 or 37 carboxyl-terminal residues of its cytoplasmic tail domain present a similar defective phenotype of *trap* KO (Kappe *et al.,* 1999). Indeed, while the function of TRAP was severely impaired upon changes on its intracellular domain, the surface presentation of the protein remained unchanged (Kappe *et al.*, 1999). In addition, mutants phenotype whose TRAP cytoplasmic tail was substituted by that of TgMIC2 did not differ from wt sporozoites in terms of infectivity and gliding, therefore suggesting that the molecular mechanism underlying sporozoites gliding and invasion is conserved among the Apicomplexa (Kappe *et al*., 1999). The role of TRAP in sporozoite gliding motility was further explored by Münter and colleagues, 2009. In this study, the authors verified that in the absence of TRAP, sporozoites could still form adhesion sites but were unable to brake them, resulting in a defective gliding pattern to which the authors named "patch gliding", similar to the gliding pattern described by Kappe and colleagues in 1999, for sporozoites harbouring mutations in the cytoplasmic tail domain of TRAP. This suggests that, although being dispensable for the formation of the initial adhesion sites, TRAP is essential for sporozoite gliding motility, coordinating the turnover of contact sites and thus ensuring a unidirectional gliding pattern (Münter *et al.,* 2009).

The ectodomain of TRAP needs to be shed for sporozoites to glide and invade a host cell. Indeed, a few years ago it was verified that TRAP can be cleaved by the rhomboid protease (ROM) 4, an enzyme highly expressed in sporozoites with a substrate transmembrane domain for cleavage (Le Roch *et al.,* 2003; Baker *et al.,* 2006). Later, this issue was further investigated using two mutant parasite lines harbouring targeted mutations in two canonical rhomboid motifs present in the transmembrane domain of TRAP, specifically the motif AGGIIGG and FFFIIGG (Ejigiri *et al.,* 2012). Interestingly, these mutations led to an accumulation of TRAP at the surface of sporozoites, suggesting that these motifs are critical for the shedding of the molecule. Moreover, these mutants displayed an impaired infectivity to mosquito salivary glands and were 10 to 100 less infectious to mice when compared to wt sporozoites. The defective phenotype of the mutant sporozoites was concomitant with a defect in gliding motility and also in cell traversal. Moreover, mutants incapable of shedding TRAP accumulate the protein all over their surface, suggesting that TRAP might be shedded in a stochastic manner, contributing for the smooth gliding pattern observed in wt sporozoites (Ejigiri *et al.,* 2012).

Finally, the whole picture was completed when it was discovered the mode of interaction of TRAP with the glideosome. Indeed, the cytoplasmic tail is anchored to the fructose-1, 6-bisphosphate aldolase, which in turn is associated to F-actin, forming a ternary complex (Kim *et al.,* 1998; Buscaglia *et al.*, 2003; Jewett & Sibley, 2003). As this enzyme is a tetramer, composed by four identical subunits, different subunits can bind at the same time with TRAP and actin (Bosch *et al.,* 2007). Biochemical and structural studies reported that the key residues of TRAP cytoplasmic tail that seems to allow the binding with the aldolase are a sub-terminal tryptophan residue along with two non-contiguous stretches of negatively charged residues. Interestingly, it was found that aldolase is localized at the surface of micronemes containing TRAP, possibly interacting with the cytoplasmic tail of TRAP, since the latest is protruding towards the cytoplasm, whereas TRAP N-terminal region is facing the lumen of micronemes. This early association between TRAP and aldolase may explain the sorting of the aldolase to the space between the IMC and the plasma membrane of sporozoites (Ngô *et al.,* 2000). Thus, the actin-aldolase-TRAP ternary complex would be assembled upon sporozoite activation (Gantt *et al.,* 2000; Bosch *et al.,* 2007).

Concerning the host side, it was reported that a 12 amino acid long-peptide, named SM1, is capable to bind to the surface of mosquito salivary glands, competing with the binding of TRAP (Ghosh *et al.,* 2009). This peptide is a mimitope of TRAP VWA-domain and it was verified that can efficiently bind to saglin, a glycosylated homodimer of 50kDa present on the surface of mosquito salivary glands (Okulate *et al.,* 2007). Indeed, the specificity of this interaction was confirmed upon observation that a recombinant TRAP VWA-domain peptide harbouring a specific mutation in the MIDAS motif was not able to bind saglin. Additionally, upon injection of α-saglin antibodies into infected mosquitoes, *P. falciparum* sporozoites displayed an impaired infection of salivary glands. Since these observations may occur due to a steric effect of the bulk antibody, saglin expression was knockdown using interference RNA in the mosquitoes. Interestingly, *P. falciparum* sporozoites barely infect the salivary glands of mosquitoes injected with saglin dsRNA, suggesting that this receptor interacts with TRAP during sporozoite infection of salivary glands (Ghosh *et al.,* 2009).

Due to the importance of TRAP in the pre-erythrocytic stage of *Plasmodium* life cycle, a number of studies tried to report inhibitory effects on sporozoite motility and/or invasion using antibodies against distinct portions of TRAP. However, the results were highly variable, since some studies reported strong inhibition (Rogers *et al.,* 1992; Spaccapelo *et al.,* 1997), whereas others reported moderate inhibition (Charoenvit *et al.,* 1997), or even no activity (Gantt *et al.,* 2000). Despite these contradicting results, a multivalent subunit malaria vaccine using TRAP as a component is being developed (Moorthy *et al.*, 2004; Rampling *et al.*, 2016). However, it is importantly to highlight that the TRAP epitopes may be altered since it was recently demonstrated that TRAP suffers post-translational modifications, being glycosylated (Swearingen *et al.,* 2016).

b. Apical membrane antigen/erythrocyte binding-like protein

MAEBL is a transmembrane protein initially described in the rodent species *P. berghei* and *P. yoelii* but was found later to be expressed across *Plasmodium* genus (Kappe *et al.,* 1998; Martinez *et al.,* 2013). MAEBL was original reported to be involved in host cell invasion by merozoites but was later described to be constitutively expressed in multiple developmental stages of *Plasmodium* life cycle, including sporozoites and late liver stages (Kappe *et al.*, 1998, 2001; Ghai *et al.,* 2002; Kariu *et al.*, 2002; Preiser *et al.*, 2004; Singh *et al.,* 2004; Srinivasan *et al.,* 2004). In *P. berghei* sporozoites, MAEBL was reported in micronemes (Kariu *et al.,* 2002), whereas other studies reported a co-localization of MAEBL with the rhoptries of *P. yoelii* and *P. falciparum* merozoites (Kappe *et al.,* 1998; Noe & Adams, 1998; Blair *et al.,* 2002; Ghai *et al.,* 2002).

The C-terminal portion of MAEBL, which includes a sequence of amino acid tandem repeats and a cysteine-rich region (C-cys) (Fig.10), was found to be structurally related with *Plasmodium* Duffy-binding like (DBL) proteins, a family of micronemal proteins produced by merozoites involved in the adhesion and formation of the TJ during erythrocyte invasion (Miller *et al.,* 1979; Adams *et al.,* 1992, 2001). This family also includes several relevant parasite antigens, such the erythrocyte binding antigen 175 (EBA-175) of *P. falciparum* (Sim *et al.,* 1990; Tolia *et al.,* 2005) and the Duffy antigen binding proteins of *P. knowlesi* and *P. vivax* (Adams *et al.,* 1990). Later, MAEBL was included in the expanded erythrocyte binding-like (EBL) family of proteins, composed not only by DBL proteins, but also by putative *P. falciparum* erythrocyte binding proteins such as the erythrocyte-binding ligand-1 (EBL-1), EBA-140 (BAEBL), EBA-165 (PEBL) and EBA-181 (JESEBL) (Adams *et al.,* 2001; Li *et al.*, 2012). However, MAEBL stands out from this group of proteins, since it contains two cysteine-rich adhesion domains homologous to the apical membrane antigen 1 (AMA-1) in its N-terminal portion, named M1 and M2, capable of binding to red blood cells *in vitro* (Fig.10) (Kappe *et al.,* 1998). Despite the protein being expressed in blood-stage parasites, the absence of MAEBL does not affect their development (Kariu *et al.*, 2002).

This chimeric protein shares other features with EBL proteins, such for example, being encoded by a gene with multi-exon structures and conserved exon/intron boundaries (Kappe *et al.,* 1998; Adams *et al.,* 2001). In *Plasmodium*, exon boundaries are delimited by consensus donor and acceptor splicing junctions, similar to most eukaryotes. Indeed, *maebl* is one of the few described *Plasmodium* genes

that suffer post-transcriptional alternative splicing (Singh *et al.,* 2004). This was not surprising, since it may act as a mechanism to allow the parasite to use the same ligand to interact with different host receptors over their complex life cycle (Singh *et al.,* 2004). Indeed, *maebl* 3' exons are alternatively spliced generating mainly two distinct MAEBL coding sequences (CDS): a CDS for an insoluble isoform (ORF1) containing C-terminal transmembrane domain and a CDS for a soluble isoform (ORF2) without the C-terminal domain. Despite these two isoforms splicing pattern occurred in sporozoites, full-length MAEBL appears to correlate better with the ORF1 transmembrane transcript (Singh *et al.,* 2004). In addition, it was demonstrated that instead of being tissue-specific, the expression of MAEBL is regulated within the developmental cycle of sporozoites: in midgut sporozoites, MAEBL is expressed as a full-length protein; after sporozoite egressing from oocyst, MAEBL undergo a post-translational processing, to be *de novo* expressed in infectious sporozoites upon invasion of mosquito salivary glands (Preiser *et al.*, 2004; Singh *et al.,* 2004).

Figure 10- Domain architecture of the apical membrane antigen/erythrocyte binding-like protein (MAEBL). MAEBL is a chimeric protein whose extracellular portion includes a signal peptide (SP), two adhesion domains homologous to AMA-1, namely M1 and M2, amino acid tandem repeats (Tandem repeats) and a cysteine-rich region (C-cys). Additionally, MAEBL has also a transmembrane domain (TD) and a cytoplasmic tail (CTD) (Adapted from Kappe *et al.,* 2004).

The role of MAEBL in sporozoite infection started to be depicted when Kariu and colleagues, 2002 engineering *maebl* KO sporozoites and verified that the protein is essential in sporozoite infection of the mosquito salivary glands. Specifically, the defect seems to involve the adherence of sporozoites to those structures. However, the lack of infectivity of *maebl* KO sporozoites to the mosquito salivary glands was not concomitant with a defective gliding motility contrasting with *Plasmodium* TRAP mutant lines created in previous gene-targeting studies (Sultan *et al.,* 1997; Kappe *et al.,* 1999). Moreover, it was later verified that MAEBL isoform ORF1 is essential for *P. falciparum* to infect the mosquito salivary glands, suggesting that the role of MAEBL in mediating this step of *Plasmodium* life cycle is conserved in different parasite species (Saenz *et al.,* 2008). It was also demonstrated that MAEBL does not have any role in sporozoite infection of the mammalian host, since *maebl* KO sporozoites could infect rat liver at the same extent as wt sporozoites (Kariu *et al.,* 2002).

As abovementioned, MAEBL is expressed (*de novo*) in infectious sporozoites, which may indicate a role in sporozoite infectivity to the mammalian host (Preiser *et al.*, 2004; Singh *et al.*, 2004). Despite the study performed by the Kariu group in 2002 indicating that expression of MAEBL is not required for the establishment of a successful liver infection by sporozoites, studies using antibodies against distinct portions of MAEBL have been reporting the opposite. Indeed, it was demonstrated that antibodies against the M1, M2 and C-cys domains of *P. yoelii* MAEBL were capable to partially inhibit sporozoites infection of mouse hepatocytes (Preiser *et al.*, 2004). Specifically, the higher inhibition was obtained when antiserum to the M1-domain was used, being capable of reducing the number of EEFs by approximately 40%. This inhibitory effect was also observed using antibodies against the M2-domain of the canonical form or against the C-terminal of the alternative form of *P. falciparum* MAEBL (Peng *et al.*, 2016). Moreover, it was recently proven that MAEBL is highly immunogenic pre-

erythrocytic antigen, since sera of immunized human volunteers under chloroquine cover could recognize at a great extent the protein (Peng *et al.,* 2016).

Chapter II

Material and Methods

Section I – Maintaining the life cycle of *P. berghei* parasites in laboratory

The general procedures concerning the maintenance of the *P. berghei*–mosquitoes-rodent system of experimental malaria are explained in this section and were divided into two subsections: maintaining parasites in the vertebrate and invertebrate hosts.

1. Maintaining *P. berghei* in the vertebrate host

NMRI or C57BL6 male or female mice were purchased from Charles River Laboratories and were housed at the Institute for Research and Innovation in Health (I3S) animal facility under a 12 hours alternating cycle of light-dark and access to food and water *ad libitum*. All the experiments were performed in accordance with the Institute for Research and Innovation in Health Animal Ethics Committee and the Portuguese National Authorities for Animal Health guidelines, according to the statements on the directive 2010/63/EU of the European Parliament and Council.

Blood-stage parasites were produced in mice, according to methods described previously (Ramakrishnan *et al.*, 2013). In brief, mice were infected either with blood-stage parasites or sporozoites, depending on the purpose of the experiment. Specifically, in case of infection with blood-stage parasites, mice became infected upon i.v. injection of heparinized blood from an infected animal or intraperitoneal (i.p.) injection of cryopreserved parasites. Alternatively, mice were infected intravenously with sporozoites in PBS.

To monitor the infection of mice, their parasitaemia was assessed by analysis of Giemsa-stained thin blood smears (Ramakrishnan *et al.,* 2013). The parasitaemia was calculated by dividing the number of infected RBCs by the total number of RBCs in the field; the average parasitaemia of 10 to 30 fields of approximately 500 RBCs per field was routinely counted. When the parasitaemia of mice was above 1%, animals were euthanized by cervical dislocation under deeply inhaled anaesthesia. For some experimental procedures, such as storage of parasites and extraction of parasite genomic DNA (gDNA), isoflurane-anesthetized animals were exsanguinated via cardiac puncture using a heparinized syringe. For the preparation of parasite stocks, the collected blood was diluted in Alsever's solution containing 10% glycerol at a ratio of 1:2 and aliquoted into several 1 ml cryogenic vials. Aliquots were frozen at -80°C and then transferred to a liquid nitrogen storage container (Sinden *et al.*, 2002).

2. Maintaining *P. berghei* in the invertebrate host

Anopheles stephensi mosquitoes (SDA 500 strain) were reared at the Centre for the Production and Infection of *Anopheles* at the Pasteur Institute, Paris, France, and then infected and maintained at the I3S, Porto, Portugal. An acclimatized room at 20°C was used as insectary, in which mosquitoes were caged in autoclavable metal-frame cages and kept inside humidified incubators at 20.5 ± 0.5°C. Moreover, they were maintained in a regular 12 hours light-dark cycle and were fed with 10% sucrose solution-soaked cotton pads placed on the netting of cages, which were changed twice a week. Two to three days after their arrival, mosquitoes were allowed to have an infectious blood meal, using mice with parasitaemia and gametocytaemia (percentage of RBCs infected with gametocytes) values

around 5% and 0.5%, respectively. The infectious blood meal procedure is described in detail by Ramakrishnan and colleagues, 2013. Briefly, mice were anesthetized through i.p. injection of ketamine/xylazine mixture (ketamine 125 mg/kg, xylazine 12.5 mg/kg) and then were laid down on the netting of mosquito cages (one or two mice per cage). Female mosquitoes were fed *ad libitum*, but in order to avoid mosquitoes overeating of blood, the position of mice was changed every 5 minutes for approximately 45 minutes. During feeding, mice were kept anaesthetized and were covered by large pieces of cotton minimizing their risk of hypothermia. After mosquitoes finish their meal, the animals were sacrificed by cervical dislocation. One week later, mosquitoes were allowed to feed on non-infected animals (naïve blood meal), as described above (Sinden *et al.*, 2002).

The dissection of mosquitoes occurred 19 to 21 days after their infectious blood meal, using a fluorescent stereoscope, and was performed as described previously (Carey *et al.,* 2013; Ramakrishnan *et al.,* 2013; Sato *et al.,* 2014). Briefly, after being collected from their cages using an electric insect vacuum, mosquitoes were transferred to a tube and placed on ice. Once anesthetized, they were washed with 70% ethanol, and then with PBS and placed on a glass slide. To collect the salivary glands, the thorax of mosquitoes was gently pressed towards the slide while their heads were pulled away with the help of two needled syringes, releasing the salivary glands that appear as a pair of three-lobed structures. The salivary glands were gently collected to and ice-cooled tube with PBS. To collect the hemolymph, the distal abdominal segment of mosquitoes was removed and their thorax was gently washed via injection of 30 µl of PBS into a pinhole located underneath their wing. The drained fluid was immediately collected and placed on an ice-cooled tube. Then, while grasping the thorax of mosquitoes with a needle, their penultimate abdominal segment was slowly removed using the other needle, exposing the midgut of mosquitoes. Midguts were gently cleaned by removing the Malpighian tubules if necessary, and were collected to an ice-cooled tube with PBS. The prevalence of *P. berghei* infection in mosquitoes was calculated by dividing the number of midgut GFP positive mosquitoes by the total number of dissected mosquitoes. To count sporozoites, midgut and salivary glands were mechanically disrupted using a sterile micropestle. Sporozoites were then diluted and counted in a plastic slide with a counting grid, under a light microscope.

Section II – Molecular biology

1. Preparation of blood and extraction of parasite genomic DNA

The preparation of infected blood for extraction of parasite gDNA was performed based on the protocol described by Ménard and Janse, 1997. In brief, blood of infected mice was collected by cardiac puncture and diluted by adding PBS to a final volume of 5 ml. The blood was allowed to pass through a Plasmodipur filter (Eurodiagnostica), previously rinsed with PBS, in order to remove leukocytes. Then, the filters were washed with PBS and the filtrate added to the filtered blood. To lysate RBCs, saponin was added to the suspension to a final concentration of 0.15% (v/v) and following an incubation period of 5 minutes at room temperature (RT), parasites were collected by centrifugation at 3200g for 20 minutes. The supernatant was discarded and the pellet washed twice

by resuspending in 2 ml of PBS and centrifugation at 12000g for 5 minutes. If not processed immediately, the parasites pellet was stored at -20°C.

The extraction of parasite gDNA was performed using the QIAamp DNA Blood Mini kit (Qiagen), following the manufacturer instructions. Quantification of the extracted gDNA was performed by using a spectrophotometer.

2. Construction of transfection vectors

For the construction of all vectors, the amplification of the homology regions was accomplished by PCR using *P. berghei* ANKA strain clone 676cl1 expressing a GFP-Luciferase genomic DNA (*P. berghei* ANKA GFP^+:LUC^+ ; Franke-Fayard *et al.,* 2008). Primer sequences are represented in Table I.

a. Targeting *maebl* in *P. berghei* parasites

Two DNA fragments corresponding to *maebl* (PBANKA_0901300.2) 5' and 3' untranslated regions (UTRs) were amplified using a high-fidelity *Taq* DNA polymerase with proofreading activity (Takara) and the primer pairs P1/P2 and P3/P4, respectively. The PCR conditions were as follows: initial denaturation step (2 minutes at 98°C), 35 cycles of denaturation (10 seconds at 98°C), annealing (30 seconds at 55°C) and elongation (40 seconds at 68°C) and a final elongation step (5 minutes at 68°C). PCR products were isolated from a 1% agarose gel after electrophoresis, using the kit NucleoSpin® Gel and PCR Clean-up (Macherey-Nagel). These fragments were cloned into a pGEM-T Easy vector (Promega), sent for sequencing and checked against *P. berghei* genome database (PlasmoDB, http://plasmodb.org/plasmo/) using the Basic Local Alignment Search Tool (BLAST). The resulting vectors were double digested with KpnI and ClaI or EcoRI and BamHI, allowing the insertion of the UTRs into either side of the selectable marker cassette (*T. gondii dhfr/ts* ORF flanked by the upstream and downstream control elements of *P. berghei dhfr/ts*) of a transfection vector pL0001 (MRA-770; MR4), yielding plasmid pΔMAEBL.

b. Targeting *trap* in *P. berghei* parasites

The regions corresponding to *trap* (PBANKA_1349800) 5' and 3' UTRs were amplified using a high-fidelity *Taq* DNA polymerase with proofreading activity (Takara) and the primer pairs P11/P12 and P15/P16, respectively. Importantly, the promoter region of *trap* was not comprised in the fragment corresponding to 5'UTR. The PCR conditions were as follows: initial denaturation (2 minutes at 98°C), 35 cycles of denaturation (10 seconds at 98°C), annealing (30 seconds at 55°C or 50°C, concerning the primer pairs P11/P12 or P15/P16, respectively) and elongation (40 seconds at 68°C) and a final elongation step (5 minutes at 68°C). PCR products were isolated from a 1% agarose gel after electrophoresis, cloned into a pGEM-T Easy vector (Promega), sequenced and checked against PlasmoDB. The promoter and open reading frame (ORF) of *trap*, henceforth called pORF, were amplified using the primer pair P13/P14 and the following PCR conditions: initial denaturation (2 minutes at 98°C), 35 cycles of denaturation (10 seconds at 98°C), annealing (30 seconds at 55°C) and elongation (40 seconds at 68°C) and a final elongation step (5 minutes at 68°C). The PCR product was

isolated from a 1% agarose gel after electrophoresis, cloned into a pCR-XL-TOPO® (Invitrogen), sequenced and checked against PlasmoDB. The resulting vector was digested with SalI and BamHI, allowing the fusion of 3'UTR with the 3'end of the pORF (pORF_3'UTR). The 5'UTR and pORF_3'UTR were inserted into a transfection vector pL0001 (MRA-770; MR4), on each site of the selectable marker cassette, using the unique cloning sites KpnI/HindIII and EcoRV/BamHI, respectively, yielding plasmid pCTR. The plasmid pCTD$^-$ harbours a truncated version of the ORF of *trap*, lacking 111 nucleotides upstream of the stop codon (Kappe *et al.,* 1999). pCTD$^-$ was engineered exactly in the same manner as plasmid pCTR, but using the primer pair P13/P21 for the amplification of a DNA fragment corresponding to *trap* promoter region and truncated ORF (pORF^{ctd-}); importantly, a stop codon was encoded in the reverse primer P21. PCR conditions were also the same as used for the amplification of pORF, with the exception that primers annealed at 53°C.

The targeting constructs were prepared to be used in the transfection of parasites accordingly Ménard and Janse, 1997. In brief, *Escherichia coli* DH5a containing the vectors pΔMAEBL, pCTR or pCTD$^-$ were inoculated in Luria Broth (LB) with ampicillin (100 µg/ml), and cultured overnight at 37 °C and 200 rpm agitation. Transfection vectors were isolated from bacteria and digested with KpnI and BamHI, yielding *maebl*, *trap* and *trap^{ctd-}* linearized targeting constructs. The constructs were isolated from a 1% agarose gel after electrophoresis, semi-quantified and stored at -20°C.

3. Transfection of parasites

The practical aspects of transfecting *P. berghei* ANKA GFP$^+$:LUC$^+$ blood-stage parasites are divided here as follows: *in vitro* synchronization of schizonts; purification of schizonts; electroporation of schizonts and injection into mice and drug selection of transfectants. All these procedures were performed based on the protocols described previously (Ménard & Janse, 1997; Janse *et al.,* 2006).

a. *In vitro* synchronization of schizonts

Mice were infected with an i.p. injection of cryopreserved *P. berghei* ANKA GFP$^+$:LUC$^+$ blood-stage parasites. Once parasitaemia was above 1%, a few microliters of its blood was transferred into two mice yielding a final parasitaemia of 0.001%. Their parasitaemia was assessed at day 3 post-infection and once it reached values around 5%, their blood was collected by cardiac puncture for the synchronization of schizonts *in vitro.* The collected blood was immediately transferred to a tube containing RPMI1640 culture medium supplemented with 20% heat inactivated fetal bovine serum (FBS). Infected RBCs were harvested by centrifugation at 450g for 8 minutes and resuspended in 50 ml of RPMI1640, 20% FBS, supplemented with neomycin (50 µg/ml). The resulting suspension was then equally distributed among two cell culture flasks T-75 and diluted with 25mL of RPMI1640, 20% FBS with neomycin (50 µg/ml). The flasks were flushed with a gas mixture (5% CO_2, 5% O_2, 90% N_2) for 90 seconds and placed in a shaker incubator at 36.5 ± 0.5°C at a speed just enough to avoid cell sedimentation. Then, schizonts were allowed to synchronize overnight for a 16 hours period (Janse *et al.,* 2006).

b. Purification of schizonts

A small sample of blood collected from the overnight cultures was smeared over a glass slide. After Giemsa-staining, the slide was analysed to assess the quality of schizonts, i.e. to check if the majority portion (70 to 80%) of parasites appeared as viable schizonts (Janse *et al.,* 2006). If it was not the case, the cultures were placed back into the incubator for 1 to 2 hours. Once fully mature, schizonts were separated from non-infected erythrocytes by density-gradient centrifugation. In brief, 50 ml of 50% (v/v) Nycodenz-PBS solution were prepared, by adding equals amounts of Nycodenz density-gradient stock solution (138 g Nycodenz powder in 500 ml 5mM Tris:HCl, 3 mM KCl, 0.3 mM $CaNa_2EDTA$, pH 7.5) and PBS. After distributing the parasite culture equally among three 50 ml Falcon tubes, 10 ml of 50% (v/v) Nycodenz-PBS solution was gently added to each tube under the culture suspension, in order to form two distinct and well-defined aqueous layers. Centrifugation occurred at 450g for 20 minutes at RT without brake. During this step, the DNA solution (needed at later steps) was prepared by diluting 10 µg of *maebl*, *trap* or *trap*$^{ctd-}$ linearized targeting constructs into 10 µl of sterile water. Meanwhile, schizonts were collected by gently aspirating the brownish grey layer at the interface between the two suspensions to a new tube. Up to 40 ml of fresh RPMI1640, 20% FBS medium was added to the collected schizonts and the suspension was centrifuged at 450g for 8 minutes. The schizonts-containing pellet was carefully resuspended in 1 ml RPMI1640, 20% FBS medium and then diluted at a final concentration of 1:10 (resuspended schizonts: medium). The suspension was then aliquoted in a way that one single tube contains the amount of parasites necessary for one transfection, i.e. 0.5 to 1x10^7parasites (Janse *et al.,* 2006).

c. Electroporation of schizonts and injection into mice

Electroporation of schizonts was performed using The Amaxa® Nucleofector® Technology (Amaxa). Schizonts were mixed with 100 µl Nucleofector solution 88A6 (Amaxa) containing already the DNA. The suspension was transferred to an electroporation cuvette, which was placed in the electroporation device, and merozoites were transfected using the program U33. Immediately after electroporation, the suspension was diluted by the addition of 50 µl of RPMI1640, 20% FBS medium and i.v. injected in two mice.

d. Drug selection of transfectants

One day after infection with transfected parasites, mice started to be treated with pyrimethamine (0.07mg/ml) given in drinking water (Janse *et al.*, 2006). Their parasitaemia began to be daily assessed one week after infection to monitor the appearance of drug-resistant parasites. The emerging parasite populations in the infected animals, henceforth referred as parental population 1 and 2 (PP1 and PP2), were allowed to multiply until infecting 1% of mice RBCs. Then, to perform another round of drug selection, 1x10^6 infected RBCs of each mouse were transferred into two mice, yielding transfer populations 1 to 4 (TP1, TP2, TP3 and TP4). Once parasitaemia was near 5% the blood of infected animals was collected by cardiac puncture for storage of parasites and genotype analysis of parental and transfer populations.

4. Cloning of parasites

After assessing the genotype of parental and transfer populations of parasites by PCR (see PCR strategies in the "Genotypic analysis of mutant parasites" subsection), a proper transfer population was selected for cloning.

Cloning of parasites was performed using the limiting dilution method described by Ménard and Janse, 1997. Briefly, a cryopreserved stock of a transfer population was intraperitoneally injected in two mice. Their parasitaemia was daily assessed and once it reached near 0.1%, their blood was collected and diluted to inject half of a parasite per mice in approximately 15 mice. The parasite populations that emerged after cloning (clonal populations) were allowed to grow and once parasitaemia was near 5%, the blood was collected by cardiac puncture for storage and genotype analysis of parasites.

5. Genotypic analysis of mutant parasites

The genotype of parasites was verified by PCR and Southern blot analysis (Ménard & Janse, 1997). The parental populations (PPs), transfer populations (TPs) and clonal populations (CPs) that emerged after transfection of wt parasites with the *maebl*, *trap* or *trap*$^{ctd-}$ targeting constructs will be hereinafter referred to as MAEBL^{-}, cTRAP or TRAP^{ctd-} PPs, TPs and CPs.

a. Genotypic analysis by PCR

The PCR screening of the recombinant locus of parasites was performed using a high-fidelity DNA polymerase (Phusion®, New England Biolabs). Thus, the general thermocycling conditions used were as follows: initial denaturation step (30 seconds at 98°C), 35 cycles of denaturation (10 seconds at 98°C), annealing (30 seconds at appropriate annealing temperature) and elongation (at least 30 seconds at 72°C) and a final elongation step (10 minutes at 72°C).

A portion of a non-related gene was amplified as a positive control for the PCR reactions. The reactions were accomplished using the primer pairs P9/P10, P23/P24 or P5/6, yielding specific products corresponding to portions of the *trsp* (PBANKA_0209100) ORF, *p38* (PBANKA_1107600) or *maebl* ORF, respectively. These reactions were performed using an annealing temperature of 65°C, 71°C or 60°C.

Furthermore, the eventual absence of the *maebl* ORF in the genome of transgenic parasites was also assessed using the primer pair P5/P6. When necessary, a central portion of the *tgdhfr* ORF was amplified using the primer pair P17/P18 at a temperature of annealing of 58°C.

The primer pair P7/P8 was used to verify whether the selectable marker was inserted in the expected site of the *maebl* recombinant loci of MAEBL^{-} PPs, TPs and CPs, since P7 is complementary to a specific sequence of the selectable marker cassette and P8 binds at a region of the 3'UTR in the locus. This reaction was accomplished by using a temperature of annealing of 60°C. A similar analysis of the *trap* recombinant loci of cTRAP and TRAP^{ctd-} PPs, TPS and CPs was performed, but using the primer pairs P19/P20 or P22/P20, respectively. In specific, whereas P19 and P22 are complementary

to the terminal end of pORF or pORF^{ctd-}, respectively, P20 is complementary to a region of the 3'UTR in the locus; all those primers annealed at 63°C.

Finally, using the *TaKaRa Ex Taq* DNA polymerase (Takara) and the primer pair P13/P14 it was possible to confirm the absence of a non-truncated *trap* ORF in the genome of TRAP^{ctd-} CPs, since P14 is complementary to the terminal nucleotides of the endogenous *trap* ORF (see PCR conditions in the "Construction of transfection vectors" subsection).

All reaction product ran on 1% agarose gel with ethidium bromide and images were digitally acquired using a UV transilluminator.

b. Genotypic analysis by Southern blot

gDNA (2 to 10 µg) of cloned parasites was digested overnight at 37°C with HindIII-HF and NruI-HF for *maebl* knockouts or ClaI and HindIII-HF for cTRAP and TRAP^{ctd-} and then separated by 0.8% agarose gel electrophoresis at 30V for 7 hours. Under gentle agitation, the gel was depurated (0.25M HCl) for 15 minutes, denatured (1.5M NaCl, 0.5M NaOH) for 30 minutes and neutralized twice (3M NaCl, 0.5M Tris-HC pH 7.0) for 15 minutes, taking care of rinsing the gel with deionized water between incubations. The gDNA was transferred to a Nytran-N membrane (Amersham Hybond N+, GE Healthcare) overnight, using sodium saline citrate 10x (0.3M Sodium Citrate, 1M NaCl) as transfer buffer. gDNA was fixed to the membrane by incubation at 65°C for 5 hours and then revealed by staining the membrane in methylene blue [0.02% (w/v) Methylene blue, 0.3mM NaOAc] for 10 to 15 minutes at RT. The hybridization probes were obtained by PCR amplification of gDNA using primer pairs P1/P2 and P11/12, yielding *maebl* and *trap* 5'UTR, respectively (see PCR conditions in the "Construction of transfection vectors" subsection). These probes were then labelled using AlkPhos Direct™ kit (GE Healthcare) according to manufacturer's instructions: i.e. the amplified gDNA was denatured by heating at 100°C for 5 minutes, mixed with reaction buffer and alkaline phosphatase and cross-linked with the enzyme using a formaldehyde-containing solution by incubation at 37°C for 30 minutes. The membrane was pre-incubated with hybridization buffer (0.25 ml per cm^2 of membrane) at 45°C for 2 hours and then hybridized with the respective labelled probe (5 ng of probe per ml of hybridization buffer) overnight at the same temperature, under gentle agitation. Then, the membrane was washed twice in preheated primary wash buffer [2M Urea, 0.1% (w/v) SDS, 50 mM NaH_2PO_4 pH 7.0, 150 mM $NaCl_2$,1 mM $MgCl_2$, 0.2% (w/v) Blocking reagent, provided by the kit] for 10 minutes at 45°C and then washed twice with secondary wash buffer (50 mM Tris:HCl, 100 mM NaCl, 2mM $MgCl_2$) for 5 minutes at RT. Labelled bands were visualized using CDP-Star detecting reagent (30 µl per cm^2 of membrane) and were digitally acquired in a ChemiDoc Imaging System (Bio-Rad Laboratories) after 1 hour exposure.

Section III – *In vivo* analysis of mutant sporozoite infectivity and capacity to target the liver

Control (wt) and mutant sporozoites (MAEBL^{-} clones B2 and G3, cTRAP clone B2 and TRAP^{ctd-} clone 9) were collected from the salivary glands or hemolymph of mosquitoes 19 to 20 days after the infectious blood meal. Sporozoites were counted and intravenously injected into young C57BL/6 mice previously treated or not with clodronate liposomes (Tavares *et al.*, 2013).

Mice were imaged according to Ploemen and colleagues*,* 2009, using an IVIS LUMINA LT (Perkin Elmer), at multiple time points depending on the assay, i.e. at 7 minutes to evaluate the sporozoites capacity to home to the liver or 24 or 44/46 hours post-infection to evaluate infectivity. In brief, animals were placed in the induction chamber and anaesthesia was induced with 2% isoflurane in 100% oxygen mixture (Tseng *et al.,* 2015). Once anaesthetized, the chest and abdominal region of mice were depilated and 2.1 mg of D-luciferin dissolved in PBS was injected subcutaneously. The animals were placed on the sample stage of the IVIS system and after an incubation period of 5 minutes, the bioluminescent signal was collected during 5 minutes. A non-infected mouse was always imaged in parallel in order to evaluate background noise signal. Mice were kept anesthetized during the acquisitions.

Bioluminescence quantitative analysis and image processing were performed using the Living Image® 4.4 software. The region of interest (ROI) was set either to measure the entire body of the animal or the abdominal area at the region of the liver and measurements were expressed as total flux (photon per second) or average radiance (photon per second per cm^2 per sr).The capacity of sporozoites to arrest in the hepatic sinusoids, expressed as percentage of bioluminescence in the liver of infected mice 7 minutes after their infection, was calculated by dividing the bioluminescent signal from the liver by the signal obtained from the animals' total body surface. Sporozoite infectivity was inferred from the parasite loads in the liver of mice at 24 and 44/46 hours post-infection, which in turns correlate with the intensity of the bioluminescent signal restricted to that organ.

Section IV – *In vitro* analysis of sporozoite infectivity, development and cell traversal

1. Host cells and parasites

HepG2 cells (ATCC) were cultured in Dulbecco's modified eagle medium, 4.5 g/L Glucose, 25mM HEPES supplemented with 10% FBS and 2mM L-glutamine, henceforth called complete medium, at 37°C, 5% CO_2 (Sinnis *et al.,* 2013). Cells were sub-cultivated and maintained following ATCC instructions (American Type Culture Collection, 2016).

For the *in vitro* assays, control (wt) and mutant sporozoites were collected from the salivary glands or hemolymph of *A. stephensi* mosquitoes 19 to 20 days after the infectious blood meal. The mutant

parasite populations used to assess the invasion capacity of *maebl* KO sporozoites were clone B2 and G3, whereas their cell traversal capacity was assessed using solely clone B2.

2. Quantification of sporozoite invasion and development by immunofluorescence microscopy

The protocols used to assess sporozoite invasion and development were adapted from the one described by Sinnis and colleagues, 2013. In brief, HepG2 cells were seeded in a Lab-Tek 8-chamber slides at 0.8 to $1x10^5$ cells per well in 200 µl complete medium. Following an incubation period of 24 hours at 37°C under 5% CO_2, the medium was removed and 1.5 to $2x10^4$ sporozoites in 200 µl complete medium were added to each well. The slides were centrifuged at 300g for 5 minutes and then incubated for 2 or 48 hours at 37°C under 5% CO_2 for assessing invasion or development, respectively. The cells were then washed with warm PBS and fixed with 4% (v/v) paraformaldehyde (PFA) in PBS for 30 minutes at RT and stored at 4°C.

To quantify the percentage of sporozoites that invaded HepG2 cells the slides were blocked with 5% (v/v) FBS in PBS, henceforth named blocking solution, for 30 minutes at RT, and then stained using a double-staining strategy (Rénia *et al.*, 1988). In brief, the surface of extracellular sporozoites was probed with mouse α-CSP monoclonal antibodies (3D11; 2 µg/ml) followed by Alexa Fluor® 568 conjugated α-mouse IgG secondary antibodies (1:500). Slides were permeabilized with 1% (v/v) Triton X-100 in PBS for 4 minutes at RT, allowing the probing of intracellular sporozoites with mouse α-CSP antibodies (3D11; 2 µg/ml), which were revealed by Alexa Fluor® 488 conjugated α-mouse IgG (1:500) secondary antibodies. To assess the development, slides were sequentially blocked and permeabilized and then labelled with mouse α-CSP (3D11; 2 µg/ml) and rabbit α-GFP primary antibodies (1:250), which were revealed using Alexa 568® conjugated α-mouse IgG (1:500) and Alexa Fluor® 488 conjugated α-rabbit IgG (1:500) antibodies. Moreover, the DNA was labelled with DAPI (1:5000) in PBS. Slides were mounted in Vectashield® (Vector Laboratories) and stored at 4°C protected from light.

Immunofluorescence of slides was observed using a upright epifluorescence microscope. For the analysis of sporozoite invasion, randomly images were acquired based on the number of host cells nuclei per optical field (usually, containing 200 to 500 nuclei), using a 20x objective and the Alexa Fluor® 488 (green), Alexa Fluor® 568 (red) and DAPI (blue) filter sets. In brief, extracellular sporozoites appeared using both red and green filters, whereas intracellular sporozoites could only be seen using the green filter. The number of extracellular, intracellular and host cells nuclei were counted in duplicate in approximately 10 to 30 fields and the sporozoite invasion capacity, expressed in percentage of infected host cells, was calculated by dividing the total number of intracellular sporozoites by the total number of host cells nuclei. For the analysis of EEF development, the number of EEFs were counted in duplicate by performing a visual scan of the whole well using a 20x objective and the red and green filters. To quantify the size of EEFs, 15 random pictures were acquired per each tested condition, using a 20x objective and the red and green filters. Moreover, representative pictures of each tested condition were taken using a 63x oil immersion objective using all filter sets.

Image processing and quantifications were performed using ImageJ (Schneider *et al.,* 2012); specifically, the oval and the polygonal selection tools were used to delimit EEFs as ROI in order to measure the area (μm^2) of parasites.

3. Quantification of sporozoite host cell traversal by flow cytometry

Host cell traversal capacity of sporozoites was assessed using the flow cytometry-based method described by Formaglio and colleagues, 2014. In brief, HepG2 cells were seed on 96 well plate at $5x10^4$ cell per well in 300 µl complete medium, and incubated overnight at 37°C under 5% CO_2. Then $1.5x10^4$ sporozoites were incubated with cells in 100 µl complete medium with 5 µg/ml of propidium iodide (PI), for 90 minutes at 37°C under 5% CO_2. Non-infected cells, i.e. cells incubated only with PI, were used as control. Cells were then washed twice with PBS and then trypsinized. The supernatant was discarded and cells were resuspended in 1% (v/v) FBS in PBS. Cells were analysed in a FACS Canto II flow cytometer (BD Biosciences) and data analysed using FlowJo software (TreeStar, Inc.). The sporozoite cell wounding capacity was assessed by quantifying the percentage of PI positive events.

Section V – Statistical analysis

Statistical analysis was performed using GraphPad Prism 6 software. An unpaired two-tailed Student's t-test assuming equal variance was used to compare the mean of two different groups and an one-way ANOVA with post-hoc testing analysis (Turkey's test) was performed to compare the means of three or more unmatched groups. Statistical significance was found when $p<0.05$.

Chapter III

Results

During this work, two genes, *maebl and trap,* were targeted in GFP-luciferase *P. berghei* parasites aiming at generating *maebl* knockouts and TRAP^{ctd-} transgenic parasites to explore their involvement in the arrest of sporozoites in the liver sinusoids. Therefore, the results are divided into two sections, each one related to the gene that was targeted.

Section I – Apical membrane antigen/erythrocyte binding-like protein

1. Generating *maebl* knockout parasites

A targeted gene replacement strategy by double crossover homologous recombination was used for the deletion of *maebl* from the GFP-luciferase *P. berghei* parasites genome (Fig.11A-B). For that *maebl* UTRs immediately up and downstream the coding sequence were amplified by PCR using gDNA as template, and then cloned in the pL0001 vector (MR4) allowing the construction of the plasmid pΔMAEBL which contains the pyrimethamine-resistant *T. gondii* dihydrofolate reductase–thymidylate synthase (*tgdhfr-ts*) selectable marker flanked by the amplified DNA fragments. The pΔMAEBL vector was verified upon digestion with specific restriction enzymes (Fig.11C). The targeting construct (pΔMAEBL) was linearized following digestion with KpnI and BamHI (Fig.11A,C) and then used for transfection. After two rounds of pyrimethamine selection, the parental and transfer parasite populations were obtained and their genome analysed by PCR to verify the successful integration of the selectable marker in the respective chromosome locus and the eventual absence of *maebl* ORF (Fig. 12A-D). By PCR, all the parental and transfer populations were positive for the integration of the selectable marker and the transfer population 1 selected for subsequent cloning. The cloning efficiency was 25%, meaning only 4 animals out of 16 became infected, yielding the clonal populations B2, B3, G3 and R5. PCR analysis revealed that only B2, B3 and G3 clones were positive for the selectable marker integration and negative for the *maebl* ORF (Fig.12C-D). Their genotype was further analysed by Southern blot and no evidence of wt maebl locus was found in these clones confirming the generation of *maebl* knockouts (Fig.12E).

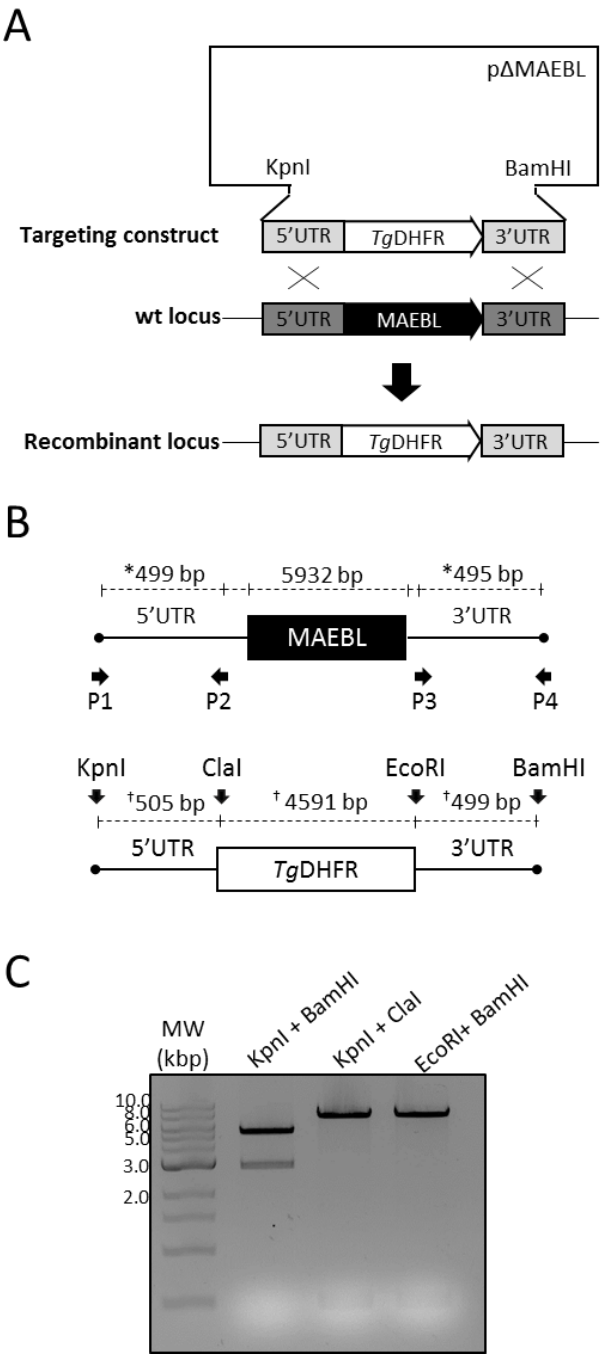

Figure 11– Targeted deletion of *maebl* in *P. berghei*. A, Schematic diagram of the strategy to delete *maebl* in *P. berghei* by double crossover homologous recombination. The *maebl* UTR's sequences were amplified by PCR (light grey boxes) and subcloned into the plasmid, pL0001 (MR4) to generate the PΔMAEBL vector. PΔMAEBL was digested with KpnI and BamHI to obtain the linearized transfection construct composed by the selectable marker cassette (white arrow box) flanked by the *maebl* UTRs. **B,** Restriction strategy used for the construction of the targeting vector. Asterisks (*) and crosses (†) depict the length of the homology regions in the wt locus and the fragments that were integrated (*maebl* UTRs; selectable marker

cassette, white box) in the recombinant locus, respectively. The length of the endogenous ORF (black box) is also depicted in the restriction map, as well as the primer pairs (horizontal black arrows, P1-P4; sequences in Table I) used to amplify the *maebl* UTRs. **C,** Digestion of pΔMAEBL plasmid using the respective restriction enzymes. Digestion products were run on 1% agarose gel containing ethidium bromide. MW, molecular weight.

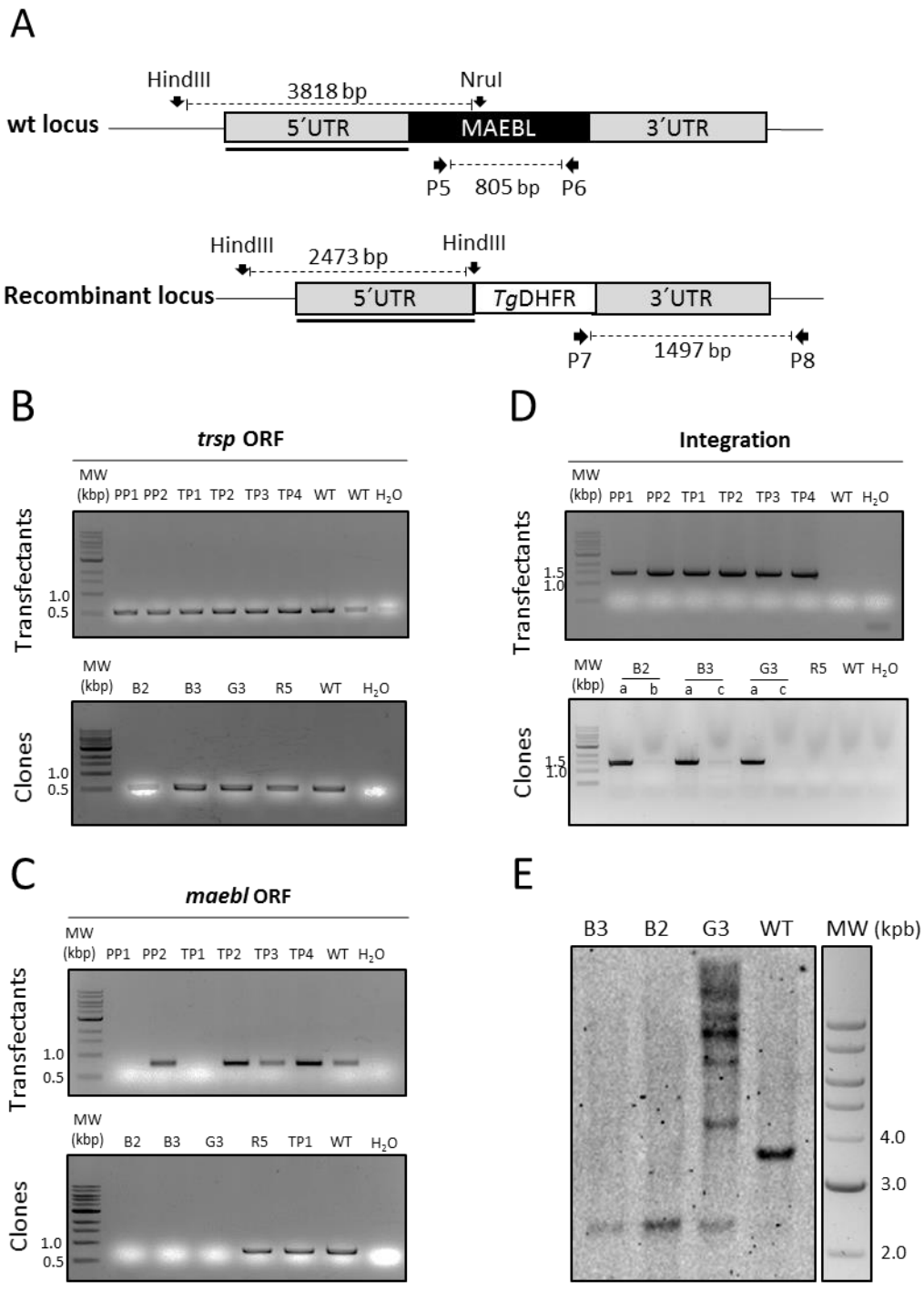

Figure 12- Genotypic analysis of MAEBL mutants. **A**. Schematic diagram of the wt and recombinant loci. Horizontal arrows (P5-P8) depict the primer pairs (sequence in Table I) used in the genotypic screening of mutants by PCR. The Southern blot approach is also schematized: vertical arrows show the cleavage site of restriction enzymes, whereas solid bars represent the probe used in the analysis. The length of the expected PCR products and fragments upon digestion of gDNA with HindIII and NruI, is also shown in the diagram. **B-D.** Genotypic analysis of mutants by PCR. A portion of the ORF from a non-related gene, the *trsp* (600 bp) was amplified as a positive control for the PCR reaction (panel B). The presence or absence of the *maebl* ORF in recombinant loci of mutants was assessed using the primer pair P5/P6 (panel C). In addition, in order to verify the correct integration of the selectable marker cassette in their recombinant loci, mutants were screen using the primers P7 and P8, as they bind to the 3' terminal end of the selectable marker cassette and at 3' of the *maebl* 3'UTR, respectively (panel D). The latter PCR was performed using different amounts of gDNA: 25 ng (a), 50 ng (b) and 100 ng (c). In every reaction, gDNA of wt parasites (WT) was used as control (panels B-D). Additionally, gDNA of transfer population 1 (TP1) was used as an additional control in the *maebl* ORF PCR analysis of MAEBL$^-$ clones (panel C). PP, parental population; TP, transfer population; H_2O, blank; MW, molecular weight. **E.** Genomic Southern blot analysis of MAEBL$^-$ clones (B2, B3 and G3), upon double digestion with HindIII and NruI and probed with the *maebl* 5'UTR probe. gDNA of wt parasites (WT) was included as a control. MW, molecular weight.

2. MAEBL$^-$ sporozoites are defective in invading the mosquito salivary glands

The successful generation of MAEBL$^-$ parasites implies that MAEBL is not essential for the growth and development of the blood-stage parasite forms, which is in agreement with previous gene-targeting studies (Kariu *et al.,* 2002). To investigate the development of MAEBL$^-$ parasites in the invertebrate host, anopheline mosquitoes were allowed to feed on mice infected with MAEBL$^-$ clones B2 or G3. Approximately 19 or 21 days after the infectious blood meal, mosquitoes were dissected and the number of sporozoites in their midgut, hemolymph and salivary glands determined. As expected, the number of sporozoites associated with the mosquito salivary glands was severely reduced for MAEBL$^-$ when compared to the wt (Fig.13). While MAEBL$^-$ sporozoites tend to accumulate in the hemolymph, no differences in the numbers of sporozoites in the midguts were found, suggesting MAEBL$^-$ have no defects in sporozoites development and egress from oocysts (Fig.13). All of these findings are in agreement with the phenotype of MAEBL$^-$ sporozoites reported by Kauri and colleagues, 2002 (Kariu *et al.*, 2002). Due to the strong defect of MAEBL$^-$ on the invasion of mosquito salivary glands, all the sporozoites used in further experiments were collected from the hemolymph.

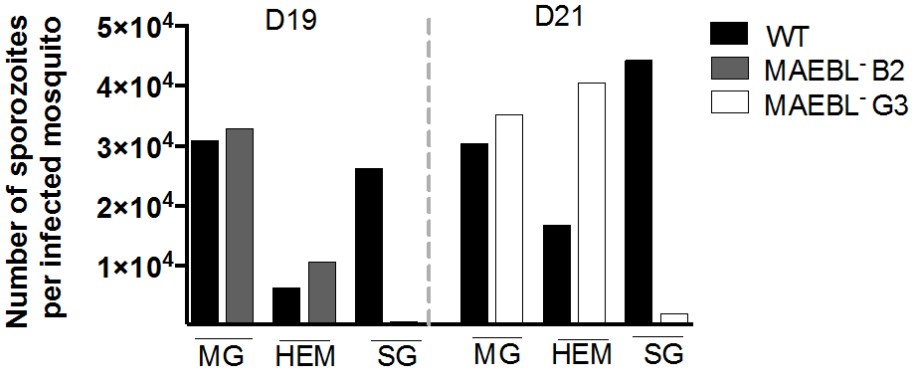

Figure 13- MAEBL$^-$ sporozoites cannot infect the mosquito salivary glands. *A. stephensi* mosquitoes were allowed to feed on mice infected with wt or MAEBL$^-$ blood-stage parasites. Mosquitoes were dissected 19 or 21 days after the infectious blood meal and sporozoites collected from mosquito midgut (MG), hemolymph (HEM) and salivary gland (SG) were counted.

The graphic shows two independent experiments, separated by a dashed horizontal line, concerning two different MAEBL$^-$ clones (MAEBL$^-$ B2, MAEBL$^-$ G3). The values correspond to the number of sporozoites collected per mosquito and are representative of 4 and 3 experiments, concerning the clone B2 and clone G3, respectively.

3. MAEBL$^-$ sporozoites have a defective capacity to infect the liver

To assess whether MAEBL$^-$ sporozoites infect the mammalian host in the same extent as the wt, $5x10^4$ sporozoites were i.v. injected into young C57BL/6 mice. The parasite burden in the liver was determined at 24 and 44 hours post-infection using whole mice live imaging to measure the bioluminescent signal following the injection of luciferin. Surprisingly, 24 hours after sporozoite inoculation, mice infected with mutant sporozoites had a significant lower parasite burden in the liver than the control group (Fig.14A). As expected, this difference was also found at 44 hours (Fig.14B). The fold-difference between the mean values of bioluminescence in the liver of mice infected with MAEBL$^-$ or WT parasites calculated at both 24 and 44 hours were highly comparable (fold-differences of ≈7), suggesting that the impaired infectivity of MAEBL$^-$ sporozoites might be due to a defect in the establishment of the liver infection rather than in the hepatic development of parasites. Only 3 mice out of 4 infected with MAEBL$^-$ sporozoites became infected in the blood presenting a 1-day delay in the prepatent period compared to control group (Fig.14C). Since each day of delay is correlated with a 10-fold decrease in the initial asexual-stages inoculum (Haussig *et al.,* 2011), our results suggest that MAEBL$^-$ sporozoites were 10 fold less infectious than wt sporozoites. The mean parasitaemia differed significantly between groups over time, but despite those differences, MAEBL$^-$ blood-stages showed a normal asexual growth kinetics compared to wt parasites as evidenced by the similar slope of the curves, thus reinforcing a dispensable role for MAEBL during this phase of the parasite life cycle (Fig.14C).

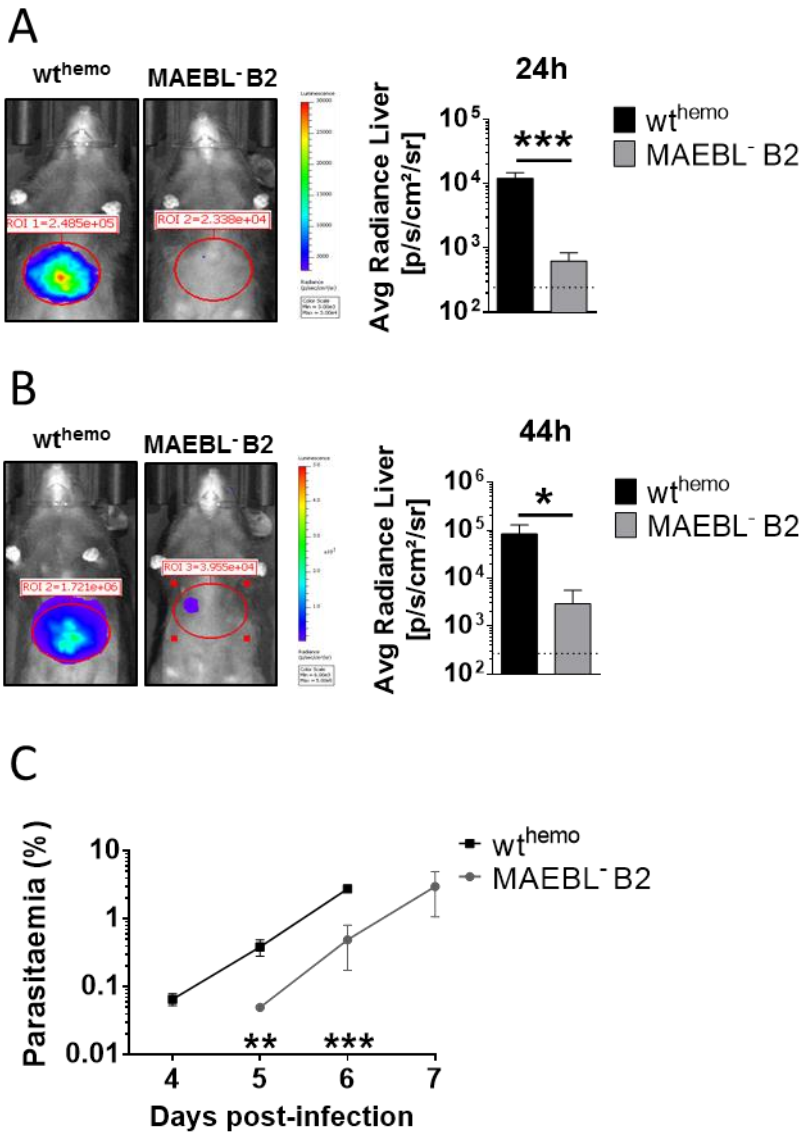

Figure 14– MAEBL⁻ sporozoites have an impaired capacity to infect the liver. C57BL/6 mice were i.v. infected with $5x10^4$ MAEBL⁻ B2 (MAEBL⁻ B2) or wt sporozoites, collected from the hemolymph 19 days after mosquito infection. **A-B.** The infectivity of mutant sporozoites was assessed by quantification of the parasite burden in the liver at 24 h (panel A) and 44 h (panel B) post-infection. The liver load was assessed by whole mice bioluminescence imaging, using an IVIS LUMINA LT upon s.c. injection of 2.1 mg of luciferin. The graphs show the values correspondent to the mean ± SD of the average radiance of bioluminescent signal (photons/second/cm^2/sr) in the liver of 3 to 4 mice. The background levels of bioluminescence calculated from non-infected mice (dotted horizontal lines) are also represented. **C.** The parasitaemia of infected animals starting at day 4 post-infection (square: wt; circles: MAEBL⁻) was determined daily by a Giemsa-stained blood smear. Importantly, only 3 from 4 mice infected with mutant sporozoites became blood-stage positive. The values depicted in the graph represent the mean percentage ± SD of parasitaemia in logarithmic scale. Statistical analysis was performed with an unpaired two-tail Student´s t-test: *, $p < 0.05$; **, $p< 0.01$; ***, $p< 0.001$.

4. MAEBL$^-$ sporozoites do not home to the liver as control sporozoites

To infect the mammalian host, sporozoites need to arrest in the liver sinusoids. In fact, once inside the circulatory system of the host, sporozoites rapidly target the liver, suggesting that this event is mediated by specific interactions between sporozoite surface proteins and host molecules (Frevert *et al.,* 2005). To evaluate whether MAEBL$^-$ sporozoites home to the liver as control sporozoites we have performed the homing assay. For that, Kupffer cells of C57BL/6 mice were first depleted by i.v. injection of clodronate liposomes two days before performing the assay (Tavares *et al.,* 2013). Approximately 1.3x10^5 MAEBL$^-$ and control sporozoites collected from mosquito hemolymph at day 19 were i.v. injected in mice and imaged 7 minutes after using a whole mice live imaging system to quantify the bioluminescent signal in the liver over the total body (Fig.15A). A non-infected mouse injected with luciferin was included to evaluate the background signal. The percentage of bioluminescent signal in the liver was found to be significantly lower in mice injected with MAEBL$^-$ sporozoites than the control, suggesting that MAEBL might be involved on the arrest of sporozoites in the sinusoids (Fig.15A). The progression of the hepatic infection was monitored at 24 (Fig.15B) and 46 hours (Fig.15C) using bioluminescence imaging. As expected, mice infected with MAEBL$^-$ sporozoites present a reduced liver load at both 24 and 46 hours compared to mice infected with control sporozoites (Fig.15B-C) resulting in a two-days delay in the prepatent period of mutant parasites (Fig.15D). No difference was seen in the progression of the blood-stage between mutant and wt parasites (Fig.15D). It is noteworthy to mention, that the lack of statistical significance (Fig.15B-C) might be due to the reduced number of animals per group, a limitation associated at this type of assay, in particular, when it has to be performed with sporozoites collected from hemolymph.

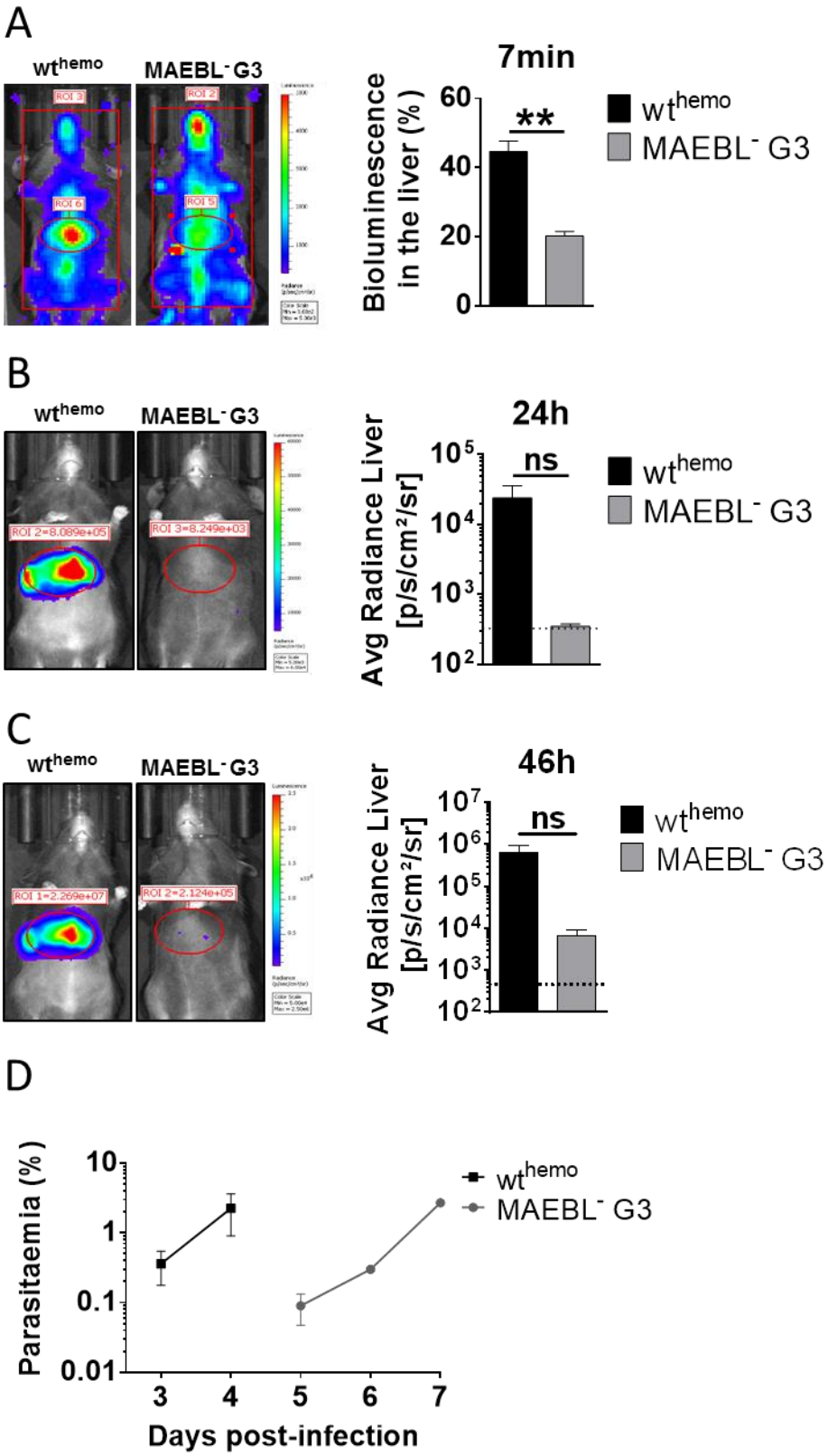
A
wthemo
MAEBL- G3
ROI 3
ROI 2
ROI 6
ROI 5
7min
Bioluminescence in the liver (%)
60
40
20
0
**
wthemo
MAEBL- G3
B
wthemo
MAEBL- G3
ROI 2=8.089e+05
ROI 3=8.249e+03
24h
Avg Radiance Liver [p/s/cm²/sr]
10⁵
10⁴
10³
10²
ns
wthemo
MAEBL- G3
C
wthemo
MAEBL- G3
ROI 1=2.269e+07
ROI 2=2.124e+05
46h
Avg Radiance Liver [p/s/cm²/sr]
10⁷
10⁶
10⁵
10⁴
10³
10²
ns
wthemo
MAEBL- G3
D
Parasitaemia (%)
10
1
0.1
0.01
3
4
5
6
7
Days post-infection
wthemo
MAEBL- G3

Figure 15– MAEBL$^-$ sporozoites cannot properly arrest in the mammalian liver. Imaging the *in vivo* arrest of MAEBL$^-$ sporozoites and monitoring the progress of liver and blood infection. **A-C.** The bioluminescent signal in clodronate treated mice and i.v. injected with 1.3x10^5 MAEBL$^-$ (MAEBL$^-$ G3; n=2) or wt sporozoites (wt^{hemo}; n=2), collected at day 19 from mosquitoes hemolymph and measured at 7 min (panel A), 24 h (panel B) and 46 h (panel C) post-infection by whole mice imaging using an IVIS LUMINA LT and upon s.c. injection of 2.1 mg of luciferin. In A the graph shows the mean percentage bioluminescent signal in the liver (%) ± SD, calculated by dividing the total flux (photons/second) in the liver by the total flux (photons/second) from the animals' total body surface previously subtracted by the respective background calculated from non-infected mice. The graphs shown in B and C depict the mean average radiance of bioluminescence (photons/second/cm^2/sr) ± SD in the liver of mice at 24 h and 46 h after sporozoite inoculation, respectively. The background values of bioluminescence are represented as a dotted horizontal line. **D.** Parasitaemia developed by mice infected with wt hemolymph (square) or MAEBL$^-$ G3 (circle) sporozoites, over time. The values correspond to the mean percentage ± SD of parasitaemia in logarithmic scale. Statistical analysis was performed with an unpaired two-tail Student´s t-test:**, $p < 0.01$; ns, non-significant.

5. MAEBL$^-$ sporozoites are defective in wounding and invading HepG2 cells *in vitro*

To better dissect the defective phenotype of MAEBL$^-$ sporozoites in infecting the liver, we performed *in vitro* assays to evaluate the ability of sporozoites to invade and develop inside host cells. For that, MAEBL$^-$ sporozoites from mosquito's hemolymph and the respective wt control collected from either hemolymph or salivary glands, were incubated with the hepatoma cell line HepG2, during two hours at 37°C. The cells were then washed and either fixed or left in culture for two additional days to evaluate respectively parasites invasion or development. To determine the percentage of cells invaded by sporozoites we used a double labelling technique to distinguish between intracellular and extracellular parasites (Rénia *et al.*, 1988). Based on that, MAEBL$^-$ showed a clear defect in invading HepG2 cells when compared to wt (hemolymph) sporozoites as determined in two independent experiments carried out for each of the two clones (Fig.16A). Additionally, we also observed that wt hemolymph sporozoites displayed a 5 to 14-fold decrease in invasion compared with wt salivary gland sporozoites (Fig.16A). As expected, an approximately 10 to 30-fold reduction in the number of EEFs formed by mutant sporozoites compared to the wt hemolymph sporozoites was observed (Fig.16B). This difference is correlated with the reduced percentage of mutant sporozoites capable of invading HepG2 cells (Fig.16A). Additionally, the number of EEFs formed by wt hemolymph sporozoites was approximately 15 to 30-fold lower than the number formed by wt salivary gland sporozoites (Fig.16B). Moreover, no differences were seen in the size of the few EEFs formed by MAEBL$^-$ compared to wt, suggesting that MAEBL is not necessary for liver-stage development (Fig.16B).

It is well known that sporozoites display an aggressive host cell wounding/traversal behaviour particularly important for their progression in the skin and in the liver (Amino *et al.,* 2008; Tavares *et al.,* 2013*)*. Although not essential for the establishment of the infection (Ishino *et al.*, 2004; 2005a), cell traversal is an important mechanism used by sporozoites either to avoid clearance by Kupffer cells or to cross the liver sinusoidal barrier (Tavares *et al.,* 2013). To evaluate MAEBL$^-$ sporozoites host cell wounding/traversal capacity, HepG2 cells were incubated for 90 min at 37°C with parasites in the presence of PI (Formaglio *et al.,* 2014). The percentage of wounded/traversed cells was determined by the quantification of PI positive cells by fluorescence-activated cell sorting (FACS) analysis (Fig.

16C). The percentage of PI^+ HepG2 cells after incubation with $MAEBL^-$ sporozoites was significant lower than the control with wt hemolymph sporozoites (Fig.16C). Indeed, the percentage of PI^+ cells after contact with $MAEBL^-$ sporozoites was similar to the condition of cells only (Fig.16C). In addition, we also found that wt hemolymph sporozoites display a significant reduction in their CT activity compared to the wt salivary glands sporozoites (Fig.16C).

Altogether these results indicate that the defective infectivity of $MAEBL^-$ sporozoites is invasion and cell traversal-related. However, we cannot ignore that the impaired capacity of these sporozoites to recognize and arrest in the liver might be responsible for the downstream defects such as in invasion and cell traversal. Moreover, our data clearly show that hemolymph sporozoites are less infectious than salivary glands sporozoites, reinforcing the idea that sporozoites maturation in the mosquito salivary glands is required to overcome the biological challenges imposed by the mammalian host.

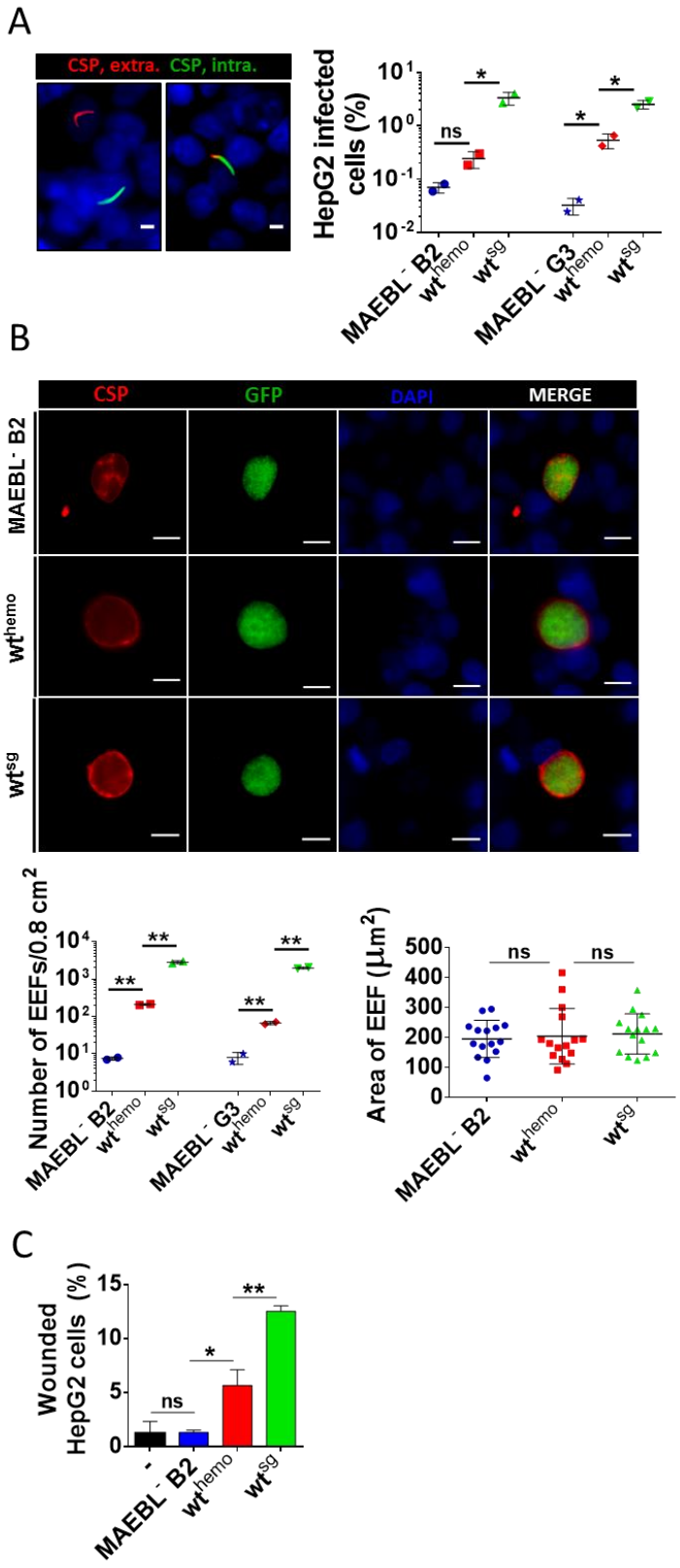
A
CSP, extra. CSP, intra.
HepG2 infected cells (%)
ns
*
*
*
MAEBL⁻ B2
wthemo
wtsg
MAEBL⁻ G3
wthemo
wtsg
B
CSP
GFP
DAPI
MERGE
MAEBL⁻ B2
wthemo
wtsg
Number of EEFs/0.8 cm2
**
**
**
**
MAEBL⁻ B2
wthemo
wtsg
MAEBL⁻ G3
wthemo
wtsg
Area of EEF (µm2)
ns
ns
MAEBL⁻ B2
wthemo
wtsg
C
Wounded HepG2 cells (%)
ns
*
**
-
MAEBL⁻ B2
wthemo
wtsg

Figure 16– MAEBL$^-$ sporozoites cannot properly infect and wound HepG2 cells. A. Quantification of the invasion capacity of MAEBL$^-$ sporozoites after incubation with HepG2 cells for 2 h at 37°C, 5% CO_2. The wide-field immunofluorescence (IFA) images show HepG2 cells infected with wt salivary glands sporozoites, depicting the double staining strategy used to quantify the sporozoites capacity to invade host cells: the surface of sporozoites was stained before and after permeabilization with Triton-X100, using mouse monoclonal anti-CSP antibody (3D11) in combination with Alexa Fluor® 568 anti-mouse IgG or Alexa Fluor® 488 anti-mouse IgG, respectively. Thus, extracellular sporozoites could be seen as red and green, whereas intracellular sporozoites would appear only in green. The nuclei of cells were labelled with DAPI and appear in blue. The red signal was highlighted in order to make it easier to distinguish between extracellular (CSP, extra.) and intracellular parasites (CSP, intra.). An incomplete invasion event of a HepG2 cell by a sporozoite is also demonstrated. The values represented in the graphic correspond to the mean percentage (%) ± SD of invaded HepG2 cells. Two clones were independently tested, clone B2 (MAEBL$^-$ B2, circle) and G3 (MAEBL$^-$ G3, star) along with wt salivary glands (wt^{sg}, triangles) and hemolymph (wt^{hemo}, squares) sporozoites. Scale bar, 5 µm. **B.** Quantification of MAEBL$^-$ EEF development, after incubation of sporozoites with HepG2 cells for 48 h at 37°C, 5% CO_2. IFA images show HepG2 cells infected with MAEBL$^-$ B2, wt salivary glands (wt^{sg}) or wt hemolymph (wt^{hemo}) parasites. Cells were permeabilized and stained with mouse anti-CSP monoclonal antibody (3D11) and rabbit α-GFP antibodies. Primary antibodies were revealed by the addition of Alexa Fluor® 568 anti-mouse IgG (red) and Alexa Fluor® 488 anti-rabbit IgG (green). DNA of parasites and host cells was stained with DAPI and appears in blue (DAPI). The values shown in graphic on the left correspond to the average number of EEFs per well ± SD of duplicates. The graphic on the right shows EEFs area; the values correspond to the mean area ± SD of a randomly chosen sample of 15 EEFs, measured considering the CSP staining. Scale bar, 10 µm. **C.** Assessment of the cell wounding capacity of MAEBL$^-$ sporozoites. MAEBL$^-$ B2, wt hemolymph (wt^{hemo}) or salivary glands (wt^{sg}) sporozoites were incubated with HepG2 cells, at a ratio of 1:2 (parasites:cells), for 90 min at 37°C, 5% CO_2 in the presence of 5 µg/mL PI. The percentage of wounded HepG2 cells was quantified by FACS analysis of PI$^+$ events. The values shown in the graph correspond to the mean ± SD of duplicates or triplicates. Statistical analysis was performed using an unpaired two-tail Student´s t-test or the one-way ANOVA for the comparison of the mean of two or multiple groups, respectively: *, $p<0.05$; **, $p<0.01$; ns, non-significant.

Section II – Thrombospondin-related adhesion protein

1. Generating a *trap* mutant line lacking the cytoplasmic tail in C-terminal

To explore the role of TRAP in mediating the arrest of sporozoites to the liver sinusoids, we have replaced by double crossover homologous recombination in the GFP-luciferase *P. berghei* the single-copy of *trap* by a truncated version lacking the cytoplasmic tail in C-terminal ($TRAP^{ctd-}$ line; Fig.17). For that, we started by constructing the transfection plasmid ($pCTD^{-}$) (Kappe *et al.,* 1999). *Trap* UTRs and the truncated ORF were amplified by PCR, using gDNA as template, and then inserted into the transfection vector pL0001 (MR4) harbouring the selectable marker cassette (TgDHFR-TS gene) (Fig.17A-B). As $TRAP^{ctd-}$ parasites would harbour a selectable marker inserted in their chromosomic locus (Fig.17B), it was necessary to generate another parasite line that could act as an integration control (cTRAP), harbouring the selectable marker inserted in the same region as $TRAP^{ctd-}$ parasites (Fig.18). Therefore, we engineered a plasmid similar to $pCTD^{-}$, named pCTR, differing only in the fact of having the entire, instead of truncated, coding sequence of *trap* (Fig.18A-B). Transfection plasmids, $pCTD^{-}$ and pCTR were digested with the respective restriction enzymes and fragments with the expected sizes obtained (Fig.17C; Fig.18C). The linearized targeting constructs, obtained upon digestion of the vectors with KpnI and BamHI (Fig.17A; Fig.18A), were used for transfections.

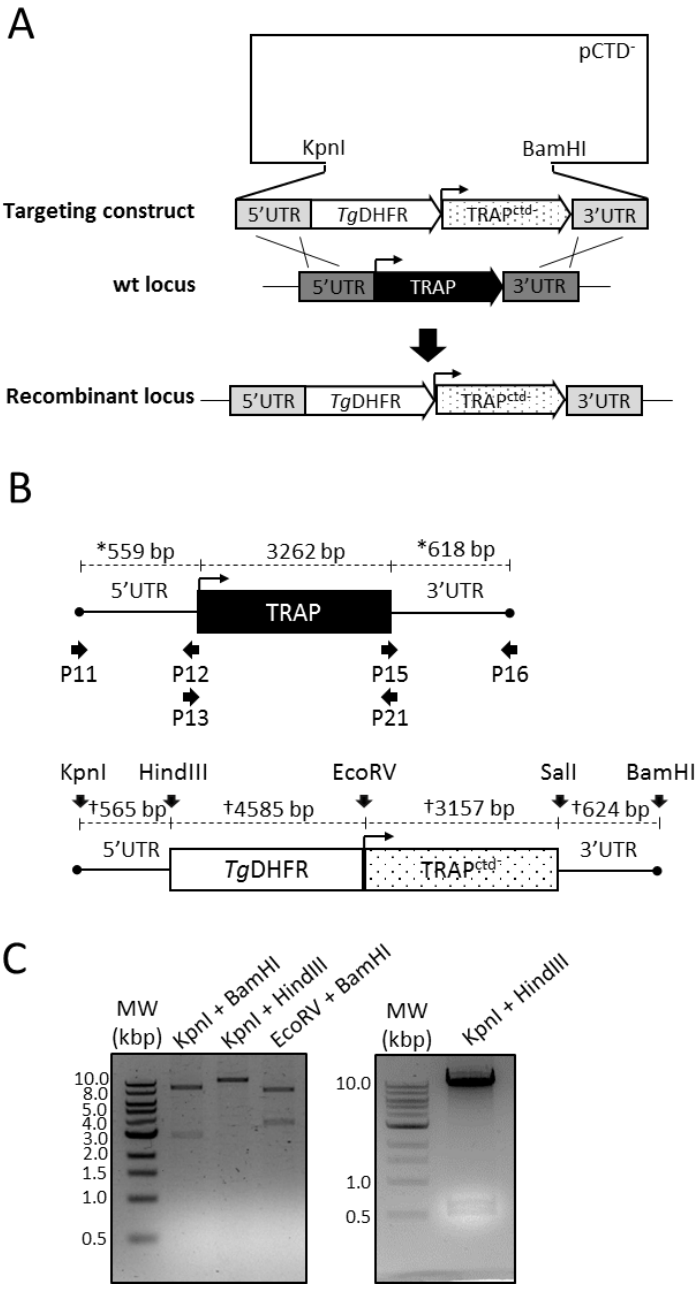

Figure 17– Deletion of TRAP cytoplasmic tail domain in *P. berghei*. A. Schematic representation of the *P. berghei trap* targeted replacement strategy. The PCR amplified *trap* UTRs (3'UTR as well as the portion at 5' of the promoter region; light grey boxes) and pORF^{ctd-} (*trap* promoter region and truncated ORF; white dotted arrow box) were subcloned into a final transfection plasmid, named pCTD^{-} (pL0001, MR4). This plasmid was digested with KpnI and BamHI, in order to obtain the linearized transfection construct, composed by pORF^{ctd-} , the selectable marker cassette (white arrow box) and by the *trap* UTRs. The selectable marker cassette harbours the *T. gondii dhfr-ts* ORF along with the upstream and downstream control elements of *P. berghei dhfr-ts*, and therefore confers pyrimethamine resistance to transfectants. The endogenous promoter and ORF sequences (black arrow box) were targeted via double-crossover homologous recombination, using the endogenous 3'UTR as well as the remaining portion of the 5'UTR (dark grey boxes) as homology regions. The recombinant locus schematizes the expected recombination event. **B.** Restriction maps of wt and recombinant loci (upper and lower diagram, respectively). Asterisks (*) depicts the length of the regions of homology, whereas crosses (†) indicate the length of the integrated regions in the recombinant locus: the UTRs (3'UTR and the portion at 5' of the promoter sequence), the

selectable marker cassette (white box) and the pORF^{ctd-} (white dotted box). The length of the endogenous promoter and ORF (black box) and the primer pairs (horizontal black arrows, P11-13; P15, P16, P21; sequences in Table I) that were used to amplify the integrated regions are depicted in the scheme. **C.** Digestion of pCTD^{-} with the proper restriction enzymes. Digestion products were analysed on 1% agarose gel containing EthBr. MW, molecular weight.

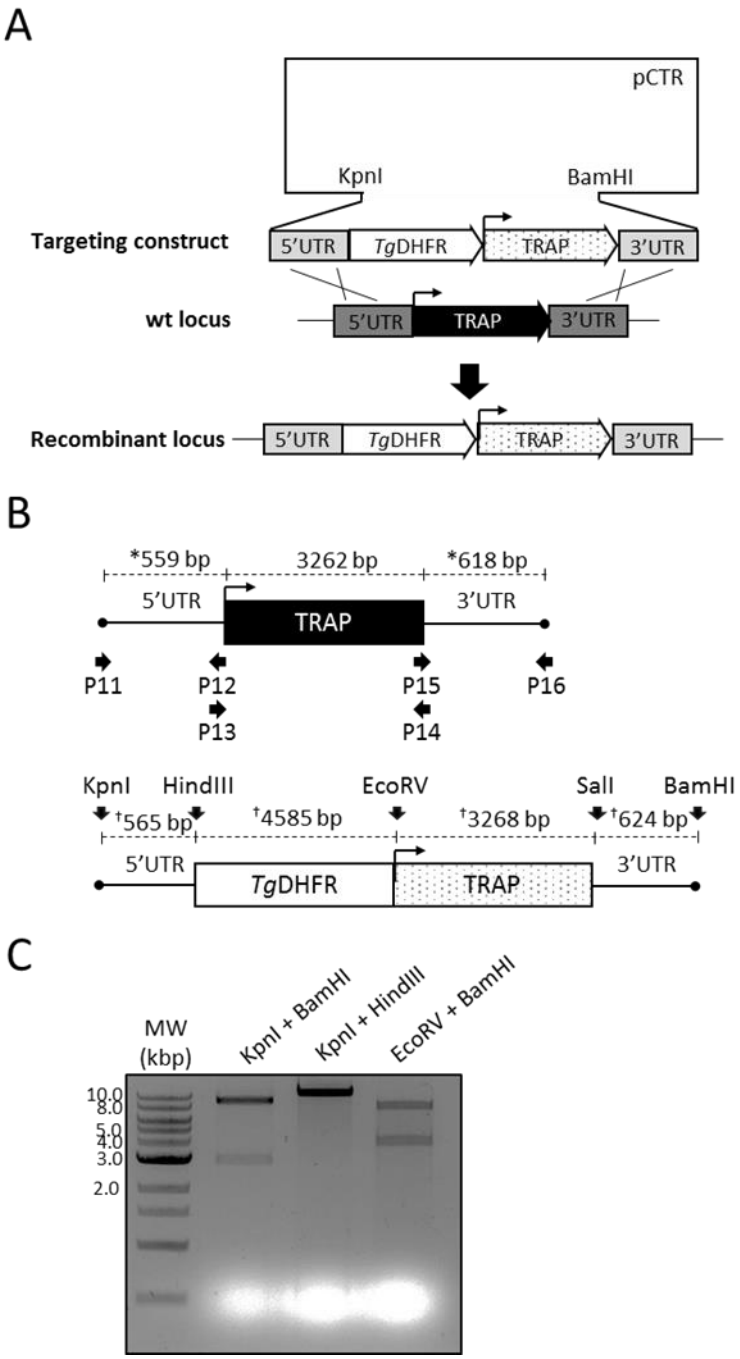

Figure 18– Targeted replacement of *trap* in *P. berghei* to generate the cTRAP line. A. Schematic diagram of the replacement strategy for *trap*. The PCR amplified *trap* UTRs (3'UTR as well as the portion at 5' of *trap* promoter region; light

grey boxes) and pORF (*trap* promoter region and ORF; white dotted arrow box) were subcloned into a final transfection plasmid, named pCTR (pL0001, MR4). The linearized transfection construct, obtained by double digestion of pCTR with KpnI and BamHI, contained the pORF, the selectable marker cassette (white arrow box) and the UTRs. The selectable marker cassette renders transfectants resistant to pyrimethamine since it has the *T. gondii dhfr-ts* ORF along with the upstream and downstream control elements of *P. berghei dhfr-ts*. The *trap* endogenous promoter and ORF sequences (black arrow box) were targeted via double-crossover homologous recombination, using the endogenous 3'UTR as well as the remaining portion of the 5'UTR (dark grey boxes) as regions of homology. The recombinant locus is also shown in the diagram. **B.** Restriction maps of wt and recombinant loci (upper and lower diagram, respectively). Asterisks (*) depict the length of the homology regions in the wt locus, whereas crosses (†) indicate the length of the integrated regions in the recombinant locus: the UTRs (the 3'UTR and the portion at 5' of the promoter sequence), the selectable marker cassette (white box) and the pORF (white dotted box). The length of the endogenous promoter region and ORF (black box), as well as the primer pairs (horizontal black arrows, P11-P16; sequences in Table I) that were used to amplify the integrated fragments are also depicted in the scheme. **C.** Digestion of pCTR with the proper restriction enzymes. Digestion products ran on 1% agarose gel with EthBr. MW, molecular weight.

The transfection of parasites and subsequent drug selection of transfectants was performed as described above. In brief, transfected merozoites were injected into 2 mice, which were treated with pyrimethamine given in drinking water. Infected blood containing the TRAP^{ctd-} or cTRAP parental populations was injected into naïve mice, yielding under drug selection transfer TRAP^{ctd-} and cTRAP populations 1 to 4, respectively. Then, the gDNA of pyrimethamine-resistant populations was analysed by PCR to verify the successful integration of the replaced *trap* ORF in the respective chromosomic locus (Fig.19A-C; Fig.20A-C). Based on the PCR results (Fig.19A-C; Fig.20A-C) cTRAP transfer population 2 and TRAP^{ctd-} transfer population 3 were chosen for cloning by limiting dilution into 14 and 16 mice, respectively. Only 4 mice from each cloning procedure became blood infected, meaning that the cloning efficiency ranged between 25% and 29%, yielding cTRAP B2, B3, R3 and R4 and TRAP^{ctd-} 5, 7, 9 and 11, respectively. Then, the genotype of all cTRAP clonal populations and TRAP^{ctd-} 9 and 11 was analysed by PCR (Fig.19A-D; Fig.20A-C). A first screening was performed to confirm whether the recombinant event occurred in the expected region of the chromosomic locus (Fig.19C; Fig.20C). Indeed, we could amplify the expected DNA fragment when using gDNA of cTRAP clones B2, R3 or R4 and TRAP^{ctd-} clones 9 and 11 as template, but not when using TRAP B3 (Fig.20C). In addition, primers capable to hybridize to the promoter region and final portion of *trap* coding sequence failed to amplify the expected DNA fragment when using gDNA of TRAP^{ctd-} 9 and 11, suggesting the successful replacement of *trap* (Fig.19D). Later, upon gDNA digestion and probing with an amplified DNA fragment corresponding to *trap* 5'UTR used in homologous recombination (Fig.19A, Fig.20A), we were capable to confirm by Southern blot analysis that the correct integration of the selectable marker in the chromosomic locus has been achieved in TRAP^{ctd-} 9 and 11 (Fig.19E) and in cTRAP B2, B3 and R4 (Fig.20D). All populations proved to be genetically homogenous and we found no evidence of wt *trap* locus (Fig.19E; Fig.20D). In the light of these results, cTRAP B2, B3 and R4 and TRAP^{ctd-} 9 and 11 were considered to be clones deserving further analysis.

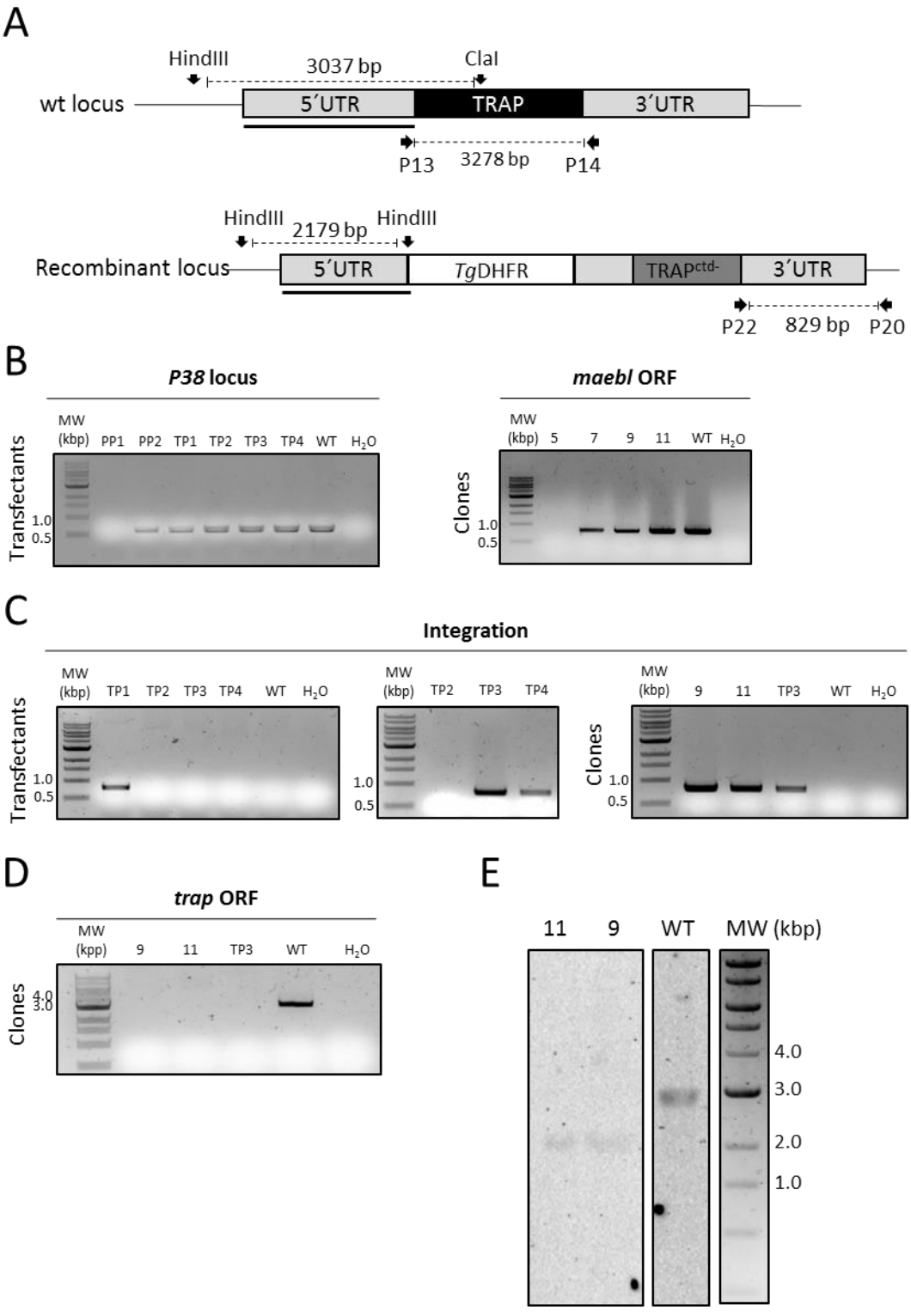

Figure 19- Genotypic analysis of TRAP^{ctd-} mutants. A. Schematic diagram of the wt and recombinant loci. Initially, a genotypic screening of transfectants was performed by PCR: horizontal arrows (P13, P14, P20, P22; sequences in Table I) depict the primer pairs used in the screening. The diagram also shows the Southern blot approach used to analyse the

genotype of mutants: vertical arrows and solid bars represent the cleavage site of restriction enzymes and the used probe, respectively. The length of the expected PCR products and fragments upon digestion of gDNA with HindIII and ClaI are also indicated in the scheme. **B-D.** Genotypic analysis of mutants by PCR. A portion of the ORF from the non-related genes, *P38* (700bp) or *maebl* (800bp) was amplified as a positive control for the PCR reactions (panel B). The integration of the truncated TRAP ORF in the recombinant loci of transfectants, was verified by PCR using the primers P22 and P20, as they bind to the terminal end of truncated ORF ($pORF^{ctd-}$) and to a region of the 3'UTR in the loci, respectively (panel C). An additional PCR analysis of the clones was performed using the primer pair P13/P14 to assess the absence of the full length *trap* ORF in their genome, since the reverse primer P14 binds to the terminal nucleotides of the endogenous *trap* ORF (panel D). In every reaction, gDNA of wt parasites (WT) was used as a control (panels B-D). PCR products were run on 1% agarose gel with EthBr. PP, parental population; TP, transfer population; H_2O, blank; MW, molecular weight. **E.** Genomic Southern blot analysis of $TRAP^{ctd-}$ clones (9 and 11), upon double digestion with HindIII and ClaI and probed with the 5'UTR probe. gDNA of wt parasites (WT) was included as a control. MW, molecular weight.

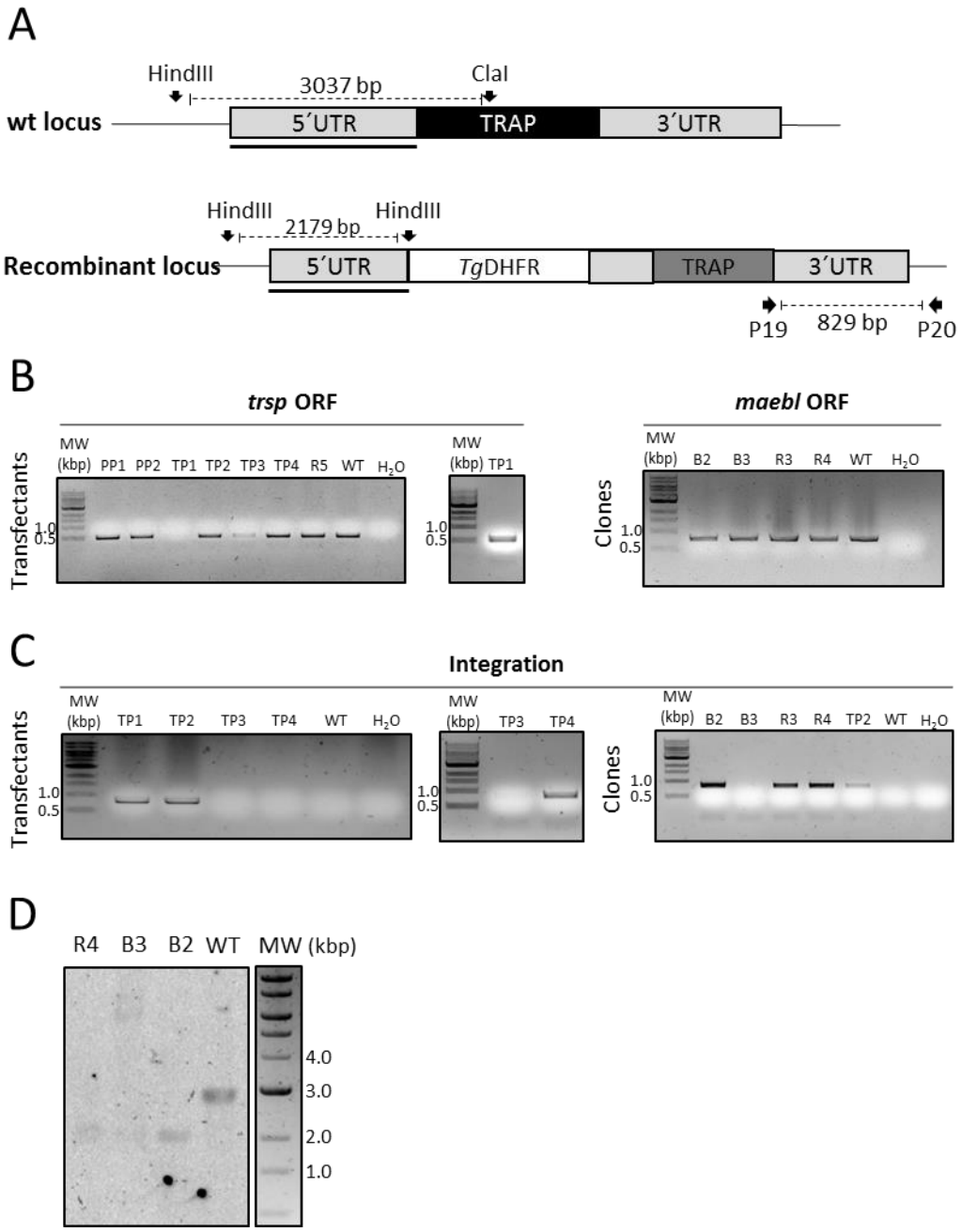

Figure 20- Genotypic analysis of the cTRAP mutants. A. Schematic diagram of the wt and recombinant loci. First, transfectants were screened by PCR; horizontal arrows (P19, P20; sequences in Table I) represent the primer pair used in the screening. Vertical arrows and solid bars are inherent to the Southern blot approach and represent the cleavage site of restriction enzymes and the probe that was used, respectively. The length of the PCR products and fragments upon digestion of gDNA with HindIII and ClaI are also shown in the diagram. **B-C.** Genotypic analysis of mutants by PCR. The amplification of non-related genes, i.e. portions of the *trsp* ORF (600bp) and *maebl* ORF (800bp), was performed as a positive control for the PCR reactions (panel B). Integration on the *trap* loci was evaluated by using the primer pair P19 and P20 as they bind to the terminal end of pORF and to a region of the *trap* 3'UTR in the loci, respectively (panel C). In every reaction, gDNA of wt parasites (WT) was used as a control (panels B-C). Additionally, gDNA of transfer population 2 (TP2)

was used a positive control in the Integration PCR analysis of cTRAP clones (panel C). PCR products were run on 1% agarose gel with EthBr. PP, parental population; TP, transfer population; H_2O, blank; MW, molecular weight. **D,** Genomic Southern blot analysis of cTRAP clones B2, B3 and R4, upon double digestion with HindIII and ClaI and probing with *trap* 5'UTR. gDNA of wt parasites (WT) was included as a control. MW, molecular weight.

2. Evaluating cTRAP and TRAP^{ctd-} parasites infectivity

According to previous studies, sporozoites with TRAP lacking a cytoplasmic tail have no defect on their asexual blood-stage, infect normally the mosquito midgut and form viable sporozoites that egress normally from oocysts when mature (Kappe *et al.*, 1999). However, TRAP^{ctd-} sporozoites failed to infect the salivary glands of mosquitoes as well as the rat liver (Kappe *et al.,* 1999).

To assess the infectivity of mutant parasites to the anopheline vector, mosquitoes were allowed to feed on mice infected with wt, cTRAP (clone B2) or TRAP^{ctd-} (clone 9) erythrocytic-stages. Mosquitoes were dissected 20 days after the infectious blood meal and the sporozoites associated with their hemolymph and salivary glands were counted. Similar numbers of sporozoites were found in the hemolymph of mosquitoes infected with the different parasites, suggesting that cTRAP (clone B2) and TRAP^{ctd-} (clone 9) sporozoites can develop and egress normally from oocysts (Fig.21). In sharp contrast, dramatically fewer sporozoites were found in the salivary glands of mosquitoes infected with TRAP^{ctd-} (clone 9) compared to cTRAP (clone B2) or wt parasites (Fig.21).

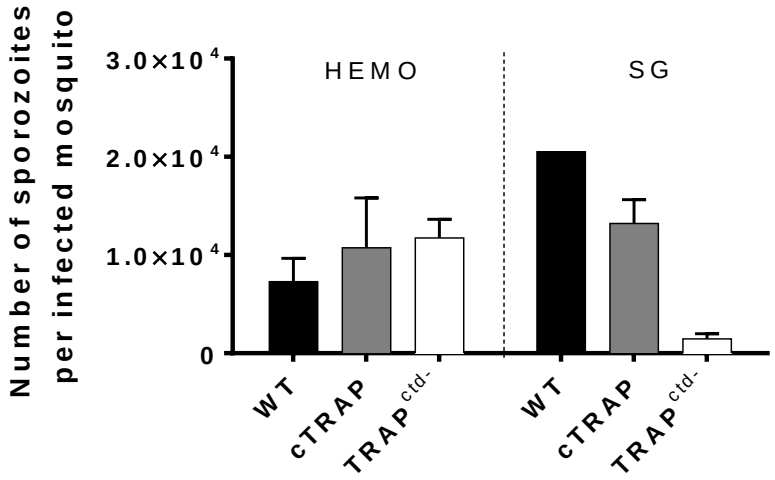

Figure 21– TRAP cytoplasmic tail is crucial for the infection of mosquito salivary glands by sporozoites. *A. stephensi* mosquitoes were allowed to fed on mice infected with wt, cTRAP (clone B2) or TRAP^{ctd-} (clone 9) erythrocytic-stages. Female mosquitoes were dissected 20 days after the infectious blood meal and the sporozoites collected from their hemolymph (HEMO) and salivary glands (SG) were quantified by microscopy. The values correspond to the mean ± SD of the number of sporozoites per mosquito and are representative of 2 independent experiments.

Then, the infectivity of cTRAP (clone B2) sporozoites to the mammalian host was assessed by whole-body bioluminescence imaging in C57BL/6 mice at 24 (Fig.22A) and 44 hours (Fig.22B) after i.v. injection. As expected, mutant sporozoites were capable of infect and develop in the liver as wt sporozoites (Fig.22A-B). Moreover, both parasite populations induced blood-infections with similar

pre-patent periods (Fig.22C). In addition, we found no differences in the mean parasitaemia of infected mice and in the growth kinetics of asexual blood-stage parasites between groups over time (Fig.22C).

Finally, we investigated whether TRAP^{ctd-} (clone 9) sporozoites were capable to infect the liver. Similar to the experiments using MAEBL^{-} sporozoites, TRAP^{ctd-} sporozoites were collected from the mosquito hemolymph. Thus, C57BL/6 mice were infected i.v. with hemolymph TRAP^{ctd-} or cTRAP sporozoites and imaged at 24 (Fig.23A) and 44 hours (Fig.23B). At 24 and 44 hours, mice infected with TRAP^{ctd-} (clone 9) sporozoites presented a significantly lower infection in the liver compared to control group (Fig.23A-B). Moreover, none of the mice infected with TRAP^{ctd-} sporozoites developed a blood infection, in sharp contrast with the control group, which became blood-stage positive at day 3 post-infection (Fig.23C).

Together, these results demonstrated that TRAP^{ctd-} sporozoites have a defect to infect both the mosquito salivary glands and rodent liver. In addition, we confirmed that the insertion of the selectable marker in the TRAP locus (cTRAP) did not compromise sporozoites fitness. Therefore, these mutant lines can be used in further experiments aiming to explore the role of TRAP in mediating the arrest of sporozoites to the liver.

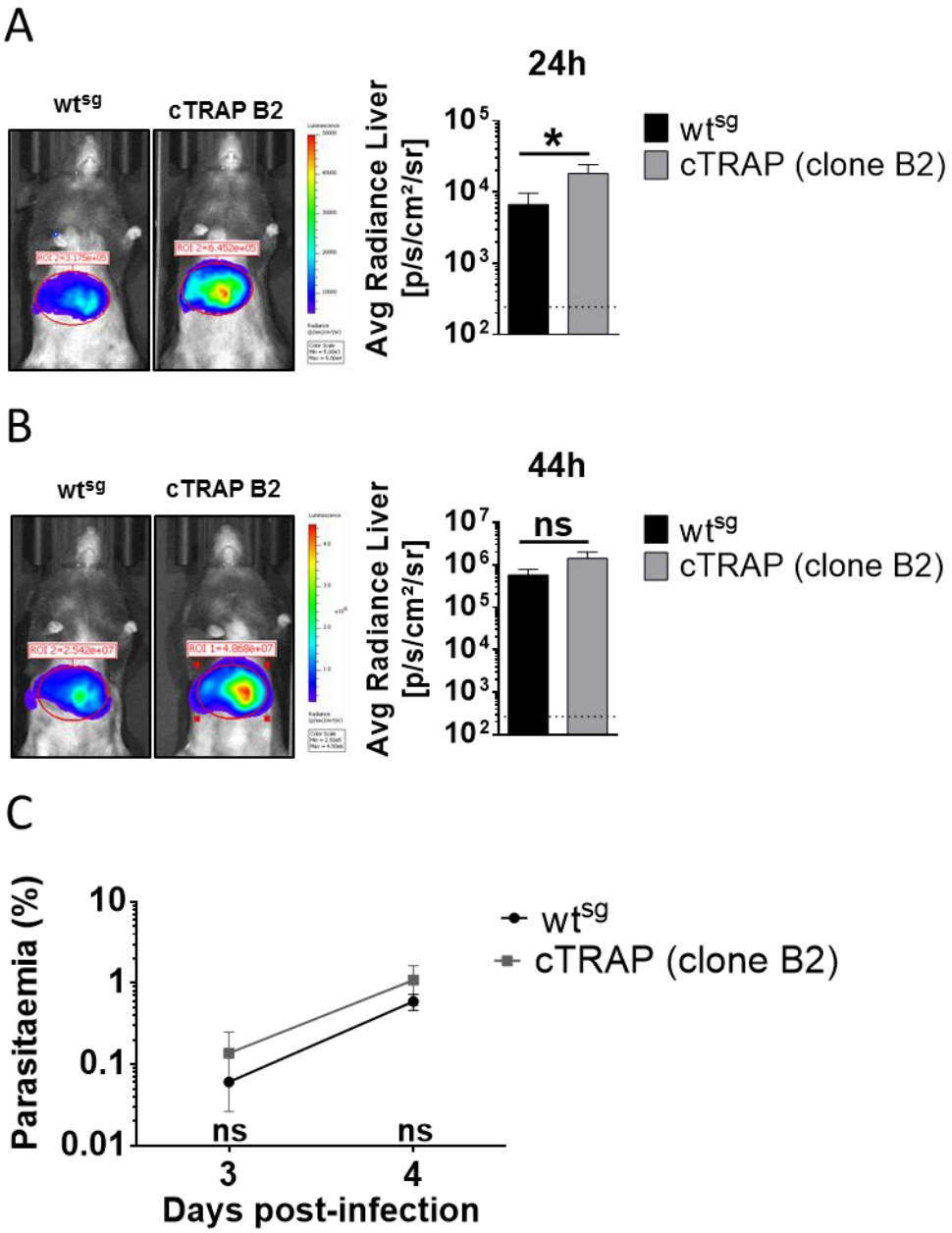

Figure 22- cTRAP sporozoites infect the liver as wt sporozoites. C57BL/6 mice were i.v. infected with $3x10^4$ sporozoites, collected from mosquitoes salivary glands 20 days after the infectious blood meal. **A-B.** cTRAP (cTRAP clone B2) and wt sporozoites infectivity to the mammalian host was assessed by quantification of the parasite burden in the liver of mice at 24h (panel A) and 44h (panel B) after infection. The liver load was quantified by whole mice bioluminescence imaging, using an IVIS LUMINA LT upon s.c. injection of 2.1 mg of luciferin. Bioluminescence was measured in average radiance and is expressed as photons per second per cm^2 per sr. The values depicted in the graphics correspond to the mean ± SD (n=3) of the average radiance, whereas the dotted horizontal line represents the background signal. **C.** Parasitaemia of infected mice over time. The values depicted in the graphic correspond to the mean parasitaemia ± SD in logarithmic scale. Statistical analysis was performed with an unpaired two-tail Student´s t-test: *, $p < 0.05$; ns, non-significant.

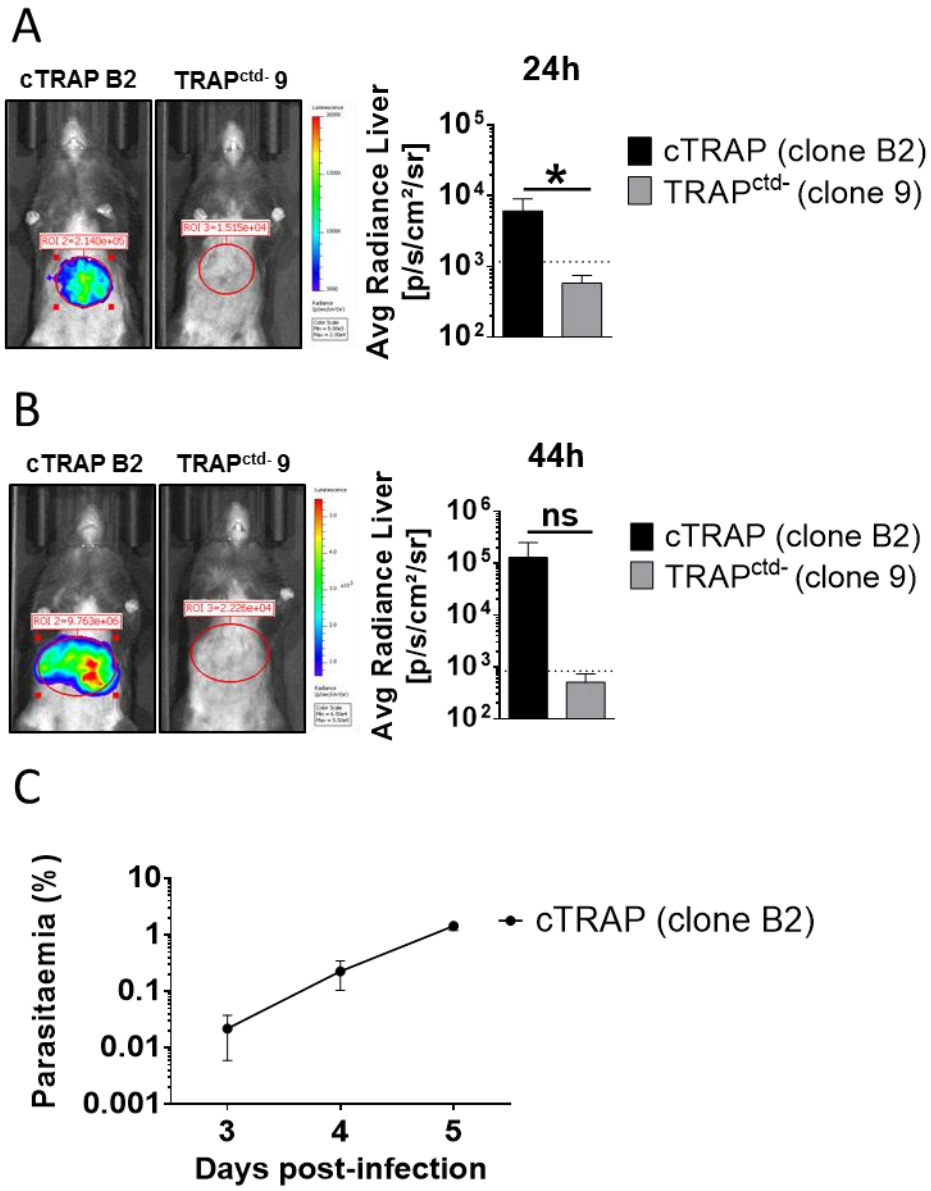

Figure 23– The cytoplasmic tail of TRAP is essential for sporozoites infection of the liver. C57BL/6 mice were infected i.v. with $3x10^4$ TRAP^{ctd-} or cTRAP sporozoites, collected from the mosquitoes' hemolymph 20 days after the infectious blood meal. **A-B.** The liver load was assessed by whole mice bioluminescence imaging, at 24h (panel A) and 44h (panel B) post-infection using an IVIS LUMINA LT upon s.c. injection of 2.1 mg of luciferin. The graphics show the mean ± SD (n=3) of the average radiance in the liver (photons/second/cm^2/sr), as well as the background level of bioluminescence (dotted horizontal line). **C.** Progress of the blood-infection, expressed as mean parasitaemia ± SD in logarithmic scale. Importantly, none of the mice infected with TRAP^{ctd-} sporozoites became infected. Statistical analysis was performed with an unpaired two-tail Student´s t-test: *, $p < 0.05$; ns, non-significant.

Chapter IV

Discussion and Conclusions

Section I – Apical membrane antigen/erythrocyte binding-like protein

1. MAEBL might be an important parasite ligand during *Plasmodium* pre-erythrocytic stage

This study provides the first genetic evidence that MAEBL might be required for the liver infection by sporozoites. Indeed, we found that *maebl* knockout sporozoites from mosquitoes' hemolymph were at least 10 fold less infectious to mice than wt (Fig.14). Moreover, the *in vivo* results were supported by the *in vitro* experiments, in which impairment in the sporozoites invasion and wounding of hepatocytes, but not in liver-stage development, was observed (Fig.16). Our findings also suggest that the impaired capacity of these sporozoites to recognize and arrest in the liver might be responsible for the downstream defects such as in invasion (Fig.15). However, some of our findings are in conflict with the Kariu *et al.* study in 2002, in which MAEBL was found to be required only for sporozoites invasion of the mosquito salivary glands but not to liver infection. It's noteworthy to mention that in contrast to our study, the *in vivo* experiments were performed using midgut rather than hemolymph sporozoites (Kariu *et al.,* 2002). It is known for long time that midgut sporozoites cannot infect the mammalian host at the same extent as hemolymph and salivary glands sporozoites (Vanderberg, 1975). Furthermore, it was demonstrated that midgut sporozoites are less motile than more mature parasite stages, such as hemolymph or salivary glands sporozoites (Hegge *et al.,* 2009; Kudryashev *et al.,* 2012; Sato *et al.,* 2014). Indeed, several genes important for the sporozoite infectivity to the mammalian host are regulated during the sporozoite journey in the mosquito, which can justify the poor infective capacity of midgut sporozoites (Matuschewski *et al.,* 2002b; Mikolajczak *et al.,* 2008). Thus, it is possible that a potential defect in the infectivity of their *maebl* knockout sporozoites may have been missed, since midgut sporozoites, are *per se*, very poorly infectious to the rodent liver. Despite this discrepancy, our results are in agreement with the Kariu's study concerning the mutant sporozoites phenotype in the invertebrate host. Moreover, we also found no differences in the kinetics of blood-stage replication of mutants compared to wt parasites (Kariu *et al.,* 2002).

Interestingly, a previous study performed by Preiser and colleagues in 2004 shows that liver stage development of *P. yoelii* parasites were inhibited from approximately 30% to 40%, when sporozoites were incubated with rabbit antiserum prepared against the extracellular domains of MAEBL (Preiser *et al*., 2004). However, in this study the authors only counted the number of schizonts formed 48 hours after infection and did not evaluate sporozoite invasion capacity in the presence of MAEBL antisera. Thus, our results refine the previous observations reported by Preiser and colleagues, since we could directly demonstrate that the absence of MAEBL hinders the sporozoite invasion of hepatocytes (Fig.16A), resulting in a lowered number of EEFs formed compared to control conditions (Fig.16B).

2. A conserved system for sporozoites recognition of distinct host cell molecules?

Our results suggest that MAEBL may be an important ligand for the sporozoite infection of the mammalian host. At first glance, it is not expected that the same recognition system operate in both,

the mosquito salivary glands and in the liver of the mammalian host. However, as different stages or specie-specific adhesins allow the interaction between apicomplexan parasites and diverse host molecules using a conserved actin-myosin motor (Münter *et al.,* 2009), we hypothesize that an analogous system is on the basis of the recognition and commitment of sporozoites invasion of distinct cells and hosts. In our hypothesis, MAEBL would act as a shapable adhesive molecule capable to interact with host molecules expressed at the surface of acinar and liver cells of the invertebrate and vertebrate host, respectively. Indeed, based on the literature, midgut sporozoites express different forms of MAEBL when compared to salivary glands. MAEBL was detected as two products with 90kDa and 96kDa majorly in mature midgut sporozoites and as a 240kDa in salivary gland sporozoites, henceforth called smaller and full-length product, respectively (Preiser *et al.*, 2004). Interestingly, an independent study suggested that the smaller products are formed due to post-translational modifications of the protein controlled in a time-dependent manner during sporozoites development in the oocyst (Singh *et al.*, 2004). Specifically, the full-length product starts to be expressed by immature midgut sporozoites 7 days after the infection of mosquitoes. However, as midgut sporozoites mature, the full-length product is post-translational modified until being completely absent from midgut sporozoites at day 14 post mosquito infection (Singh *et al.,* 2004). Thus, the smaller products appear to be representations of amino and carboxyl fragments originated from the post-translational modification of the protein (Preiser *et al.,* 2004). In addition, during sporozoite maturation in the oocyst, the subcellular localization of MAEBL also varies. At day 15 post-mosquito infection, MAEBL is still restricted to the apical pole of sporozoites, however, from that day forward, MAEBL starts to be distributed among the sporozoite surface, in agreement with the fact that MAEBL is required for the sporozoite infection of mosquito salivary glands (Srinivasan *et al.*, 2004). Once inside the salivary glands, sporozoites re-express the full-length MAEBL product spread over the parasite surface (Srinivasan *et al.,* 2004*;* Preiser *et al.,* 2004*;* Singh *et al.,* 2004), possibly required for the establishment of a successful infection of the mammalian host liver. Hypothetically speaking, sporozoites could resort to post-translational modifications of MAEBL to refine the affinity of a conserved system, also composed by several others important adhesins such as TRAP and CSP, in order to recognize different host receptors. Thus, it would be interesting to suggest that the smaller products of MAEBL, expressed majorly by mature midgut sporozoites (Singh *et al.,* 2004; Preiser *et al.*, 2004), and possibly by hemolymph sporozoites, may contribute for the infectivity of mosquito salivary glands, whereas the full-length product participates in the sporozoite infectivity of the liver. To explore this hypothesis, it would be interesting to first, confirm by western blot that hemolymph sporozoites do not express the full-length product of MAEBL and second, to assess whether sporozoites expressing the former product were capable to infect the mosquito salivary gland as the same extent as hemolymph sporozoites. Specifically, this could be tested, for example, by injecting wt salivary glands or hemolymph sporozoites into the hemolymph of non-infected mosquitoes and then determine their capacity to infect the mosquito salivary glands.

It was previously suggested that the reduced number of *maebl* knockout sporozoites collected from the mosquito salivary glands was correlated with the sporozoite incapacity to adhere to acinar

cells of the mosquito salivary glands, contrarily to *trap* knockout sporozoites, which can form a trypsin-sensitive junction with those cells, to be shortly thereafter arrested due to their lack of motility (Sultan *et al.,* 1997; Kariu *et al.,* 2002). A similar phenomenon may occur during the infectivity of the mammalian host liver by sporozoites, i.e. *maebl* knockout sporozoites may not be able to properly adhere to host molecules specifically expressed by liver cells. Indeed, our results showed that MAEBL$^-$ sporozoites display an impaired capacity to home to the liver (Fig.15A), as well as impaired invasion and hepatocyte traversal capacity *in vitro* (Fig.16A,C). Altogether, these findings suggest that MAEBL may act as an adhesin capable to bind to molecules expressed by hepatocytes and thus contribute for the establishment of a successful infection in the mammalian host liver.

In this work, we show that sporozoites use a conserved MAEBL dependent-mechanism to infect the salivary glands and the liver of invertebrate and vertebrate host, respectively. In addition, we speculate that this phenomenon might be regulated through post-translational modifications of the protein. In apicomplexan parasites, post-translational modification of proteins are associated with important processes such as gliding motility, invasion of host cells, growth and cell regulation and gene expression (Jortzik *et al.,* 2011). This may acquire a particular importance in *Plasmodium* parasites due to their relatively small genome, which does not reflect the complexity of their life cycle (Singh *et al.,* 2004). Although important, MAEBL will not certainly be the unique protein that participates in the process of sporozoite host cell recognition. Instead, we suggest that MAEBL may act along with other surface sporozoite proteins such as TRAP (Fig.8) and CSP (Coppi *et al.* 2011), for host cell recognition. The strong defective phenotype of *maebl* knockout sporozoites in both hosts might suggest a possible role of MAEBL as an "adapter" protein in the conserved molecular system, allowing the sporozoite interaction with distinct host molecules without having to completely modify the whole system during its journey from the vector to the mammalian host liver.

3. Future directions

The unexpected phenotype of MAEBL$^-$ in the mammalian host is worth to be further investigated. The next step is undoubtedly to complement the *maebl* knockout parasites, in order to confirm that their defective phenotype is due to the absence of MAEBL. The figure 24 depict a possible strategy to complement MAEBL$^-$ parasites. In brief, the complementation plasmid will be linearized under the *maebl* 5'UTR, to promote its insertion via single crossover homologous recombination in the recombinant loci of MAEBL$^-$ parasites. The re-insertion of *maebl* needs to be performed using the *maebl* 5'UTR as homology region, since this gene is transcribed together with the upstream gene, as a bicistronic transcript (Balu *et al.,* 2009). To distinguish between complemented from *maebl* knockout parasites, the human *dhfr* (*hdhfr*) will be used as selectable marker, rendering transfectants resistant to the anti-folate drug WR99210 (Sultan *et al.,* 2001). We expect that, once the targeting construct is inserted into the *maebl* locus, complemented parasites will be able to express MAEBL and their defective phenotype restored.

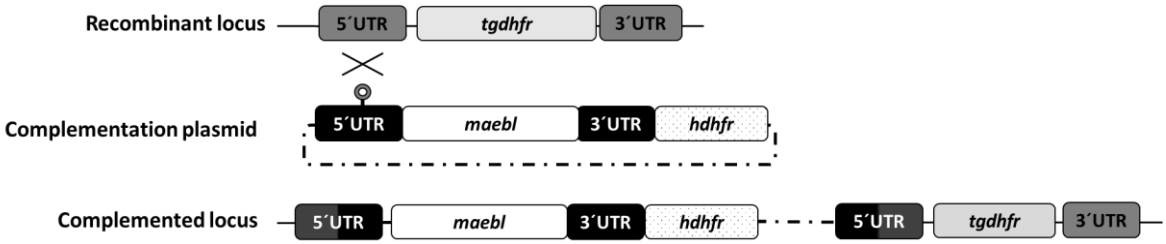

Figure 24- Genetic complementation of MAEBL⁻ parasites. Schematic diagram showing the recombinant locus of MAEBL⁻ parasites, the complementation plasmid and the expected complemented locus. The recombinant locus, containing the *tgdhfr* (light grey box) flanked by the *maebl* UTRs (dark grey boxes), will be targeted via single crossover homologous recombination using the 5'UTR as homology region and upon linearization of the complementation plasmid. The complementation plasmid will be engineered in order to contain the *hdhfr* (dotted white box), the MAEBL gene (white box) along with the *maebl* UTR's (black boxes); the plasmid backbone is represented as a dashed line. The complemented locus will result from the insertion of the whole complementation plasmid in the recombinant locus of MAEBL⁻ parasites.

In addition, it would be interesting to clarify the controversy over the secretory organelle to which MAEBL is associated. Indeed, MAEBL was found to be associated with the rhoptries of *P. yoelii* (Kappe *et al.,* 1998; Noe & Adams, 1998) and *P. falciparum* blood-stage parasites (Blair *et al.,* 2002; Ghai *et al.,* 2002). In addition, a punctuated immunofluorescent pattern limited to the apical pole of *P. berghei* merozoites upon their staining with anti-MAEBL antibodies also suggests that this protein is associated with the rhoptries of parasites (Kappe *et al.,* 1997). Surprisingly, MAEBL was found in association not with the rhoptries by with the micronemes of *P. berghei* sporozoites (Kariu *et al.,* 2002). Thus, it would be interesting to find an independent evidence that MAEBL co-localizes with the sporozoite micronemes, using a specific micronemal marker, such as TRAP (Rennenberg *et al.,* 2010). If so, the localization of MAEBL in *P. berghei* blood-stages would have to be assessed again, in order to understand if MAEBL is capable to associate with different secretory organelles in a specie or parasite developmental stage-dependent fashion.

Lastly, it will be necessary to generate another mutant line capable to replace MAEBL⁻ as control in further experiments aiming the assessment of the homing capacity of mutant sporozoites. Using a genome-wide expression screen with *P. yoelii*, it was discovered several genes upregulated in midgut sporozoites and downregulated in salivary glands sporozoites (Mikolajczak *et al.,* 2008). Among them, the *upregulated in oocyst sporozoites 3* (*UOS3*) seems to constitute a potential candidate to be used in future experiments, since it was proven that UOS3-null mutants are incapable to infect the mosquito salivary glands, but have no defect in their infectivity to the mammalian host (Mikolajczak *et al.*, 2008).

4. Significance of the study

The findings of this study contributed to the overall knowledge about the molecular mechanisms that occur during host-parasite interactions in the pre-erythrocytic stage of *Plasmodium* life cycle. Indeed, we provide the first genetic evidence that in the absence of MAEBL, sporozoites have a defect in their capacity to target and then infect the liver. Furthermore, we hypothesize that a model based on the existence of a conserved system in which the post-translational modifications of MAEBL may

contribute for the successful sporozoite infection of both the mosquito salivary glands and the mammalian liver. The importance of this protein in the establishment of sporozoites liver infection, along with the fact of being highly immunogenic (Peng *et al.,* 2016), renders MAEBL as a promising target to be included in a multivalent pre-erythrocytic-stage malaria vaccine.

Section II - Thrombospondin-related adhesion protein

According with previous studies, genetic modifications of the cytoplasmic tail of TRAP render parasites non-infectious for the mosquito salivary glands and the rodent liver (Kappe *et al.,* 1999; Heiss *et al.,* 2008). In agreement, we observed that TRAP^{ctd-} sporozoites were barely found in association with the mosquito salivary glands (Fig.21) and failed to infect the liver (Fig.23A-B) and consequently, the blood (Fig.23C). Thus, we consider that our results provide an independent evidence for the essentiality of TRAP cytoplasmic tail in sporozoite infectivity to the mammalian host. This may be particularly important since, to the best of our knowledge, this is the first study to analyse TRAP cytoplasmic tail mutant sporozoites phenotype in the mammalian host by real-time *in vivo* bioluminescence imaging.

As the next step, it would be interesting to explore the defective phenotype of TRAP^{ctd-} sporozoites in the mammalian host, since their lack of infectivity may also be associated with a defective homing capacity to the liver. The absence of the C-terminal portion of the cytoplasmic tail of TRAP may lead to cumulative defects in sporozoites infectivity to the mammalian host if it renders sporozoites incapable to arrest in the liver sinusoids besides affecting their motility and invasion capacity. If so, it will be possible to assess the importance of gliding motility in the sporozoites homing to the liver. But before using TRAP^{ctd-} sporozoites in further experiments, it is imperative to firstly check if these mutant parasites are capable to properly express TRAP at their surface, since the phenotype of TRAP^{ctd-} sporozoites is undistinguishable from the phenotype of *trap* knockout sporozoites (Sultan *et al.,* 1997).

The homing capacity of TRAP^{ctd-} sporozoites can be easily tested using whole-body bioluminescence imaging of infected animal. However, the existence of a control line is required to exclude the hypothesis that any detectable impairment in the homing capacity of TRAP^{ctd-} sporozoites is due to the presence of the selectable marker cassette in their genome. Thus, we constructed the cTRAP parasite line to act as an integration control. As we have shown, the insertion of the *tgdhfr-ts* gene in the *trap* locus does not interfere with sporozoites capacity to infect both, the invertebrate and the mammalian host (Fig.21; Fig.22).

Taking in consideration these results, we conclude that the TRAP^{ctd-} and cTRAP mutant lines are valuable tools to be used in future experiments aiming the study of the role of TRAP as an adhesive molecule and/or TRAP associated-gliding motility in mediating the homing of the sporozoites to the liver.

Chapter V

Annex

Table I- List of primers used in this study. The table shows the primers used for the construction of pΔMAEBL, pCTR and pCTD$^-$, as well as for the genotypic analysis of mutant parasites. The restriction sites are underlined.

	Primer name	Sequence (5' – 3')
P1	MAEBL_5'UTR F	TTGGTACCGCAAAGAACAACATGCATAC
P2	MAEBL_5'UTR R	GCATCGATGAAAGACACGAAACACAAG
P3	MAEBL_3'UTR F	GGGAATTCTCGCCCCAATTATATTACC
P4	MAEBL_3'UTR R	TTGGATCCGCTAAGAAAGCTTGCCATAC
P5	MAEBL_ORF_F	GGGCATAGATAACCCACAAG
P6	MAEBL_ORF_R	ACATGGCCCGATACAATGAG
P7	TgDHFR/TS_ORF_end_F	CCCATTGTGAACATCCTCAAC
P8	MAEBL_LOCUS_3'_R2	CAACCGTCGAAGGCATAAATTAG
P9	TRSP_ORF_F	GTGCTCAAATAATCAACCTGTTG
P10	TRSP_ORF_R	TCCCTTCAGAATTGTCAGGAC
P11	TRAP_5'UTR_F	AAGGTACCAAATAATCAAATTGGAGGTATC
P12	TRAP_5'UTR_R	GGAAGCTTAGGAATAATATGGGTAAGAC
P13	TRAP_PROM_F	CGGATATCGTGGTGGATATTATTTATGAG
P14	TRAP_ORF_R	TTGTCGACTTAGTTCCAGTCATTATCTTC
P15	TRAP_3'UTR_F	CCGTCGACTTTTAATAAACATATATATC
P16	TRAP_3'UTR_R	AAGGATCCACTTAAGAGTATTATTTTTG
P17	TgDHFT/TS_ORF_F	CCACTTGACCACAGATTTC
P18	TgDHFR/TS_ORF_R	GTTGAGGATGTTCACAATGG
P19	TRAP_INT_R	GAAGATAATGACTGGAACTAAGTCGAC
P20	TRAP_3'locus_F	CTCCAGACATAATAACACAGATATGA
P21	TRAPctd$^-$_ORF_R	TTGTCGACTTAGCTACTTCCTGCTATAAAA
P22	TRAPctd$^-$_INT_R	TTTATAGCAGGAAGTAGCTAAGTCGAC
P23	P38_ORF_F	CGACTGTTTCCCCTGGTGATGCA
P24	P38_locus_R	TGGTACGCAATGTGTGAATTTCCGT

Chapter VI

References

Abrahamsen, M.S., Templeton, T.J., Enomoto, S., Abrahante, J.E., Zhu, G., Lancto, C.A., Deng, M., Liu, C., Widmer, G., Tzipori, S., Buck, G.A., Xu, P., Bankier, A.T., Dear, P.H., Konfortov, B.A., Spriggs, H.F., Iyer, L., Anantharaman, V., Aravind, L. & Kapur, V. (2004). Complete genome sequence of the apicomplexan, *Cryptosporidium parvum*. *Science*, 304(5669), pp.441–5.

Adams, J.H., Hudson, D.E., Torii, M., Ward. G.E., Wellems, T.E., Aikawa, M. & Miller L.H. (1990). The Duffy receptor family of *Plasmodium knowlesi* is located within the micronemes of invasive malaria merozoites. *Cell*, 63(1), pp.141–53.

Adams, J.H., Sim, B. K., Dolan, S.A., Fang, X., Kaslow, D.C., & Miller, L.H. (1992). A family of erythrocyte binding proteins of malaria parasites. *Proceedings of the National Academy of Sciences of the United States of America*, 89(15), pp.7085–9.

Adams, J.C. & Tucker, R.P. (2000). The thrombospondin type 1 repeat (TSR) superfamily: diverse proteins with related roles in neuronal development. *Developmental Dynamics*, 218(2), pp.280–99.

Adams, J.H., Blair, P.L., Kaneko, O. & Peterson, D.S. (2001). An expanding ebl family of *Plasmodium falciparum*. *Trends in parasitology*, 17(6), pp.297–9.

Akhouri, R.R., Bhattacharyya, A., Pattnaik, P., Malhotra, P. & Sharma, A. (2004). Structural and functional dissection of the adhesive domains of *Plasmodium falciparum* thrombospondin-related anonymous protein (TRAP). *The Biochemical Journal*, 379(3), pp.815–22.

Aley, S.B., Bates, M.D., Tam, J.P. & Hollingdale, M.R. (1986). Synthetic peptides from the circumsporozoite proteins of *Plasmodium falciparum* and *Plasmodium knowlesi* recognize the human hepatoma cell line HepG2-A16 in vitro. *The Journal of Experimental Medicine*, 164(6), pp.1915–22.

American Type Culture Collection. (2016). Hep G2 [HEPG2] (ATCC® HB8065™), pp.1–3. Retrieved from https://www.atcc.org/~/ps/HB-8065.ashx.

Amino, R., Thiberge, S., Martin, B., Celli, S., Shorte, S., Frischknecht, F., & Ménard, R. (2006). Quantitative imaging of *Plasmodium* transmission from mosquito to mammal. *Nature Medicine*, 12(2), pp.220–24.

Amino, R., Giovannini, D., Thiberge, S., Gueirard, P., Boisson, B., Dubremetz, J.F., Prévost, M.C., Ishino, T., Yuda, M. & Ménard, R. (2008). Host cell traversal is important for progression of the malaria parasite through the dermis to the liver. *Cell Host & Microbe*, 3(2), pp.88–96.

Anstey, N.M., Douglas, N.M., Poespoprodjo, J.R., & Price, R.N. (2011). *Plasmodium vivax*: clinical spectrum, risk factors and pathogenesis. *Advances in Parasitology*, 80, pp.151-201.

Antony, H.A. & Parija, S.C. (2016). Antimalarial drug resistance: an overview. *Tropical Parasitology*, 6(1), pp.30–41.

Aravind, L., Iyer, L.M., Wellems, T.E. & Miller, L.H. (2003). *Plasmodium* biology: genomic gleanings. *Cell*, 115(7), pp.771–85.

Ashley, E.A., Dhorda, M., Fairhurst, R.M., Amaratunga, C., Lim, P., Suon, S., Sreng, S., Anderson, J.M., Mao, S., Sam, B., Sopha, C., Chuor, C.M., Nguon, C., Sovannaroth, S., Pukrittayakamee, S., Jittamala, P., Chotivanich, K., Chutasmit, K., Suchatsoonthorn, C., Runcharoen, R., Hien, T.T., Thuy-Nhien, N.T., Thanh, N.V., Phu, N.H., Htut, Y., Han, K., Aye, K.H., Mokuolu, O.A., Olaosebikan, R.R., Folaranmi, O.O., Mayxay, M., Khanthavong, M.,

Hongvanthong, B., Newton, P.N., Onyamboko, M.A., Fanello, C.I., Tshefu, A.K., Mishra, N., Valecha, N., Phyo, A.P., Nosten, F., Yi, P., Tripura, R., Borrmann, S., Bashraheil, M., Peshu, J., Faiz, M.A., Ghose, A., Hossain, M.A., Samad, R., Rahman, M.R., Hasan, M.M., Islam, A., Miotto, O., Amato, R., MacInnis, B., Stalker, J., Kwiatkowski, D.P., Bozdech, Z., Jeeyapant, A., Cheah, P.Y., Sakulthaew, T., Chalk, J., Intharabut, B., Silamut, K., Lee, S.J., Vihokhern, B., Kunasol, C., Imwong, M., Tarning, J., Taylor, W.J., Yeung, S., Woodrow, C.J., Flegg, J.A., Das, D., Smith, J., Venkatesan, M., Plowe, C.V., Stepniewska, K., Guerin, P.J., Dondorp, A.M., Day, N.P. & White, N.J. (2014). Spread of artemisinin resistance in *Plasmodium falciparum* malaria. *The New England Journal of Medicine*, 371(5), pp.411–23.

Autino, B., Noris, A., Russo. R. & Castelli, F. (2012). Epidemiology of malaria in endemic areas. *Mediterranean Journal of Hematology and Infectious Diseases*, 4(1), pp.e2012060.

Baer, K., Roosevelt, M., Clarkson, A.B.J., van Rooijen, N., Schnieder, T. & Frevert, U. (2007). Kupffer cells are obligatory for *Plasmodium yoelii* sporozoite infection of the liver. *Cellular Microbiology*, 9(2), pp.397–412.

Baer, K., Klotz, C., Kappe, S.H., Schnieder, T. & Frevert, U. (2007). Release of hepatic *Plasmodium yoelii* merozoites into the pulmonary microvasculature. *PLoS Pathogens*, 3(11), p.e171.

Baird, K., (2015). Origins and implications of neglect of G6PD deficiency and primaquine toxicity in *Plasmodium vivax* malaria. *Pathogens and Global Health*, 109(3), pp.93–106.

Baker, R.P., Wijetilaka, R. & Urban, S. (2006). Two *Plasmodium* rhomboid proteases preferentially cleave different adhesins implicated in all invasive stages of malaria. *PLoS Pathogens*, 2(10), pp.e113.

Balu, B., Blair, P.L. & Adams, J.H. (2009). Identification of the transcription initiation site reveals a novel transcript structure for *Plasmodium falciparum maebl*. *Experimental Parasitology*, 121(1), pp.110–4.

Bannister, L.H., Hopkins, J.M., Fowler, R.E., Krishna, S. & Mitchell, G.H. (2000). A brief illustrated guide to the ultrastructure of *Plasmodium falciparum* asexual blood stages. *Parasitology Today*, 16(10), pp.427–33.

Baum, J., Richard, D., Healer. J., Rug, M., Krnajski, Z., Gilberger, T.W., Green, J.L., Holder, A.A. & Cowman, A.F. (2006). A conserved molecular motor drives cell invasion and gliding motility across malaria life cycle stages and other apicomplexan parasites. *Journal of Biological Chemistry*, 281(8), pp.5197–208.

Besteiro, S., Dubremetz, J.F. & Lebrun, M. (2011). The moving junction of apicomplexan parasites: A key structure for invasion. *Cellular Microbiology*, 13(6), pp.797–805.

Bhanot, P., Frevert, U., Nussenzweig, V. & Persson C. (2003). Defective sorting of the thrombospondin-related anonymous protein (TRAP) inhibits *Plasmodium* infectivity. *Molecular and Biochemical Parasitology*, 126(2), pp.263–73.

Bhanot, P., Schauer, K., Coppens, I. & Nussenzweig, V. (2005). A surface phospholipase is involved in the migration of *Plasmodium* sporozoites through cells. *The Journal of Biological Chemistry*, 280(8), pp.6752–60.

Blair, P.L., Kappe, S.H., Maciel, J.E., Balu, B. & Adams JH. (2002). *Plasmodium falciparum* MAEBL is a unique member of the ebl family. *Molecular and Biochemical Parasitology*, 122(1), pp.35–44.

Bosch, J., Buscaglia, C.A., Krumm, B., Ingason, B.P., Lucas, R., Roach, C., Cardozo, T., Nussenzweig, V. & Hol, W.G. (2007). Aldolase provides an unusual binding site for thrombospondin-related anonymous protein in the invasion machinery of the malaria parasite. *Proceedings of the National Academy of Sciences of the United*

States of America, 104(17), pp.7015–20.

Boucher, L.E. & Bosch, J. (2015). The apicomplexan glideosome and adhesins - Structures and function. *Journal of Structural Biology*, 190(2), pp.93–114.

Brayton, K.A., Lau, A.O., Herndon, D.R., Hannick, L., Kappmeyer, L.S., Berens, S.J., Bidwell, S.L., Brown, W.C., Crabtree, J., Fadrosh, D., Feldblum, T., Forberger, H.A., Haas, B.J., Howell, J.M., Khouri, H., Koo, H., Mann, D.J., Norimine, J., Paulsen, I.T., Radune, D., Ren, Q., Smith, R.K.J., Suarez, C.E., White, O., Wortman, J.R., Knowles, D.P.J., McElwain, T.F. & Nene, V.M. (2007). Genome sequence of *Babesia bovis* and comparative analysis of apicomplexan hemoprotozoa. *PLoS Pathogens*, 3(10), pp.1401–13.

Buscaglia, C.A., Coppens, I., Hol, W.G. & Nussenzweig, V. (2003). Sites of interaction between aldolase and thrombospondin-related anonymous protein in *Plasmodium*. *Molecular Biology of the Cell*, 14(12), pp.4947–57.

Carey, A.F., Ménard, R. & Bargieri, D.Y. (2013). Scoring sporozoite motility. In Ménard, R. ed. *Malaria, Methods and Protocols*. Humana Press, pp. 371–83.

Carey, A.F., Singer, M., Bargieri, D., Thiberge, S., Frischknecht, F., Ménard, R. & Amino R. (2014). Calcium dynamics of *Plasmodium berghei* sporozoite motility. *Cellular Microbiology*, 16(5), pp.768–83.

Carrolo, M., Giordano, S., Cabrita-Santos, L., Corso, S., Vigário, A.M., Silva, S., Leirião, P., Carapau, D., Armas-Portela, R., Comoglio, P.M., Rodriguez, A. & Mota, M.M. (2003). Hepatocyte growth factor and its receptor are required for malaria infection. *Nature Medicine*, 9(11), pp.1363–9.

Cerami, C., Frevert, U., Sinnis, P., Takacs, B., Clavijo, P., Santos, M,J. & Nussenzweig, V. (1992). The basolateral domain of the hepatocyte plasma membrane bears receptors for the circumsporozoite protein of *Plasmodium falciparum* sporozoites. *Cell*, 70(6), pp.1021–33.

Chakravarty, S., Cockburn, I.A., Kuk, S., Overstreet, M.G., Sacci, J.B. & Zavala F. (2007). $CD8^+$ T lymphocytes protective against malaria liver stages are primed in skin-draining lymph nodes. *Nature Medicine*, 13(9), pp.1035–41.

Chamchod, F. & Beier, J.C. (2013). Modeling *Plasmodium vivax*: relapses, treatment, seasonality, and G6PD deficiency. *Journal of Theoretical Biology*, 316, pp.25–34.

Charoenvit, Y., Fallarme, V., Rogers, W.O., Sacci, J.B., Kaur,M., Aguiar, J.C., Yuan, L.F., Corradin, G., Andersen, E., Wizel, B., Houghten, R.A, Oloo, A., De la Vega, P. & Hoffman, S.L. (1997). Development of two monoclonal antibodies against *Plasmodium falciparum* sporozoite surface protein 2 and mapping of B-cell epitopes. *Infection and Immunity*, 65(8), pp.3430–7.

Chobotar, W. & Scholtyseck, E. (1982). Ultrastructure. In Long, P.L. ed. *The Biology of the Coccidia*. University Park Press, pp. 101–65.

Clements, A.N. (2011). *The Biology of Mosquitoes, Transmission of Viroses and Interactions with Bacteria*, CABI, pp-116.

Clyde, D.F. & Shute, G.T. (1957). Resistance of *Plasmodium falciparum* in Tanganyika to pyrimethamine administered at weekly intervals. *Transactions of the Royal Society of Tropical Medicine and Hygiene*, 51(6), pp.505–13.

Combe, A., Moreira, C., Ackerman, S., Thiberge, S., Templeton, T.J. & Ménard R. (2009). TREP, a novel protein necessary for gliding motility of the malaria sporozoite. *International Journal for Parasitology*, 39(4), pp.489–96.

Coppi, A., Pinzon-Ortiz, C., Hutter, C. & Sinnis, P. (2005). The *Plasmodium* circumsporozoite protein is proteolytically processed during cell invasion. *The Journal of experimental medicine*, 201(1), pp.27–33.

Coppi, A., Tewari, R., Bishop, J.R., Bennett, B.L., Lawrence, R., Esko, J.D., Billker, O. & Sinnis, P. (2007). Heparan sulfate proteoglycans provide a signal to *Plasmodium* sporozoites to stop migrating and productively invade host cells. *Cell Host and Microbe*, 2(5), pp.316–27.

Coppi, A., Natarajan, R., Pradel, G., Bennett, B.L., James, E.R., Roggero, M.A., Corradin, G., Persson, C., Tewari, R. & Sinnis, P. (2011). The malaria circumsporozoite protein has two functional domains, each with distinct roles as sporozoites journey from mosquito to mammalian host. *Journal of Experimental Medicine*, 208(2), pp.341–56.

Cowman, A.F. & Crabb, B.S. (2006). Invasion of red blood cells by malaria parasites. *Cell*, 124(4), pp.755–66.

Demeure, C.E., Brahimi, K., Hacini, F., Marchand, F., Péronet, R., Huerre, M., St-Mezard, P., Nicolas, J.F., Brey, P., Delespesse, G. & Mécheri, S. (2005). *Anopheles* mosquito bites activate cutaneous mast cells leading to a local inflammatory response and lymph node hyperplasia. *Journal of Immunology,* 174(7), pp.3932–40.

Desai, M., ter Kuile, F.O., Nosten, F., McGready, R., Asamoa, K., Brabin, B. & Newman, R.D. (2007). Epidemiology and burden of malaria in pregnancy. *The Lancet Infectious Diseases*, 7(2), pp.93–104.

van Dijk, M.R., Douradinha, B., Franke-Fayard, B., Heussler, V., van Dooren, M.W,, van Schaijk, B., van Gemert, G.J., Sauerwein, R.W., Mota, M.M., Waters, A.P. & Janse, C.J. (2005). Genetically attenuated, P36p-deficient malarial sporozoites induce protective immunity and apoptosis of infected liver cells. *Proceedings of the National Academy of Sciences of the United States of America*, 102(34), pp.12194–9.

Duffy, P.E., Sahu, T., Akue, A., Milman, N. & Anderson, C. (2012). Pre-erythrocytic malaria vaccines: identifying the targets. *Expert Review of Vaccines*, 11(10), pp.1261–80.

Ebrahimkhani, M.R., Mohar, I. & Crispe, I.N. (2011). Cross-presentation of antigen by diverse subsets of murine liver cells. *Hepatology,* 54(4), pp.1379–87.

Ejigiri, I., Ragheb, D.R., Pino, P., Coppi, A., Bennett, B.L., Soldati-Favre, D., & Sinnis, P. (2012). Shedding of TRAP by a rhomboid protease from the malaria sporozoite surface is essential for gliding motility and sporozoite infectivity. *PLoS Pathogens*, 8(7), p.e1002725.

Emsley, J., Cruz, M., Handin, R., Liddington, R. (1998). Crystal structure of the von Willebrand Factor A1 domain and implications for the binding of platelet glycoprotein Ib. *The Journal of Biological Chemistry*, 273(17), pp.10396–401.

Ferguson, D.J., Balaban, A.E., Patzewitz, E.M., Wall, R.J., Hopp, C.S., Poulin, B., Mohmmed, A., Malhotra, P., Coppi, A., Sinnis, P. & Tewari, R. (2014). The repeat region of the circumsporozoite protein is critical for sporozoite formation and maturation in *Plasmodium*. *PLoS ONE*, 9(12), p.e113923.

Formaglio, P., Tavares, J., Ménard, R. & Amino, R. (2014). Loss of host cell plasma membrane integrity following

cell traversal by *Plasmodium* sporozoites in the skin. *Parasitology International*, 63(1), pp.237–44.

Franke-Fayard, B., Djokovic, D., Dooren, M.W., Ramesar, J., Waters, A.P., Falade, M.O., Kranendonk, M., Martinelli, A., Cravo, P. & Janse C.J. (2008). Simple and sensitive antimalarial drug screening *in vitro* and *in vivo* using transgenic luciferase expressing *Plasmodium berghei* parasites. *InternationalJ for Parasitology*, 38(14), pp.1651–62.

Frevert, U., Sinnis, P., Cerami, C., Shreffler, W,, Takacs, B. & Nussenzweig V. (1993). Malaria circumsporozoite protein binds to heparan sulfate proteoglycans associated with the surface membrane of hepatocytes. *Journal of Experimental Medicine*, 177(5), pp.1287-98.

Frevert, U., (2004). Sneaking in through the back entrance: the biology of malaria liver stages. *Trends in Parasitology*, 20(9), pp.417–24.

Frevert, U., Engelmann, S., Zougbédé, S., Stange, J., Ng, B., Matuschewski, K., Liebes, L. & Yee, H. (2005). Intravital observation of *Plasmodium berghei* sporozoite infection of the liver. *PLoS Biology*, 3(6), pp.e192.

Frevert, U., Usynin, I., Baer, K. & Klotz, C. (2006). Nomadic or sessile: can Kupffer cells function as portals for malaria sporozoites to the liver? *Cellular Microbiology*, 8(10), pp.1537–46.

Frischknecht, F., Baldacci, P., Martin, B., Zimmer, C., Thiberge, S., Olivo-Marin, J.C., Shorte, S.L. & Ménard R. (2004). Imaging movement of malaria parasites during transmission by *Anopheles* mosquitoes. *Cellular Microbiology*, 6(7), pp.687–94.

Gaffar, F.R., Yatsuda, A.P., Franssen, F.F. & de Vries, E. (2004). A *Babesia bovis* merozoite protein with a domain architecture highly similar to the thrombospondin-related anonymous protein (TRAP) present in *Plasmodium* sporozoites. *Molecular and Biochemical Parasitology*, 136(1), pp.25–34.

Gantt, S., Persson, C., Rose, K., Birkett, A.J., Abagyan, R. & Nussenzweig, V. (2000). Antibodies against thrombospondin-related anonymous protein do not inhibit *Plasmodium* sporozoite infectivity *in vivo*. *Infection and Immunity*, 68(6), pp.3667–73.

Gardner, M.J., Bishop, R., Shah, T., de Villiers, E.P., Carlton, J.M., Hall, N., Ren, Q., Paulsen, I.T., Pain, A., Berriman, M., Wilson, R.J., Sato, S., Ralph, S.A., Mann, D.J., Xiong, Z., Shallom, S.J., Weidman, J., Jiang, L., Lynn, J., Weaver, B., Shoaibi, A., Domingo, A.R., Wasawo, D., Crabtree, J., Wortman, J.R., Haas, B., Angiuoli, S.V., Creasy, T.H., Lu, C., Suh, B., Silva, J.C., Utterback, T.R., Feldblyum, T.V., Pertea, M., Allen, J., Nierman, W.C., Taracha, E.L., Salzberg, S.L., White, O.R., Fitzhugh, H.A., Morzaria, S., Venter, J.C., Fraser, C.M. & Nene, V. (2005). Genome sequence of *Theileria parva*, a bovine pathogen that transforms lymphocytes. *Science,* 309(5731), pp.134–7.

Gething, P.W., Elyazar, I.R., Moyes, C.L., Smith, D.L., Battle, K.E., Guerra, C.A., Patil, A.P., Tatem, A.J., Howes, R.E., Myers, M.F., George, D.B., Horby, P., Wertheim, H.F., Price, R.N., Müeller, I., Baird, J.K. & Hay, S.I. 2012. A long neglected world malaria map: *Plasmodium vivax* endemicity in (2010). *PLoS Neglected Tropical Diseases*, 6(9), pp.e1814.

Ghai, M., Dutta, S., Hall, T., Freilich, D. & Ockenhouse, C.F. (2002). Identification, expression, and functional characterization of MAEBL, a sporozoite and asexual blood stage chimeric erythrocyte-binding protein of *Plasmodium falciparum*. *Molecular and Biochemical Parasitology*, 123(1), pp.35–45.

Ghosh, A.K., Devenport, M., Jethwaney, D., Kalume, D.E., Pandey, A., Anderson, V.E., Sultan, A.A., Kumar, N & Jacobs-Lorena, M. (2009). Malaria parasite invasion of the mosquito salivary gland requires interaction

between the *Plasmodium* TRAP and the *Anopheles* saglin proteins. *PLoS Pathogens*, 5(1), p.e1000265.

Gueirard, P., Tavares, J., Thiberge, S., Bernex, F., Ishino, T., Milon, G., Franke-Fayard, B., Janse, C.J., Ménard, R. & Amino, R. (2010.) Development of the malaria parasite in the skin of the mammalian host. *Proceedings of the National Academy of Sciences of the United States of America*, 107(43), pp.18640–45.

Hamaoka, B.Y. & Ghosh, P. (2014). Structure of the essential *Plasmodium* host cell traversal protein SPECT1. *PloS One*, 9(12), pp.e114685.

Harding, C.R. & Meissner, M. (2014). The inner membrane complex through development of *Toxoplasma gondii* and *Plasmodium*. *Cellular Microbiology*, 16(5), pp.632–41.

Haussig, J.M., Matuschewski, K. & Kooij, T.W.A. (2011). Inactivation of a *Plasmodium* apicoplast protein attenuates formation of liver merozoites. *Molecular Microbiology*, 81(6), pp.1511–25.

Hegge, S., Kudryashev, M., Smith, A. & Frischknecht, F. (2009). Automated classification of *Plasmodium* sporozoite movement patterns reveals a shift towards productive motility during salivary gland infection. *Biotechnology Journal*, 4(6), pp.903–13.

Heintzelman, M.B. (2015). Gliding motility in apicomplexan parasites. *Seminars in Cell & Developmental Biology*, 46, pp.135-42.

Heiss, K., Nie, H., Kumar, S., Daly, T.M., Bergman, L.W. & Matuschewski, K. (2008). Functional characterization of a redundant *Plasmodium* TRAP family invasin, TRAP-like protein, by aldolase binding and a genetic complementation test. *Eukaryotic Cell*, 7(6), pp.1062–70.

Hemingway, J., (2014). The role of vector control in stopping the transmission of malaria: threats and opportunities. *Philosophical Transactions of the Royal Society of London B: Biological Sciences*, 369(1645),pp. 20130431.

Holt, R.A., Subramanian, G.M., Halpern, A., Sutton, G.G., Charlab, R., Nusskern, D.R., Wincker, P., Clark, A.G., Ribeiro, J.M., Wides, R., Salzberg, S.L., Loftus, B., Yandell, M., Majoros, W.H., Rusch, D.B., Lai, Z., Kraft, C.L., Abril, J.F., Anthouard, V., Arensburger, P., Atkinson, P.W., Baden, H., de Berardinis, V., Baldwin, D., Benes, V., Biedler, J., Blass, C., Bolanos, R., Boscus, D., Barnstead, M., Cai, S., Center, A., Chaturverdi, K., Christophides, G.K., Chrystal, M.A., Clamp, M., Cravchik, A., Curwen, V., Dana, A., Delcher, A., Dew, I., Evans, C.A., Flanigan, M., Grundschober-Freimoser, A., Friedli, L., Gu, Z., Guan, P., Guigo, R., Hillenmeyer, M.E., Hladun, S.L., Hogan, J.R., Hong, Y.S., Hoover, J., Jaillon, O., Ke, Z., Kodira, C., Kokoza, E., Koutsos, A., Letunic, I., Levitsky, A., Liang, Y., Lin, J.J., Lobo, N.F., Lopez, J.R., Malek, J.A., McIntosh, T.C., Meister, S., Miller, J., Mobarry, C., Mongin, E., Murphy, S.D., O'Brochta, D.A., Pfannkoch, C., Qi, R., Regier, M.A., Remington, K., Shao, H., Sharakhova, M.V., Sitter, C.D., Shetty, J., Smith, T.J., Strong, R., Sun, J., Thomasova, D., Ton, L.Q., Topalis, P., Tu, Z., Unger, M.F., Walenz, B., Wang, A., Wang, J., Wang, M., Wang, X., Woodford, K.J., Wortman, J.R., Wu, M., Yao, A., Zdobnov, E.M., Zhang, H., Zhao, Q., Zhao, S., Zhu, S.C., Zhimulev, I., Coluzzi, M., della Torre, A., Roth, C.W., Louis, C., Kalush, F., Mural, R.J., Myers, E.W., Adams, M.D., Smith, H.O., Broder, S., Gardner, M.J., Fraser, C.M., Birney, E., Bork, P., Brey, P.T., Venter, J.C., Weissenbach, J., Kafatos, F.C., Collins, F.H. & Hoffman, S.L. (2002). The genome sequence of the malaria mosquito *Anopheles gambiae*. *Science*, 298(5591), pp.129–49

Ishibashi, H., Nakamura, M., Komori, A., Migita, K. & Shimoda, S. (2009). Liver architecture, cell function, and disease. *Seminars in Immunopathology*, 31(3), pp.399–409.

Ishino, T., Yano, K., Chinzei, Y. & Yuda, M. (2004). Cell-passage activity is required for the malarial parasite to cross

the liver sinusoidal cell layer. *PLoS Biology*, 2(1), p.e4.

Ishino, T., Chinzei, Y. & Yuda, M. (2005a). A *Plasmodium* sporozoite protein with a membrane attack complex domain is required for breaching the liver sinusoidal cell layer prior to hepatocyte infection. *Cellular Microbiology*, 7(2), pp.199–208.

Ishino, T., Chinzei, Y. & Yuda, M., (2005b). Two proteins with 6-cys motifs are required for malarial parasites to commit to infection of the hepatocyte. *Molecular Microbiology*, 58(5), pp.1264–75.

Janse, C.J., Ramesar, J. & Waters, A.P. (2006). High-efficiency transfection and drug selection of genetically transformed blood stages of the rodent malaria parasite *Plasmodium berghei*. *Nature Protocols*, 1(1), pp.346–56.

Jayabalasingham, B., Bano, N. & Coppens, I. (2010). Metamorphosis of the malaria parasite in the liver is associated with organelle clearance. *Cell Research*, 20(9), pp.1043–59.

Jensenius, M., Han, P.V., Schlagenhauf, P., Schwartz, E., Parola, P., Castelli, F., von Sonnenburg, F., Loutan, L., Leder, K., Freedman, D.O. & GeoSentinel Surveillance Network. (2013). Acute and potentially life-threatening tropical diseases in western travelers-A GeoSentinel multicenter study, 1996-2011. *The American Journal of Tropical Medicine and Hygiene*, 88(2), pp.397–404.

Jewett, T.J. & Sibley, L.D. (2003). Aldolase forms a bridge between cell surface adhesins and the actin cytoskeleton in apicomplexan parasites. *Molecular Cell*, 11(4), pp.885–94.

Jin, Y., Kebaier, C. & Vanderberg, J. (2007). Direct microscopic quantification of dynamics of *Plasmodium berghei* sporozoite transmission from mosquitoes to mice. *Infection and Immunity*, 75(11), pp.5532–9.

Jortzik, E., Kehr, S. & Becker, K. (2011). Post-translational modifications in apicomplexan parasites. In Mehlhorn, H. ed. *Progress in Parasitology*. Springer Berlin Heidelberg, pp. 93–120.

Kaiser, K., Camargo, N. & Kappe, S.H. (2003). Transformation of sporozoites into early exoerythrocytic malaria parasites does not require host cells. *The Journal of Experimental Medicine*, 197(8), pp.1045–50.

Kaiser, K., Matuschewski, K., Camargo, N., Ross, J., Kappe, S.H. (2004). Differential transcriptome profiling identifies *Plasmodium* genes encoding pre-erythrocytic stage-specific proteins. *Molecular Microbiology*, 51(5) pp.1221–32.

Kappe, S,H., Curley, G.P., Noe, A.R., Dalton, J.P. & Adams, J.H. (1997). Erythrocyte binding protein homologues of rodent malaria parasites. *Molecular and Biochemical Parasitology*, 89(1), pp.137–48.

Kappe, S.H., Noe, A.R., Fraser, T.S., Blair, P.L., & Adams, J.H. (1998). A family of chimeric erythrocyte binding proteins of malaria parasites. *Proceedings of the National Academy of Sciences of the United States of America*, 95(3), pp.1230–5.

Kappe, S.H, Bruderer, T., Gantt, S., Fujioka, H., Nussenzweig, V. & Ménard R. (1999). Conservation of a gliding motility and cell invasion machinery in apicomplexan parasites. *The Journal of Cell Biology*, 147(5), pp.937–43.

Kappe, S.H., Gardner, M.J., Brown, S.M., Ross, J., Matuschewski, K., Ribeiro, J.M., Adams, J.H., Quackenbush, J., Cho, J., Carucci, D.J., Hoffman, S.L. & Nussenzweig, V. (2001). Exploring the transcriptome of the malaria sporozoite stage. Proceedings of the National Academy of Sciences of the United States of America, 98(17),

pp.9895–900.

Kappe, S.H., Buscaglia, C.A & Nussenzweig, V. (2004). *Plasmodium* sporozoite molecular cell biology. *Annual Review of Cell and Developmental Biology*, 20, pp.29–59.

Kariu, T., Yuda, M., Yano, K. & Chinzei, Y. (2002). MAEBL is essential for malarial sporozoite infection of the mosquito salivary gland. *The Journal of Experimental Medicine*, 195(10), pp.1317–23.

Kariu, T., Ishino, T., Yano, K., Chinzei, Y. & Yuda, M. (2006). CelTOS, a novel malarial protein that mediates transmission to mosquito and vertebrate hosts. *Molecular Microbiology*, 59(5), pp.1369–79.

Kaushansky, A., Douglass, A.N., Arang, N., Vigdorovich, V., Dambrauskas, N., Kain, H.S., Austin, L.S., Sather, D.N. & Kappe, S.H. (2015). Malaria parasites target the hepatocyte receptor EphA2 for successful host infection. *Science*, 350(6264), pp.1089–92.

Kebaier, C. & Vanderberg, J.P. (2006). Re-ingestion of *Plasmodium berghei* sporozoites after delivery into the host by mosquitoes. *The American Journal of Tropical Medicine and Hygiene*, 75(6), pp.1200–4.

Killeen, G.F., Seyoum, A., Gimnig, J.E., Stevenson, J.C., Drakeley, C.J. & Chitnis, N. (2014). Made-to-measure malaria vector control strategies: rational design based on insecticide properties and coverage of blood resources for mosquitoes. *Malaria Journal*, 13, pp.146.

Kim, H., Certa, U., Döbeli, H., Jakob, P. & Hol, W.G. (1998). Crystal structure of fructose-1,6-bisphosphate aldolase from the human malaria parasite *Plasmodium falciparum*. *Biochemistry*, 37(13), pp.4388–96.

Kiszewski, A., Mellinger, A., Spielman, A., Malaney, P., Sachs, S.E. & Sachs, J. (2004). A global index representing the stability of malaria transmission. *The American Journal of Tropical Medicine and Hygiene*, 70(5), pp.486–98.

Krishna, M. (2013). Microscopic anatomy of the liver. *Clinical Liver Disease*, 2(S1), pp.S4–7.

Kudryashev, M., Münter, S., Lemgruber, L., Montagna, G., Stahlberg, H., Matuschewski, K., Meissner, M., Cyrklaff, M. & Frischknecht, F. (2012). Structural basis for chirality and directional motility of *Plasmodium* sporozoites. *Cellular Microbiology*, 14(11), pp.1757–68.

Labaied, M., Camargo, N. & Kappe, S.H. (2007). Depletion of the *Plasmodium berghei* thrombospondin-related sporozoite protein reveals a role in host cell entry by sporozoites. *Molecular and biochemical parasitology*, 153(2), pp.158–66.

Lacroix, C. & Ménard, R. (2008). TRAP-like protein of *Plasmodium* sporozoites: linking gliding motility to host-cell traversal. *Trends in Parasitology*, 24(10), pp.431–34.

Lasonder, E., Janse, C.J., van Gemert, G.J., Mair, G.R., Vermunt, A.M., Douradinha, B.G., van Noort, V., Huynen, M.A., Luty, A.J., Kroeze, H., Khan, S.M., Sauerwein, R.W., Waters, A.P., Mann, M. & Stunnenberg, H.G. (2008). Proteomic profiling of *Plasmodium* sporozoite maturation identifies new proteins essential for parasite development and infectivity. *PLoS Pathogens*, 4(10), pp.e1000195.

Lefèvre, T., Vantaux, A., Dabiré, K.R., Mouline, K., Cohuet, A. & Lefèvre, T. (2013). Non-genetic determinants of mosquito competence for malaria parasites. *PLoS Pathogens*, 9(6), pp.e1003365.

Leirião, P., Albuquerque, S.S., Corso, S., van Gemert, G.J., Sauerwein, R.W., Rodriguez, A., Giordano, S. & Mota, M.M. (2005). HGF/MET signalling protects *Plasmodium*-infected host cells from apoptosis. *Cellular Microbiology*, 7(4), pp.603–9.

Levine, N.D. (1973). *Protozoan Parasites of Domestic Animals and of Man*, Burgess Pub. Co.

Li, R., Rieu, P., Griffith, D.L., Scott, D. & Arnaout, M.A. (1998). Two functional states of the CD11b A-domain: correlations with key features of two Mn^{2+}-complexed crystal structures. *The Journal of Cell Biology*, 143(6), pp.1523–34.

Li, X., Marinkovic, M., Russo, C., McKnight, C.J., Coetzer, T.L. & Chishti, A.H. (2012). Identification of a specific region of *Plasmodium falciparum* EBL-1 that binds to host receptor glycophorin B and inhibits merozoite invasion in human red blood cells. *Molecular and Biochemical Parasitology*, 183(1), pp.23–31.

Lovett, J.L., Howe, D.K. & Sibley, L.D. (2000). Molecular characterization of a thrombospondin-related anonymous protein homologue in *Neospora caninum*. *Molecular and Biochemical Parasitology*, 107(1), pp.33–43.

Lyon, M., Deakin, J.A. & Gallagher, J.T. (1994). Liver heparan sulfate structure. A novel molecular design. *The Journal of biological chemistry*, 269(15), pp.11208–15.

Martinez, C., Marzec, T., Smith, C.D., Tell, L.A. & Sehgal, R.N. (2013). Identification and expression of maebl, an erythrocyte-binding gene, in *Plasmodium* gallinaceum. *Parasitology research*, 112(3), pp.945–54.

Matsuoka, H., Yoshida, S., Hirai, M & Ishii, A. (2002). A rodent malaria, *Plasmodium berghei*, is experimentally transmitted to mice by merely probing of infective mosquito, *Anopheles stephensi*. *Parasitology International*, 51(1), pp.17–23.

Matuschewski, K., Nunes, A.C., Nussenzweig, V. & Ménard, R. (2002a). *Plasmodium* sporozoite invasion into insect and mammalian cells is directed by the same dual binding system. *The EMBO journal*, 21(7), pp.1597–606.

Matuschewski, K., Ross, J., Brown, S.M., Kaiser, K., Nussenzweig, V. & Kappe, S.H. (2002b). Infectivity-associated changes in the transcriptional repertoire of the malaria parasite sporozoite stage. *Journal of Biological Chemistry*, 277(44), pp.41948–53.

Matuschewski, K., (2006). Getting infectious: formation and maturation of *Plasmodium* sporozoites in the *Anopheles* vector. *Cellular Microbiology*, 8(10), pp.1547–56.

Mauduit, M., Grüner, A.C., Tewari, R., Depinay, N., Kayibanda, M., Chavatte, J.M., Franetich, J.F., Crisanti, A., Mazier, D., Snounou, G. & Rénia, L. (2009). A role for immune responses against non-CS components in the cross-species protection induced by immunization with irradiated malaria sporozoites. *PloS One*, 4(11), pp.e7717.

McCutchan, T.F., Kissinger, J.C., Touray, M.G., Rogers, M.J., Li, J., Sullivan, M., Braga, E.M., Krettli, A.U. & Miller, L.H. (1996). Comparison of circumsporozoite proteins from avian and mammalian malarias: biological and phylogenetic implications. *Proceedings of the National Academy of Sciences of the United States of America*, 93(21), pp.11889–94.

Medica, D.L. & Sinnis, P. (2005). Quantitative dynamics of *Plasmodium yoelii* sporozoite transmission by infected anopheline mosquitoes. *Infection and Immunity*, 73(7), pp.4363–9.

Meis, J.F., Verhave, J.P., Jap, P.H. & Meuwissen, J.H. (1983). An ultrastructural study on the role of Kupffer cells in the process of infection by *Plasmodium berghei* sporozoites in rats. *Parasitology*, 86 (2), pp.231–42.

Meis, J.F., Verhave, J.P., Brouwer, A. & Meuwissen, J.H. (1985). Electron microscopic studies on the interaction of rat Kupffer cells and *Plasmodium berghei* sporozoites. *Zeitschrift für Parasitenkunde*, 71(4), pp.473–83.

Ménard, R. (2001). Gliding motility and cell invasion by Apicomplexa: Insights from the *Plasmodium* sporozoite. *Cellular Microbiology*, 3(2), pp.63–73.

Ménard, R. & Janse, C. (1997). Gene targeting in malaria parasites. *Methods*, 13(2), pp.148–57.

Ménard, R., Tavares, J., Cockburn, I., Markus, M., Zavala, F. & Amino R. (2013). Looking under the skin: the first steps in malarial infection and immunity. *Nature Reviews Microbiology*, 11(10), pp.701–12.

Mercier, C., Adjogble, K.D., Däubener, W. & Delauw, M.F. (2005). Dense granules: are they key organelles to help understand the parasitophorous vacuole of all apicomplexa parasites? *International Journal for Parasitology*, 35(8), pp.829–49.

Mikolajczak, S.A., Silva-Rivera, H., Peng, X., Tarun, A.S., Camargo, N., Jacobs-Lorena, V., Daly, T.M., Bergman, L.W., De la Vega, P., Williams, J., Aly, A.S. & Kappe S.H. (2008). Distinct malaria parasite sporozoites reveal transcriptional changes that cause differential tissue infection competence in the mosquito vector and mammalian host. *Molecular and Cellular Biology*, 28(20), pp.6196–207.

Miller, L.H., Aikawa, M., Johnson, J.G. & Shiroishi, T. (1979). Interaction between cytochalasin B-treated malarial parasites and erythrocytes. Attachment and junction formation. *The Journal of Experimental Medicine*, 149(1), pp.172–84.

Mizushima, N. & Sahani, M.H. (2014). ATG8 localization in apicomplexan parasites: apicoplast and more? *Autophagy*, 10(9), pp.1487–94.

Montoya, J.G. & Liesenfeld, O. (2004). Toxoplasmosis. *Lancet*, 363(9425), pp.1965–76.

Moody, A.H. & Chiodini, P.L. (2000). Methods for the detection of blood parasites. *Clinic and Laboratory Haematology*, 22(4), pp.189–202.

Moorthy, V.S., Imoukhuede, E.B., Milligan, P., Bojang, K., Keating, S., Kaye, P., Pinder, M., Gilbert, S.C., Walraven, G., Greenwood, B.M. & Hill, A.S. (2004). A randomised, double-blind, controlled vaccine efficacy trial of DNA/MVA ME-TRAP against malaria infection in Gambian adults. *PLoS Medicine*, 1(2), pp.e33.

Morahan, B.J., Wang, L. & Coppel, R.L., (2009). No TRAP, no invasion. *Trends in Parasitology*, 25(2), pp.77–84.

Moreira, C.K., Templeton, T.J., Lavazec, C., Hayward, R.E., Hobbs, C.V., Kroeze, H., Janse, C.J., Waters, A.P., Sinnis, P. & Coppi, A. (2008). The *Plasmodium* TRAP/MIC2 family member, TRAP-Like Protein (TLP), is involved in tissue traversal by sporozoites. *Cellular Microbiology*, 10(7), pp.1505–16.

Morrissette, N.S. & Sibley, L.D. (2002). Cytoskeleton of apicomplexan parasites. *Microbiology and Molecular Biology Reviews*, 66(1), pp.21–38.

Mota, M.M., Pradel, G., Vanderberg, J.P., Hafalla, J.C., Frevert, U., Nussenzweig, R.S., Nussenzweig, V. & Rodríguez, A. (2001). Migration of *Plasmodium* sporozoites through cells before infection. *Science*, 291(5501),

pp.141–4.

Mota, M.M., Hafalla, J.C. & Rodriguez, A., (2002). Migration through host cells activates *Plasmodium* sporozoites for infection. *Nature Medicine*, 8(11), pp.1318–22.

Motta, P.M., (1984). The three-dimensional microanatomy of the liver. *Archivum Histologicum Japonicum*, 47(1), pp.1–30.

Müller, H.M., Reckmann, I., Hollingdale, M.R., Bujard, H., Robson, K.J. & Crisanti, A. (1993). Thrombospondin related anonymous protein (TRAP) of *Plasmodium falciparum* binds specifically to sulfated glycoconjugates and to HepG2 hepatoma cells suggesting a role for this molecule in sporozoite invasion of hepatocytes. *The EMBO Journal*, 12(7), pp.2881–9.

Münter, S., Sabass, B., Selhuber-Unkel, C., Kudryashev, M., Hegge, S., Engel, U., Spatz, J.P., Matuschewski, K., Schwarz, U,S. & Frischknecht, F. (2009). *Plasmodium* sporozoite motility is modulated by the turnover of discrete adhesion sites. *Cell Host and Microbe*, 6(6), pp.551–62.

Nair, S., Williams, J.T., Brockman, A., Paiphun, L., Mayxay, M., Newton, P.N., Guthmann, J.P., Smithuis, F.M., Hien, T.T., White, N.J., Nosten, F., Anderson, T.J. (2003). A selective sweep driven by pyrimethamine treatment in southeast asian malaria parasites. *Molecular Biology and Evolution*, 20(9), pp.1526–36.

Neafsey, D.E., Waterhouse, R.M., Abai, M.R., Aganezov, S.S., Alekseyev, M.A., Allen, J.E., Amon, J., Arcà, B., Arensburger, P., Artemov, G., Assour, L.A., Basseri, H., Berlin, A., Birren, B.W., Blandin, S.A., Brockman, A.I., Burkot, T.R., Burt, A., Chan, C.S., Chauve, C., Chiu, J.C., Christensen, M., Costantini, C., Davidson, V.L., Deligianni, E., Dottorini, T., Dritsou, V., Gabriel, S.B., Guelbeogo, W.M., Hall, A.B., Han, M.V., Hlaing, T., Hughes, D.S., Jenkins, A.M., Jiang, X., Jungreis, I., Kakani, E.G., Kamali, M., Kemppainen, P., Kennedy, R.C., Kirmitzoglou, I.K., Koekemoer, L.L., Laban, N., Langridge, N., Lawniczak, M.K., Lirakis, M., Lobo, N.F., Lowy, E., MacCallum, R.M., Mao, C., Maslen, G., Mbogo, C., McCarthy, J., Michel, K., Mitchell, S.N., Moore, W., Murphy, K.A., Naumenko, A.N., Nolan, T., Novoa, E.M., O'Loughlin, S., Oringanje, C., Oshaghi, M.A., Pakpour, N., Papathanos, P.A., Peery, A.N., Povelones, M., Prakash, A., Price, D.P., Rajaraman, A., Reimer, L.J., Rinker, D.C., Rokas, A., Russell. T.L., Sagnon, N., Sharakhova, M.V., Shea, T., Simão, F.A., Simard, F., Slotman, M.A., Somboon, P., Stegniy, V., Struchiner, C.J., Thomas, G.W., Tojo, M., Topalis, P., Tubio, J.M., Unger, M.F., Vontas, J., Walton, C., Wilding, C.S., Willis, J.H., Wu, Y.C., Yan, G., Zdobnov, E.M., Zhou, X., Catteruccia, F., Christophides, G.K., Collins, F.H., Cornman, R.S., Crisanti, A., Donnelly, M.J., Emrich, S.J., Fontaine, M.C., Gelbart, W., Hahn, M.W., Hansen, I.A., Howell, P.I., Kafatos, F.C., Kellis, M., Lawson, D., Louis, C., Luckhart, S., Muskavitch, M.A., Ribeiro, J.M., Riehle, M.A., Sharakhov, I.V., Tu Z., Zwiebel, L.J. & Besansky, N.J. (2015). Mosquito genomics. highly evolvable malaria vectors: the genomes of 16 *Anopheles* mosquitoes. *Science*, 347(6217), pp.1258522.

Ngô, H.M., Hoppe, H.C. & Joiner, K.A. 2000. Differential sorting and post-secretory targeting of proteins in parasitic invasion. *Trends in Cell Biology*, 10(2), pp.67–72.

Nichols, B.A. & Chiappino, M.L. (1987). Cytoskeleton of *Toxoplasma gondii*. *The Journal of Protozoology*, 34(2), pp.217–26.

Noe, A.R. & Adams, J.H., (1998). *Plasmodium yoelii* YM MAEBL protein is coexpressed and colocalizes with rhoptry proteins. *Molecular and Biochemical Parasitology*, 96(1–2), pp.27–35.

Oddoux, O., Debourgogne, A., Kantele, A., Kocken, C.H., Jokiranta, T.S., Vedy, S., Puyhardy, J.M. & Machouart, M. (2011). Identification of the five human *Plasmodium* species including P. *knowlesi* by real-time polymerase chain reaction. *European Journal of Clinical Microbiology & Infectious Diseases*, 30(4), pp.597–601.

Offeddu, V., Rauch, M., Silvie, O. & Matuschewski, K. (2014). The *Plasmodium* protein P113 supports efficient sporozoite to liver stage conversion *in vivo*. *Molecular and Biochemical Parasitology*, 193(2), pp.101–9.

Okulate, M.A., Kalume, D.E., Reddy, R., Kristiansen, T., Bhattacharyya, M., Chaerkady, R., Pandey, A. & Kumar, N. (2007). Identification and molecular characterization of a novel protein Saglin as a target of monoclonal antibodies affecting salivary gland infectivity of *Plasmodium* sporozoites. *Insect Molecular Biology*, 16(6), pp.711–22.

Pain, A., Renauld, H., Berriman, M., Murphy, L., Yeats, C.A., Weir, W., Kerhornou, A., Aslett, M., Bishop, R., Bouchier, C., Cochet, M., Coulson, R.M., Cronin, A., de Villiers, E.P., Fraser, A., Fosker, N., Gardner, M., Goble, A., Griffiths-Jones, S., Harris, D.E., Katzer, F., Larke, N., Lord, A., Maser, P., McKellar, S., Mooney, P., Morton, F., Nene, V., O'Neil, S., Price, C., Quail, M.A., Rabbinowitsch, E., Rawlings, N.D., Rutter, S., Saunders, D., Seeger, K., Shah, T., Squares, R., Squares, S., Tivey, A., Walker, A.R., Woodward, J., Dobbelaere, D.A., Langsley, G., Rajandream, M.A., McKeever, D., Shiels, B., Tait, A., Barrell, B. & Hall, N. (2005). Genome of the host-cell transforming parasite *Theileria* annulata compared with T. *parva*. *Science*, 309(5731), pp.131–3.

Payne, D., 1987. Spread of chloroquine resistance in *Plasmodium falciparum*. *Parasitology Today*, 3(8), pp.241–6.

Peng, K., Goh, Y.S., Siau, A., Franetich, J.F., Chia, W.N., Ong, A.S., Malleret, B., Wu, Y.Y., Snounou, G., Hermsen, C.C. Adams, J.H., Mazier, D., Preiser, P.R., Sauerwein, R.W., Grüner, A.C. & Rénia, L. (2016). Breadth of humoral response and antigenic targets of sporozoite-inhibitory antibodies associated with sterile protection induced by controlled human malaria infection. *Cellular Microbiology*.

Pihlajamaa, T., Kajander, T., Knuuti, J., Horkka, K., Sharma, A. & Permi, P. (2013). Structure of *Plasmodium falciparum* TRAP (thrombospondin-related anonymous protein) A domain highlights distinct features in apicomplexan von Willebrand factor A homologues. *Biochemical Journal*, 450(3).

Paulo FP Pimenta, P.F.P, Orfano, A.S., Bahia, A.C., Duarte, A.P.M., Ríos-Velásquez, C.M., Melo, F.F., Pessoa, F.A.C., Oliveira, G.A., Campos, K.M.M., Villegas, L.M., Rodrigues, N.B., Nacif-Pimenta, R., Simões, R.C., Monteiro, W.M., Amino, R., Traub-Cseko, Y.M., Lima, J.B.P, Barbosa, M.G.V., Lacerda, M.V.G., Tadei, W.P., & Secundino, N.F.C. (2015). An overview of malaria transmission from the perspective of Amazon *Anopheles* vectors. *Memórias do Instituto Oswaldo Cruz*, 110(1), pp.23–47.

Pradel, G. & Frevert, U., (2001). Malaria sporozoites actively enter and pass through rat Kupffer cells prior to hepatocyte invasion. *Hepatology,* 33(5), pp.1154–65.

Pradel, G., Garapaty, S. & Frevert, U. (2002). Proteoglycans mediate malaria sporozoite targeting to the liver. *Molecular Microbiology*, 45(3), pp.637–651.

Pradel, G., Garapaty, S. & Frevert, U. (2004). Kupffer and stellate cell proteoglycans mediate malaria sporozoite targeting to the liver. *Comparative Hepatology*, 3 (1), pp.S47.

Preiser, P., Rénia, L., Singh, N., Balu, B., Jarra, W., Voza, T., Kaneko, O., Blair, P., Torii, M., Landau, I. & Adams, J.H. (2004). Antibodies against MAEBL ligand domains M1 and M2 inhibit sporozoite development *in vitro. Infection and Immunity*, 72(6), pp.3604–8.

Protzer, U., Maini, M.K. & Knolle, P.A. (2012). Living in the liver: hepatic infections. *Nature Reviews Immunology*, 12(3), pp.201–13.

Prudêncio, M., Mota, M.M. & Mendes, A.M. (2011). A toolbox to study liver stage malaria. *Trends in Parasitology*, 27(12), pp.565–74.

Ramakrishnan, C., Delves, M.J., Lal, K., Blagborough, A.M., Butcher, G., Baker, K.W. Sinden, R. E. (2013). Laboratory maintenance of rodent malaria parasites. In Ménard, R., ed. *Malaria, Methods and Protocols*. Humana Press, pp. 51–72.

Ramasamy, R. (2014). Zoonotic malaria - global overview and research and policy needs. *Frontiers in Public Health*, 2, pp.123.

Rampling, T., Ewer, K.J., Bowyer, G, Bliss, C.M., Edwards, N.J., Wright, D., Payne, R.O., Venkatraman, N., de Barra, E., Snudden, C.M., Poulton, I.D. de Graaf, H., Sukhtankar, P., Roberts, R., Ivinson, K., Weltzin, R., Rajkumar, B.Y., Wille-Reece, U., Lee, C.K., Ockenhouse, C.F., Sinden, R.E. Gerry, S., Lawrie, A.M., Vekemans, J., Morelle, D., Lievens, M., Ballou, R.W., Cooke, G.S., Faust, S.N., Gilbert, S., Hill, A.V. (2016). Safety and high level efficacy of the combination malaria vaccine regimen of RTS,S/AS01B with chimpanzee Adenovirus 63 and modified vaccinia Ankara vectored vaccines expressing ME-TRAP. *The Journal of infectious diseases*, 214(5), pp.772–81.

Ranson, H., N'guessan, R., Lines, J., Moiroux, N., Nkuni, Z. & Corbel, V. (2011). Pyrethroid resistance in African anopheline mosquitoes: what are the implications for malaria control? *Trends in Parasitology*, 27(2), pp.91–8.

Rathore, D., Sacci, J.B., De la Vega, P. & McCutchan, T.F. (2002). Binding and invasion of liver cells by *Plasmodium falciparum* sporozoites. Essential involvement of the amino terminus of circumsporozoite protein. *The Journal of Biological Chemistry*, 277(9), pp.7092–8.

Rénia, L., Miltgen, F., Charoenvit, Y., Ponnudurai, T., Verhave, J.P., Collins, W.E. & Mazier, D. (1988). Malaria sporozoite penetration. A new approach by double staining. *Journal of Immunological Methods*, 112(2), pp.201–5.

Rennenberg, A., Lehmann, C., Heitmann, A., Witt, T., Hansen, G., Nagarajan, K., Deschermeier, C., Turk, V., Hilgenfeld, R. & Heussler, V.T. (2010). Exoerythrocytic *Plasmodium* parasites secrete a cysteine protease inhibitor involved in sporozoite invasion and capable of blocking cell death of host hepatocytes. *PLoS Pathogens*, 6(3), pp.e1000825.

Risco-Castillo, V., Topçu, S., Marinach, C., Manzoni, G., Bigorgne, A.E., Briquet, S., Baudin, X., Lebrun, M., Dubremetz, J.F. & Silvie, O. (2015). Malaria sporozoites traverse host cells within transient vacuoles. *Cell Host & Microbe*, 18(5), 593-603.

Riveron, J.M., Irving, H., Ndula, M., Barnes, K.G., Ibrahim, S.S., Paine, M.J. & Wondji, C.S. (2013). Directionally selected cytochrome P450 alleles are driving the spread of pyrethroid resistance in the major malaria vector *Anopheles funestus*. *Proceedings of the National Academy of Sciences of the United States of America*, 110(1), pp.252–7.

Robson, K.J., Hall, J.R., Jennings, M.W., Harris, T.J. R., Marsh, K., Newbold, C.I., Tate, V.E. & Weatherall, D.J. (1988). A highly conserved amino-acid sequence in thrombospondin, properdin and in proteins from sporozoites and blood stages of a human malaria parasite. *Nature*, 335(6185), pp.79–82

Robson, K.J., Frevert, U., Reckmann, I., Cowan, G., Beier, J., Scragg, I.G., Takehara, K., Bishop, D.H., Pradel, G. & Sinden, R. (1995). Thrombospondin-related adhesive protein (TRAP) of *Plasmodium falciparum*: expression during sporozoite ontogeny and binding to human hepatocytes. *The EMBO Journal*, 14(16), pp.3883–94.

Le Roch, K.G., Zhou, Y., Blair, P.L., Grainger, M., Moch, J.K., Haynes, J.D., De La Vega, P., Holder, A.A., Batalov, S., Carucci, D.J. & Winzeler, E.A. (2003). Discovery of gene function by expression profiling of the malaria parasite life cycle. *Science*, 301(5639), pp.1503–8.

Rodrigues, C.D., Hannus, M., Prudêncio, M., Martin, C., Gonçalves, L.A., Portugal, S., Epiphanio, S., Akinc, A., Hadwiger, P., Jahn-Hofmann, K., Röhl, I., van Gemert, G.J., Franetich, J.F., Luty, A.J., Sauerwein, R., Mazier, D., Koteliansky, V., Vornlocher, H.P., Echeverri, C.J., Mota, M.M. (2008). Host scavenger receptor SR-BI plays a dual role in the establishment of malaria parasite liver infection. *Cell Host & Microbe*, 4(3), pp.271–82.

Rogers, W.O., Malik, A., Mellouk, S., Nakamura, K., Rogers, M.D., Szarfman, A., Gordon, D.M., Nussler, A.K., Aikawa, M. & Hoffman, S.L. (1992). Characterization of *Plasmodium falciparum* sporozoite surface protein 2. *Proceedings of the National Academy of Sciences of the United States of America*, 89(19), pp.9176–80.

Roper, C., Pearce, R., Bredenkamp, B., Gumede, J., Drakeley, C., Mosha, F., Chandramohan, D. & Sharp, B. (2003). Antifolate antimalarial resistance in southeast Africa: a population-based analysis. *Lancet*, 361(9364), pp.1174–81.

Russell, D.G. & Burns, R.G. (1984). The polar ring of coccidian sporozoites: a unique microtubule-organizing centre. *Journal of Cell Science*, 65, pp.193–207.

Saenz, F. E., Balu, B., Smith, J., Mendonca, S.R., & Adams, J.H. (2008). The transmembrane isoform of *Plasmodium falciparum* MAEBL is essential for the invasion of *Anopheles* salivary glands. *PLoS One*, 3(5), pp.e2287.

Sato, Y., Montagna, G.N. & Matuschewski, K., (2014). *Plasmodium berghei* sporozoites acquire virulence and immunogenicity during mosquito hemocoel transit. *Infection and Immunity*, 82(3), pp.1164–72.

Schliwa, M. (1982). Action of cytochalasin D on cytoskeletal networks. *The Journal of Cell Biology*, 92(1), pp.79–91.

Schneider, C.A., Rasband, W.S. & Eliceiri, K.W. (2012). NIH Image to ImageJ: 25 years of image analysis. *Nature Methods*, 9(7), pp.671–5.

Senoo, H. (2004). Structure and function of hepatic stellate cells. *Medical Electron Microscopy*, 37(1), pp.3–15.

Siden-Kiamos, I. & Louis, C. (2004). Interactions between malaria parasites and their mosquito hosts in the midgut. *Insect Biochemistry and Molecular Biology*, 34(7), pp.679–85.

Sidjanski, S. & Vanderberg, J.P. (1997). Delayed migration of *Plasmodium* sporozoites from the mosquito bite site to the blood. *The American Journal Of Tropical Medicine And Hygiene*, 57(4), pp.426–9.

Silvie, O., Rubinstein, E., Franetich, J.F., Prenant, M., Belnoue, E., Rénia, L., Hannoun, L., Eling, W,, Levy, S., Boucheix, C. & Mazier, D. (2003). Hepatocyte CD81 is required for *Plasmodium falciparum* and *Plasmodium yoelii* sporozoite infectivity. *Nature Medicine*, 9(1), pp.93–6.

Sim, B.K., Orlandi, P.A., Haynes, J.D., Klotz, F.W., Carter, J.M., Camus, D., Zegans, M.E. & Chulay, J.D. (1990). Primary structure of the 175K *Plasmodium falciparum* erythrocyte binding antigen and identification of a peptide which elicits antibodies that inhibit malaria merozoite invasion. *The Journal Of Cell Biology*, 111(5), pp.1877–84.

Sinden, R.E. (1978). Cell biology. In Killick-Kendrick, R. & Jones, W. eds. *Rodent malaria*. Academic Press, Inc.,

London, pp. 85–168.

Sinden, R.E., Butcher, G.A & Beetsma, A.L. (2002). Maintenance of the *Plasmodium berghei* life cycle. In Doolan, D.L. ed. *Methods in Molecular Medicine*. Humana Press, pp. 25–40.

Singh, N., Preiser, P., Rénia, L., Balu, B., Barnwell, J., Blair, P., Jarra, W., Voza, T., Landau, I. & Adams, J.H. (2004). Conservation and developmental control of alternative splicing in *maebl* among malaria parasites. *Journal of Molecular Biology*, 343(3), pp.589–99.

Sinka, M.E., Bangs, M.J., Manguin, S., Rubio-Palis, Y., Chareonviriyaphap, T., Coetzee, M., Mbogo, C.M., Hemingway, J., Patil, A.P., Temperley, W.H., Gething, P.W., Kabaria, C.W., Burkot, T.R., Harbach, R.E. & Hay, S.I. (2012). A global map of dominant malaria vectors. *Parasites & Vectors*, 5(1), pp.69.

Sinnis, P., Clavijo, P., Fenyö, D., Chait, B. T., Cerami, C., & Nussenzweig, V. (1994). Structural and functional properties of region II-plus of the malaria circumsporozoite protein. *Journal of Experimental Medicine*, 180(1), pp.297-306.

Sinnis, P., De La Vega, P.,Coppi, A., Krzych, U., Mota, M.M. & Sinnis, P. (2013). Quantification of sporozoite invasion, migration, and development by microscopy and flow cytometry. In Ménard, R. ed. *Malaria, Methods and Protocols*. Humana Press, pp. 385–400.

Spaccapelo, R., Naitza, S., Robson, K.J., & Crisanti, A. (1997).Thrombospondin-related adhesive protein (TRAP) of *Plasmodium berghei* and parasite motility. *Lancet*, 350(9074), pp.335.

Spano, F., Putignani, L., Naitza, S., Puri, C., Wright, S., & Crisanti, A. (1998). Molecular cloning and expression analysis of a *Cryptosporidium parvum* gene encoding a new member of the thrombospondin family. *Molecular and Biochemical Parasitology*, 92(1), pp.147–62.

Springer, T.A. (2006). Complement and the multifaceted functions of VWA and integrin I domains. *Structure*, 14(11), pp.1611–6.

Srinivasan, P., Abraham, E.G., Ghosh, A.K., Valenzuela, J., Ribeiro, J.M., Dimopoulos, G., Kafatos, F.C., Adams, J.H., Fujioka, H. & Jacobs-Lorena, M. (2004). Analysis of the *Plasmodium* and *Anopheles* transcriptomes during oocyst differentiation. *The Journal of Biological Chemistry*, 279(7), pp.5581–7.

Stewart, M.J., Nawrot, R.J., Schulman, S. & Vanderberg, J.P. (1986). *Plasmodium berghei* sporozoite invasion is blocked *in vitro* by sporozoite-immobilizing antibodies. *Infection and Immunity*, 51(3), pp.859–64.

Stewart, M.J. & Vanderberg, J.P. (1988). Malaria sporozoites leave behind trails of circumsporozoite protein during gliding motility. *The Journal of Protozoology*, 35(3), pp.389–93.

Stewart, M.J. & Vanderberg, J.P. (1991). Malaria sporozoites release circumsporozoite protein from their apical end and translocate it along their surface. *The Journal of Protozoology*, 38(4), pp.411–21.

Stokkermans, T.J., Schwartzman, J.D., Keenan, K., Morrissette, N.S., Tilney, L.G. & Roos, D.S. (1996). Inhibition of *Toxoplasma gondii* replication by dinitroaniline herbicides. *Experimental Parasitology*, 84(3), pp.355–70.

Suarez, J.E., Urquiza, M., Puentes, A., Garcia, J.E., Curtidor, H., Ocampo, M., Lopez, R., Rodriguez, L.E., Vera, R., Cubillos, M., Torres, M.H. & Patarroyo, M.E. (2001). *Plasmodium falciparum* circumsporozoite (CS) protein peptides specifically bind to HepG2 cells. *Vaccine*, 19(31), pp.4487–95.

Sultan, A.A., Thathy, V., Frevert, U., Robson, K.J., Crisanti, A., Nussenzweig, V., Nussenzweig, R.S. & Ménard, R. (1997). TRAP is necessary for gliding motility and infectivity of *Plasmodium* sporozoites. *Cell*, 90(3), pp.511–22.

Sultan, A.A., (1999). Molecular interactions involved in the invasion of salivary glands by sporozoites. *International Microbiology*, (2), pp.155–60.

Sultan, A.A., Thathy, V., de Koning-Ward, T.F. & Nussenzweig, V. (2001). Complementation of *Plasmodium berghei* TRAP knockout parasites using human dihydrofolate reductase gene as a selectable marker. *Molecular and Biochemical Parasitology*, 113(1), pp.151–6.

Swearingen, K.E., Lindner, S.E., Shi, L., Shears, M.J., Harupa, A., Hopp, C.S., Vaughan, A.M., Springer, T.A., Moritz, R.L., Kappe, S.H. & Sinnis, P. (2016). Interrogating the *plasmodium* sporozoite surface: identification of surface-exposed proteins and demonstration of glycosylation on CSP and TRAP by mass spectrometry-based proteomics. *PLoS Pathogens*, 12(4),e1005606.

Sylvie, M., Pierre, C. & Jean, M. (2008). *Biodiversity of Malaria in the World*, John Libbey Eurotext.

Talman, A.M., Lacroix, C., Marques, S.R., Blagborough, A.M., Carzaniga, R., Ménard,R. & Sinden, R.E. (2011). PbGEST mediates malaria transmission to both mosquito and vertebrate host. *Molecular Microbiology*, 82(2), pp.462–74.

Tavares, J., Formaglio, P., Thiberge, S., Mordelet, E., Van Rooijen, N., Medvinsky, A., Ménard, R. & Amino, R. (2013). Role of host cell traversal by the malaria sporozoite during liver infection. *Journal of Experimental Medicine*, 210(5), pp.905–15.

The RTS,S Clinical Trials Partnership. (2014). Efficacy and safety of the RTS,S/AS01 malaria vaccine during 18 months after vaccination: a phase 3 randomized, controlled trial in children and young infants at 11 African sites. *PLoS Medicine*, 11(7),p.e1001685.

Tolia, N.H., Enemark, E.J., Sim, B.K.L., & Joshua-Tor, L. (2005).Structural basis for the EBA-175 erythrocyte invasion pathway of the malaria parasite *Plasmodium falciparum*. *Cell*, 122(2), pp.183–93.

Tomley, F. M., Billington, K. J., Bumstead, J. M., Clark, J. D., & Monaghan, P. (2001). EtMIC4: a microneme protein from *Eimeria tenella* that contains tandem arrays of epidermal growth factor-like repeats and thrombospondin type-I repeats. *International Journal for Parasitology*, 31(12), pp.1303–10.

Tossavainen, H., Pihlajamaa, T., Huttunen, T. K., Raulo, E., Rauvala, H., Permi, P., & Kilpeläinen, I. (2006). The layered fold of the TSR domain of P. *falciparum* TRAP contains a heparin binding site. *Protein Science*, 15(7), pp.1760–8.

Trottein, F., Triglia, T. & Cowman, A.F. (1995). Molecular cloning of a gene from *Plasmodium falciparum* that codes for a protein sharing motifs found in adhesive molecules from mammals and Plasmodia. *Molecular and Biochemical Parasitology*, 74(2), pp.129–41.

Tseng, J.C., Vasquez, K. & Peterson, J.D. (2015). Optical Imaging on the IVIS Spectrum CT System: General and Technical Considerations for 2D and 3D Imaging, pp.1-18. Retrieved from: http://www.perkinelmer.com/product/ivis-instrument-spectrum-ct-120v-128201.

Vanderberg, J.P. (1975). Development of infectivity by the *Plasmodium berghei* sporozoite. *Journal of*

Parasitology, 61(1), pp.43–50.

Vanderberg, J.P., Chew, S. & Stewart, M.J. (1990). *Plasmodium* sporozoite interactions with macrophages in vitro: a videomicroscopic analysis. *The Journal of Protozoology*, 37(6), pp.528–36.

Vanderberg, J.P. & Frevert, U. (2004). Intravital microscopy demonstrating antibody-mediated immobilisation of *Plasmodium berghei* sporozoites injected into skin by mosquitoes. *International Journal for Parasitology*, 34(9), pp.991–6.

Vreden, S. G., Sauerwein, R. W., Verhave, J. P., Van Rooijen, N., Meuwissen, J. H., & Van Den Broek, M. F. (1993). Kupffer cell elimination enhances development of liver schizonts of *Plasmodium berghei* in rats. *Infection and Immunity*, 61(5), pp.1936–9.

Wan, K. L., Carruthers, V. B., Sibley, L. D., & Ajioka, J. W. (1997). Molecular characterisation of an expressed sequence tag locus of *Toxoplasma gondii* encoding the micronemal protein MIC2. *Molecular and Biochemical Parasitology*, 84(2), pp.203–14.

White, M.T., Verity, R., Griffin J.T., Asante, K.P., Owusu-Agyei, S., Greenwood, B., Drakeley, C., Gesase, S., Lusingu, J., Ansong, D., Adjei, S., Agbenyega, T., Ogutu, B., Otieno, L., Otieno, W., Agnandji, A.T., Lell, B., Kremsner, P., Hoffman, I., Martinson, F., Kamthunzu, P., Tinto, H., Valea, I., Sorgho, H., Oneko, M., Otieno, K., Hamel, M.J., Salim, N., Mtoro, A., Abdulla, S., Aide, P., Sacarlal, J., Aponte, J.J., Njuguna, P., Marsh, K., Bejon, P., Riley, E.M. & Ghani, A.C. (2015). Immunogenicity of the RTS,S/AS01 malaria vaccine and implications for duration of vaccine efficacy: secondary analysis of data from a phase 3 randomised controlled trial. *The Lancet Infectious Diseases*, 15(12), pp.1450–8.

World Health Organisation, 2010. Global report on antimalarial drug efficacy and drug resistance: 2000-2010. WHO Press. Retrieved from: http://www.who.int/malaria/publications/atoz/9789241500470/en/.

World Health Organization, 2014. World Malaria Report 2014. WHO Press. Retrieved from: http://www.who.int/malaria/publications/world_malaria_report_2014/en/.

World Health Organization, 2015a. World Malaria Report 2015. WHO Press. Retreived from: http://www.who.int/malaria/publications/world-malaria-report-2015/report/en/.

World Health Organization, 2015b. Guidelines For The Treatment of Malaria, WHO Press. http://www.who.int/malaria/publications/atoz/9789241549127/en/.

World Health Organization, 2016a. Malaria, Entomology and vector control. Retrieved from: http://www.who.int/malaria/areas/vector_control/en/.

World Health Organization, 2016b. Malaria Vaccine Rainbow Tables. Retrieved from: http://www.who.int/vaccine_research/links/Rainbow/en/index.html.

Yalaoui, S., Huby, T., Franetich, J.F., Gego, A., Rametti, A., Moreau, M., Collet, X., Siau, A., van Gemert, G.J., Sauerwein, R.W., Luty, A.J., Vaillant, J.C., Hannoun, L., Chapman, J., Mazier, D. & Froissard, P. (2008). Scavenger receptor BI boosts hepatocyte permissiveness to *Plasmodium* infection. *Cell Host & Microbe*, 4(3), pp.283–92.

Yamauchi, L. M., Coppi, A., Snounou, G. & Sinnis, P. (2007). *Plasmodium* sporozoites trickle out of the injection site. *Cellular Microbiology*, 9(5), pp.1215–22.

Ying, P., Shakibaei, M., Patankar, M. S., Clavijo, P., Beavis, R.C., Clark, G. F. & Frevert, U. (1997). The malaria circumsporozoite protein: interaction of the conserved regions I and II-plus with heparin-like oligosaccharides in heparan sulfate. *Experimental Parasitology*, 85(2), pp.168–82.

Zheng, H., Tan, Z. & Xu, W. (2014). Immune evasion strategies of pre-erythrocytic malaria parasites. *Mediators of Inflammation*, 2014.